FACULDADE DE ENGENHARIA DA UNIVERSIDADE DO PORTO

Development of an insole for ulcer detection among diabetic patients

Tomás Guerreiro da Veiga

DISSERTATION

Integrated Master in Bioengineering - Biomedical Engineering

Supervisor at FEUP: Prof. Joaquim Gabriel Magalhães Mendes

Supervisor at MACE: Prof. Andrew Weightman

September 17, 2018

Development of an insole for ulcer detection among diabetic patients

Tomás Guerreiro da Veiga

Integrated Master in Bioengineering - Biomedical Engineering

September 17, 2018

Abstract

Diabetes mellitus is a global epidemic disease being responsible for over 4 million fatalities in 2017, affecting other 450 million people. Furthermore, its prevalence is increasing due to non-healthy habits. In addition to being a chronic condition, diabetes brings several complications that further burden and diminish the patients' quality of life, such as the diabetic foot. As a matter of fact, the diabetic foot and its ulcers are the diabetic complications with the largest impact on patients' lives, both in economic and social aspects. Moreover, foot ulcers when not correctly or early treated may lead to lower-limb amputation putting patients' lives at risk.

Being foot ulcers highly avoidable, an effort should be made in order to diminish this diabetes complication. The current clinical practice has proven to be ineffective by not fulfilling patients' needs. For this reason, there has been an increase in the development of new devices that are able to predict diabetic foot ulcers by monitoring critical variables of the foot, such as temperature. Consequently, the incidence of the diabetic foot is expected to lower, as well as its burden to both patients and healthcare systems around the world.

However, existing and emerging healthcare devices have yet a lot of drawbacks needing further research and development. Most of them require expert knowledge, are expensive for the average patient and/or are meant for clinical environments. Being self-monitoring very important in the prevention of foot ulcers, devices intended to be used by patients at home continuously should be further developed.

Being silicone rubber an excellent material for foot orthosis for diabetic patients and low-cost, it is a great material to be used as the substrate for such devices. Therefore, the embedment of temperature sensors within silicone rubber was studied in terms of thermal response and mechanical resistance. In addition, silicone rubber filled with carbon nanotubes was also investigated.

Three-dimensional printing has evolved in recent years and it is now possible to 3D print fully integrated electrical systems. In fact, this technology allows the creation of customised devices at a lower cost. This way, by using three-dimensional printing, the development of patient-specific devices for predicting and monitoring foot ulcers at a lower cost will be possible. For these reasons, three dimensional printing was also studied as a suitable manufacturing method of such a device.

It was found that silicone rubber with temperature sensors embedded at 1.0 mm are capable of withstanding 6 months of walking use. Furthermore, by adding CNT at 2.96wt%, the durability, as well as the thermal response, are improved. Silicone rubber 3D printed objects were found to have lower mechanical stability but faster thermal responses.

Taking into consideration the previous conclusions, a customised insole made of silicone rubber was 3D printed and tested. The developed insole was able to monitor foot temperature in four different regions of the sole of the foot both in static and dynamic conditions. In fact, the insole noticed a temperature increase during physical activity.

Acknowledgements

This dissertation is the culmination of five years of work and study and symbolises the end of another chapter in my life.

Because life, and learning for that matter, is a continuum act, it cannot be separated from the previous experiences and, therefore, I would like to acknowledge every single person that has ever played a role in my life as insignificant as that might have been.

Nevertheless, some people are worth singling out due to their contribution either to the work here described or personally.

Firstly, I would like to thank Dr. Andrew Weightman for receiving me and for all the encouragement given throughout the development of this dissertation. I would also like to thank Professor Joaquim Gabriel for all the support given throughout.

I would like to thank Coimbrinhas. Despite the fact that each one of us is living in their own city, we have always been there and supported each other whenever it was needed.

Five years ago I moved to a new city without knowing anyone, which was to become my home during the following years. During these years I have met the most wonderful people and had some of the best moments so far. I will take with me the nights spent partying and the days that followed. I will take the nights spent studying and the random ideas that would cross our minds during. The sunsets at Passeio das Virtudes, the great tascus papers before dinners and the evenings where 40 people would be having dinner in my small living room. The trips to McDrive without a car and, most of all, the breaks between lectures.

During these five years, I also had the opportunity to start my "long" adventures abroad. Thank you to all the people that I left in Stockholm. I will not forget the sunsets at Skinnarviksberget. The night outs at Slakthuset and the random weekend activities that someone would think of. Thank you to the Macanese, or wannabes, for the great nights at Cubic, beers by the lake and entertainment provided during typhoons and rainstorms. At last, I would like to thank all the people left in Manchester for turning a not so pretty city into a great and amazing city.

At last, I would like to thank my family whom without I would not have had the opportunity to accomplish what I have so far.

Now it is time to move on and do great things. So long and thanks for all the fish.

Tomás Veiga

"When you come out of the storm,
you won't be the same person who walked in.
That's what this storm's all about."

Haruki Murakami

Contents

List of Figures

List of Tables

List of Abbreviations

AM	Additive manufacturing
CNTs	Carbon nanotubes
DM	Diabetes Mellitus
DF	Diabetic Foot
DFU	Diabetic Foot Ulcers
EVA	Ethylene vinyl acetate
FBG	Fibre Bragg gratings
GNS	Graphene nanosheet
GO	Graphene oxide
IC	Integrated circuit
IR	Infrared radiation
LCT	Liquid crystal thermography
MDT	Multidisciplinary specialist footcare teams
MWNT	Multi walled carbon nanotubes
NICE	National Institute for Health and Care Excellence
PDMS	Polydimethylsiloxane
PEDOT:PSS	Poly(3,4-ethylenedioxythiophene) polystyrene sulfonate
phr	Parts per hundred rubber
PID	Proportional integral derivative
PVD	Peripheral vascular disease
RTD	Resistance temperature detectors
SWNT	Single walled carbon nanotubes
TCR	Temperature coefficient of resistance
TLC	Thermochromic liquid crystals
3D	Three dimensions
3DP	Three dimensional printing

Chapter 1

Introduction

1.1 Diabetes Mellitus and Diabetic Foot

Glucose is a simple sugar being humans' primary source of energy. In fact, glucose is present in humans' blood at all times [1], more commonly known as blood sugar, and its level is kept under a strict narrow range in order to ensure normal body function [2].

When food is eaten, blood sugar levels increase and insulin-producing cells in the pancreas are induced to release insulin into the bloodstream [1]. As a matter of fact, it is this pancreatic hormone that is responsible for promoting cellular glucose uptake, and by increasing its blood levels, blood sugar levels decrease [3].

A deficiency in insulin leads to abnormally high blood sugar levels, which characterises the chronic disease Diabetes Mellitus (DM). There are two types of diabetes depending on the mechanism that lays in the source of the problem. Type 1 diabetes, an autoimmune disease, occurs when the body self-destroys insulin-producing cells, meaning that there is no insulin in the body [4]. On the other hand, type 2 diabetes, a metabolic disorder, occurs when the body is not able to use effectively the insulin produced [5]. In order to compensate for this ineffectiveness, the insulin production initially increases, but it fails to supply the body needs [6].

DM is an important public health threat, being one of the four priority non-communicable diseases targeted for action by world leaders [7].

Globally, in 2017, it was responsible for an estimated 4.0 million deaths in the age group of 20-79 years old, corresponding to 10.5% of the global all-cause mortality [8]. Of these deaths, 47% occurred in those under 60 years of age [8, 9]. Its prevalence has almost quadruple from 108 million in 1980 [7] to 451 million in 2017 [8], nearly doubling its percentage in terms of global population, from 4.7% to 8.8%. Its incidence rate is still growing and it is expected to affect 693 million people by 2045, with higher increase rates in the low and middle-income countries [8].

More specifically, in the United Kingdom, 3.5 million people were living with the disease in 2015 and 1 million more was estimated to be living undiagnosed [9], accounting for 6% of its population. Its prevalence has more than doubled from the 1.4 million in 1996 [9] and it is

expected to reach 5 million by 2025 [10]. Furthermore, it was responsible for around 116,000 deaths in 2015, according to the National Diabetes Audit [11].

In Portugal, in 2015, it was estimated that 13.3% of the population aged between 20 and 79 was living with the disease [12], accounting for more than 1 million people. Following the same pattern as the rest of the world, the incidence is increasing, since in 2009 only 11.7% of the population was living with the disease (corresponding to 905,000 people) [13]. Furthermore, it was responsible for 4.0% of all deaths in 2015 [12].

This disease, although incurable, can be well managed with the right lifestyle and diet in order to keep blood sugar levels under control [14]. However, if this is not done, other serious complications, such as neuropathy, retinopathy, and cardiovascular diseases, can arise contributing to mortality, costs and poor quality of life [15].

Diabetic Foot (DF) refers to the presence of ulceration, infection and/or destruction of deep tissues in the lower limb of patients with type 1 or type 2 diabetes [16, 17] and is one of the most common diabetes complications. In fact, up to a quarter of all diabetic patients is affected by a foot ulcer at some point in their lifetime [18].

Globally, the prevalence of DF is, on average, 6.4% ranging between 3% in Oceania and 13% in North America [8]. The annual incidence among people with diabetes, in high-income countries, is around 2.5% [8, 9]. This value is higher in low and middle-income countries [8]. In addition, its incidence is increasing due to the rise in diabetes prevalence and the prolonged life expectancy of its patients [8].

In the U.K., there are about 86,000 people with foot ulcers and around 7,400 diabetes-related amputations every year [9, 19]. Meaning that 8.6% of people who develop a foot ulcer get amputated.

In fact, people with diabetes are 30 times more likely to have an amputation than the general population [9]. Amputations, on their own, are associated with high mortality. Indeed, up to 80% of people who get an amputation die within 5 years after the procedure [19].

Besides the negative impacts of the DM, such as a reduction in life expectancy of up to 11 years [9], patients who suffer from DF are burdened with additional impacts. First, its treatment requires a considerable amount of time at hospitals and clinics and frequent changes of wound dressings, affecting both the patients and family's working and social lives [20]. The patients' have reduced independence due to the lack of mobility and often suffer from depression and discrimination [21]. Furthermore, living with DF can be painful and diminish peoples' ability to work [21].

This diabetes complication not only has a huge impact on the patients' quality of life as it also has in its overall costs. In fact, diabetic people with foot ulcers have care costs 5.4 times higher than diabetic people without foot ulcers, making it one of the most expensive diabetes complications [8].

In addition to the patients' burden, DM and the DF also impose a significant economic impact on health care systems worldwide [8]. Globally, in 2017, around USD 727 billion was spent in total healthcare expenditure on diabetes [8]. Regarding the U.K., it is currently estimated that around

GBP 10 billion is spent, per year, in diabetes by the National Health Service (NHS), corresponding to 10% of its annual budget [9]. In Portugal, the picture is very similar with 10% of the total health expenditures being spent on diabetes [12].

When it comes to DF and amputation, in the U.K., around GBP 1 billion is spent yearly [20], corresponding to 10% of the total NHS diabetes annual budget. In addition, 86% of the total inpatient care costs were for ulcer admission in 2015 [22].

1.2 Motivation

Being DM and DF an international health threat and DFU highly predictable and preventable, extra efforts to address this issue should be made.

Although there are preventive measures regarding foot ulcers, there is still a lack of knowledge within the medical and patient community about the issue [8]. Additionally, the current clinical practice of the diabetic foot ulcers assessment requires regular visits from the patient to health care facilities [23]. In busy centres, this can be highly impractical and reduce the reliability of the assessment [24]. Furthermore, this leads to the patient's non-adherence [25].

Being the diabetic foot such a critical problem of today, and due to the ineffective current prevention and guidance of the issue, several devices have been emerging to aid the problem [26]. In fact, by measuring some physiological variables, such as foot temperature, one can predict the ulcer onset [27].

However, currently available technologies are still insufficient to be used in a continuous way and are mainly targeted for clinical environment [24]. Being home monitoring and self foot check crucial in the early detection of foot ulcers, further efforts in the development of such devices should be made [26].

Three-dimensional printing (3DP), a manufacturing technology which suffered huge advances in recent years, is now starting to contribute to the electrical objects field [28]. In fact, the medical field is an excellent example where this technology is of utmost usefulness and importance. Developing multifunctional 3D printed devices will more easily provide customised patient-specific medical devices at a lower cost [29], further increasing its quality and access to the patient.

Applying this manufacturing technology in the diabetic foot problem might be a turning point.

1.3 Objectives

The main objective of this dissertation is to develop a 3D printed temperature measurement device for the diabetic foot, capable of predicting foot ulcer onset. Furthermore, the device should be able to continuously monitor the foot temperature, whether in static or dynamic conditions.

In order to achieve this, this research project investigates different sensor depths, different manufacturing methods and different carbon nanotubes loading concentrations in silicone rubber in terms of thermal conductivity and wear and tear resistance upon cyclic loads.

1.4 Structure of the dissertation

In addition to this introductory chapter, this dissertation contains 5 more chapters. In Chapter 2 it is presented the theoretical background and literature review performed. In Chapter 3 it is presented the methodology for the investigation of sensor depth, manufacturing methods and carbon nanotubes loading as well as its results and discussion. In Chapter 4 it is described the methodology for the development of the insole and its results and discussion. Lastly, in Chapter 5 final conclusions and future work are presented.

Chapter 2

Background and Literature Review

This chapter provides the theoretical background and literature review conducted for the development of this dissertation.

It starts with an overview of the diabetic foot ulceration and its monitoring and assessment devices, followed by the existing temperature sensors suitable for monitoring foot temperatures. The following section covers the general design and common materials used on orthoses for diabetic patients, while the last section reports three dimensional printing as a manufacturing method and its use in object sensorisation.

2.1 Diabetic foot ulceration

Ulcers are defined as skin wounds that penetrate the full thickness of the dermis [17]. Diabetic foot ulcer is the general term to describe an ulcer below the ankle in a patient with diabetes [30].

2.1.1 Diabetic foot ulcers formation and infection

There are several etiologic factors in foot ulceration that alone do not present a risk but rather a combination of them. The most common ones are peripheral neuropathy (present in 86% of the cases [31]), peripheral vascular disease (PVD) (present in 49% of the cases [31]) and trauma [16, 17].

In fact, high blood sugar levels over the years in diabetic patients lead to a progressive damage to nerve fibres and blood vessels, causing peripheral neuropathy and PVD, respectively [8]. Peripheral neuropathy is characterised by a progressive loss of nerve fibre function [32], whereas, PVD is characterised by an atherosclerotic narrowing of blood vessels constraining the amount of blood in the lower extremities [16, 33]. In truth, these two conditions are widely common in diabetic patients, being peripheral neuropathy the one with the highest prevalence affecting nearly 50% of all diabetic patients [32] and PVD affecting between 15-30% [16].

The pathway to ulcer formation is complex and involves consequences of both these conditions. The pathway is depicted in Figure 2.1.

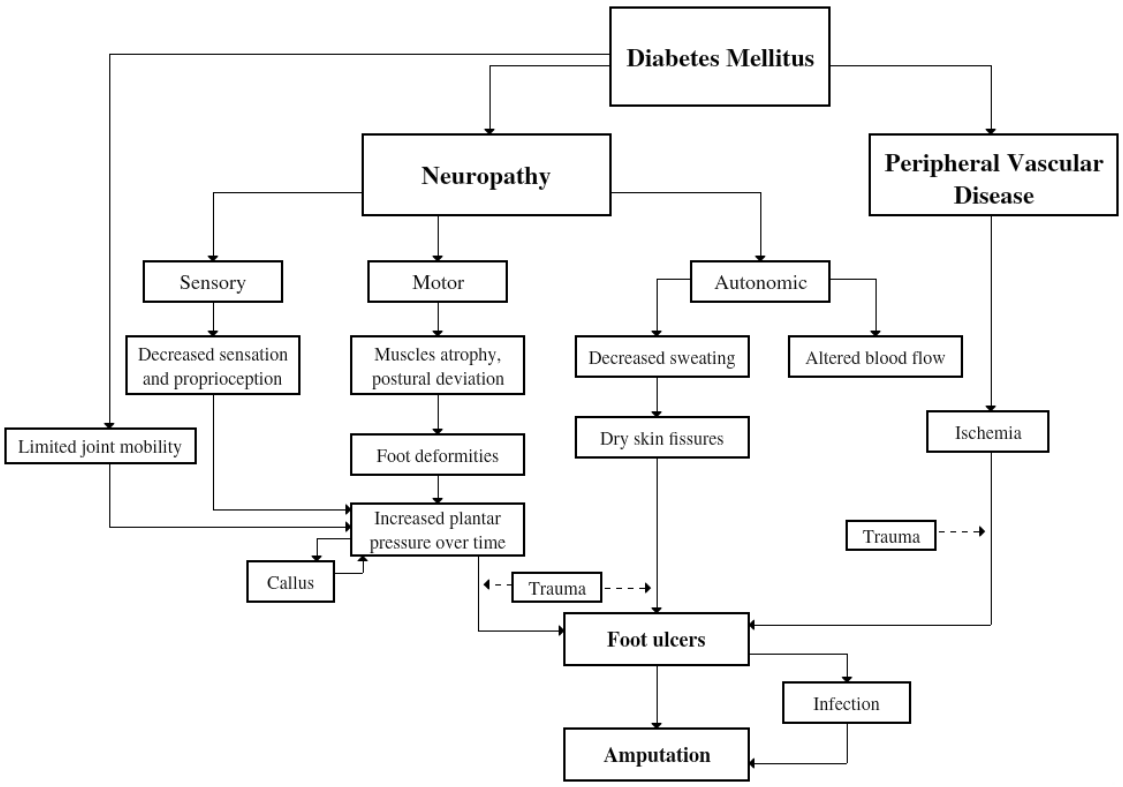

Figure 2.1: Pathways to foot ulceration. Adapted from [16, 34]

Due to neuropathy, the damaged motor nerves lead to atrophy and weakness of the intrinsic foot muscles. This causes deformities, such as clawed toes, exposing non-desirable areas to higher pressure [16, 35]. In addition to the damaged motor nerves, the chronic hyperglycemia limits the joints' mobility and cause a reduction in the tissue's elasticity [35]. These factors combined lead to a rigid and unstable foot with altered weight bearing areas and walking pattern. This increases plantar pressures. After repetitive walking trauma, plantar calluses are likely formed [34]. These calluses, further increase the local pressure, damaging the skin and finally leading to foot ulceration, see Figure 2.2 [16, 34, 35].

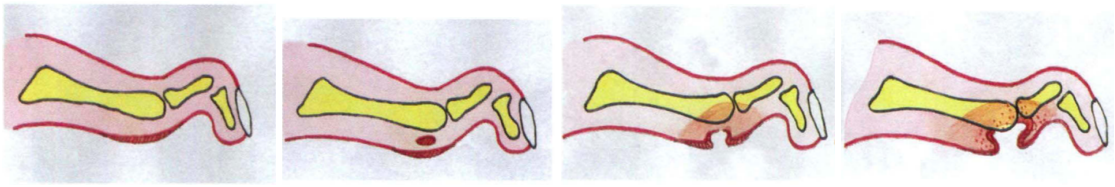

(a) (b) (c) (d)

Figure 2.2: Stages of plantar ulcer. (a) Callus formation. (b) Soft tissue damage. (c) Ulceration. (d) Infected ulcer. Reproduced from [35]

Furthermore, the loss of protective sensation, due to the damage to sensory nerves, also contributes to the increase in plantar pressure. For example, a healthy person feels discomfort after

standing for too long and changes positions, shifting the applied pressure to other areas of the feet. However, in a neuropathic person, such discomfort is not felt and pressure continues being applied in the same area for a long period of time, contributing, in the long run, to foot ulceration. [35]

Additionally, the damage to the autonomic nerves causes a reduction or elimination of sweating. This leads to plantar xerosis, making the skin drier and prone to fissures, cracks, and calluses [35]. It has been stated that reduced sweating is associated with an increased risk of foot ulceration [16].

PVD, on its own, is also a major contributing factor for foot ulceration [16]. The blood flow reduction, due to the narrowing of blood vessels, leaves the skin more susceptible to higher biomechanical stress which in combination with trauma, can lead to ulceration [34].

Trauma to the foot can be internal, such as calluses, ingrown nails or foot deformities; or external, for example from ill-fitting shoes, burns or foreign bodies [16]. Shoe related trauma is the most common one [34] but all these traumas are enough to break the skin. This rupture causes, initially, minor injuries which, by not being perceived by the patient, increase in size leading to ulceration and often to infection afterwards [16].

On the onset of a foot injury, invasion of its tissues by microorganisms, accompanied by an inflammatory response, may follow [16]. Foot infections are highly common in the diabetic population [36] affecting more than half of the DFU [37]. Infection is associated with long-term morbidity and amputation [35].

Infected ulcers are often asymptomatic due to the peripheral neuropathy [16]. Normal host response includes five different signs of inflammation: heat, redness, tenderness, swelling, and loss of function. However, due to the underlying neuropathy in diabetic patients, two of these signs, tenderness, and loss of function, are absent. Since there is no pain, there is no loss of function, therefore the patient continues to ambulate facilitating the spread of infection [35].

In addition to being a major contributing factor for foot ulceration, PVD is also a major predictor of the ulcer outcome [16]. When an injury happens, especially if complicated by infection, the local blood demands increase even more [16]. However, due to PVD, the blood supply does not meet the required amount, thus the white blood cells migration, as well as antibiotics, into the site of infection is compromised. This increases the difficulty in the foot ulcer healing process [36].

This way, what started as a simple plantar infection, rapidly progresses to a limb, or even life, threatening infection [35].

Lower limb amputation is the most devastating incident in the life of the diabetic population [35]. In fact, around 85% of all amputations are preceded by foot ulcers [8, 16, 19, 35].

2.1.2 Characteristics of diabetic foot ulcers

The distribution of foot ulcers has been reported in several studies [38, 39, 40]. Although their anatomic site depends on the population from where the participants are drawn from [41], all studies have concluded that the majority of foot ulcers are within the plantar region [38, 40]. This is expected since it is well established that high pressures potentiate ulcer formation.

In Table 2.1 it is presented the results of two studies which analysed the distribution of DFU along the plantar region [38, 39]. As it can be seen, although there are some differences between them, the regions with the highest incidence are the hallux, the heel, and the first and fifth metatarsal head. Figure 2.3 depicts these areas.

Table 2.1: Distribution of diabetic foot ulcers in plantar region. [38, 39]

	Perell *et al.* [39]	Cowley *et al.* [38]
Region of lesion on plantar site	%	%
Hallux	**18.8**	**36.2**
2nd to 5th toe	10.0	14.2
1st metatarsal head	**16.6**	**7.0**
2nd to 4th metatarsal head	25.9	8.5
2nd	11.0	–
3rd	8.3	–
4th	0.6	–
5th metatarsal head	**13.8**	**8.5**
Heel	**11.0**	**20.5**
Lateral forefoot	2.2	1.5
Medial forefoot	1.7	3.6

Figure 2.3: Anatomic regions with high ulceration. (1) Hallux, (2) first metatarsal head, (3) fifth metatarsal head, (4) heel. Adapted from [25]

When it comes to the size of the ulcers, two studies inferred this property among diabetic patients [42, 43]. The average ulcer size was found to be 2.8 cm^2 [42] and 5.9 cm^2 [43].

2.1.3 Current health care preventive practices in Diabetic Foot

Developing foot ulceration and consecutive lower limb amputation is a risk of all diabetic patients. However, this can be prevented with the right attention and care at an early stage, since it has been shown that the longer the delay in taking action, the more likely foot ulcers will be severe and take longer to heal [19]. Comprehensive footcare programs can reduce the occurrence of foot problems in up to 50% of diabetic patients [35, 44].

Preventing foot complications starts by identifying at-risk patients and educating them about the seriousness of the problem and how to examine their feet [35]. Healthcare providers should also be educated on how to assess foot problems and examine every high-risk foot upon clinic visit [16].

Personal preventive measures against the diabetic foot, in addition to managing diabetes, include a regular feet self-examination, usage of appropriate footwear and never walking barefoot in order to reduce trauma to the feet [16]. Furthermore, patients should seek treatment of any non-ulcerative pathology [8, 16].

In addition to the personal measures, every diabetic patient should have an annual quality foot check and, if at risk, referred to a specialist assessment [19].

Despite the existence of these preventing measures, they are not actually put into practice. In the U.K, in 2014-2015, 27% of people with type 1 diabetes and 13% of people with type 2 diabetes did not receive their annual quality foot check [19]. Additionally, most of the foot checks do not meet the National Institute for Health and Care Excellence (NICE) guidance standards [19].

Moreover, 29% of diabetic patients stated that they did not receive information about the annual quality foot check, and of these, 35% did not receive information about self-examination of the feet and legs [19].

When diabetic patients are admitted to the hospital, their feet should be examined. However, in 2015, only 29% of them had their feet checked within 24 hours of admission [19].

Those with an active foot problem should be referred to multidisciplinary specialist footcare teams (MDT) within one working day, according to NICE [22]. However, 31% of hospitals are without MDT and only 58% of patients were seen within the stipulated time [19]. This is a serious problem since patients who wait longer for specialist care tend to have more severe ulcers, taking longer to heal [22].

As it can be seen, the footcare practices still need to be improved in order to reach and treat every patient in need. There is still a lack of knowledge both from patients and the medical community on how to diagnose, assess and treat DF [8, 19].

2.2 Devices for an early detection of diabetic foot ulcers

As stated earlier, DFU are highly preventable and risk assessment and determination of foot status are done routinely in several countries [26]. However, improvements in these procedures are needed in order to further decrease the DFU incidence and subsequent amputations [24, 26].

The assessment of DFU is normally done by a clinician through the evaluation of several risk factors such as neuropathy, PVD, history of ulceration/amputation and plantar pressures [23, 44]. This requires regular visits from patients to doctors, which are considered intrusive and costly [23]. In addition, currently available technologies are not easy for daily self-assessment due to impracticality, dependence of expert knowledge and time consumption [23, 24].

In an attempt to improve this process, over the past years, several studies and devices have been emerging to evaluate foot at risk and to predict or monitor foot ulcers. Most of them rely on plantar pressure and/or foot temperature. Furthermore, recent studies have been emerging taking into account other parameters such as pH [31] and joint range of motion [24].

Diabetic patients with neuropathy and/or ulcers have higher plantar pressures when compared to healthy people [45], further increasing the risk of foot ulceration [24]. This way, by monitoring plantar pressures one can evaluate a foot at risk [46].

However, there is no consensus on the threshold for plantar pressure for considering a foot at risk with minimum false detection [24, 35, 46]. This comes from the fact that DFU are caused by a combination of factors and not only by high plantar pressures. For example, people with low plantar pressures can ulcerate due to high levels of activity or walking barefoot, whereas people with high plantar pressures might not ulcerate due to low levels of activity or other preventive measures, such as adequate footwear [35]. Thus, setting a plantar pressure threshold may introduce false positives and false negatives, depending on the value of the threshold [46]. This affects the system's validity and usability [46] and could reduce patients' adherence [24]. Therefore, this type of device should be patient-specific which is currently not available [46]. Furthermore, it has been concluded that plantar pressures by themselves are a poor tool to predict foot ulceration [47].

On the other hand, ulcers, just like any other wound, are preceded by inflammation [48] being heat one of its five signs. In fact, an increase in foot temperature can be predictive of an ulcer onset [35, 48, 49] even one week before it starts [23, 31]. Therefore, temperature methods can predict outcomes earlier than pressure or observational methods [47]. This way, monitoring foot temperature is an effective way to predict ulcers [35, 48, 49] and, doing it so at home has been indicated to significantly limit the re-ulceration rates in diabetic patients [26].

Manual palpation is the current temperature assessment in healthcare practice [26]. However, this is not effective since the temperature change might be too subtle to be detected manually [26]. In addition, regular monitoring of foot temperatures has not, so far, been integrated into standard diabetes care [26].

Given this, in this overview two groups of devices were considered – solely based on temperature and based on temperature and other measurements.

2.2.1 Temperature based methods

Temperature based methods are able to predict foot ulcers by monitoring foot temperature. In order to evaluate the obtained measurements, a reference value needs to be used [26, 50].

Foot temperature distribution depends on several parameters, such as ambient temperature, level of activity or even the person's weight [26, 51] (see Section 2.2.3). Therefore, there is not a standard reference value or distribution of a healthy foot for comparison [51].

As a result, the most frequently used reference value is the one in the corresponding area on the contralateral foot [26]. These temperatures normally do not differ more than 1°C and a temperature difference above 2.2°C is considered to be abnormal [26, 50, 51]. Therefore, an accentuated temperature difference between corresponding sites of the left and right foot is an early warning of foot disease in diabetes [26].

Temperature methods can be grouped depending on the technique used to measure temperature: liquid crystal thermography; infrared thermometry and thermography; and electrical contact thermometry. These will be explained in detail in the following subsections.

2.2.1.1 Liquid crystal thermography

Thermochromic liquid crystals (TLC) are materials that change their reflected colour as a function of temperature [52]. Liquid crystal thermography (LCT) correlates the colour response of a surface treated with TLC with its temperature. This way, by placing a foot in this type of surfaces, LCT provides a coloured foot imprint that is proportional to the foot temperature [26, 53].

Currently, there are two commercial products that use LCT to measure foot temperature, SpectraSole Pro 1000 [54] and TempStat™ [55].

Spectra Sole Pro 1000 [54] has been in the market since 2004 [26] and it is depicted in Figure 2.4. Targeted for the clinical environment, it was developed for preventive diagnostics and for following the healing of foot complications [56]. It consists of two rectangular plates with several layers of encapsulated TLC [56]. Each layer changes colours within a certain temperature interval, engendering temperature-specific patterns [56].

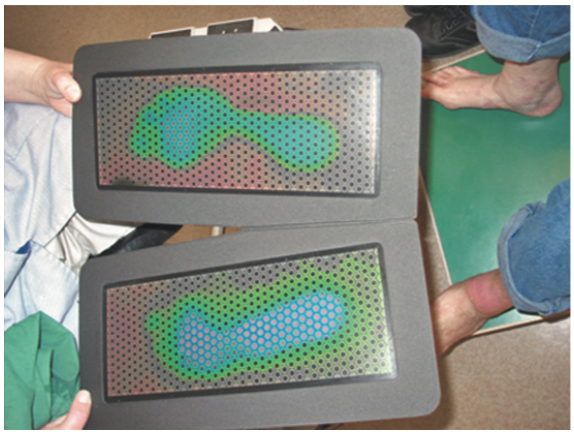

Figure 2.4: SpectraSole Pro 1000. Reproduced from [56]

The patient starts by placing his or her feet on the plates for 1 minute while standing or sitting [57]. The temperature is transferred from the feet to the plates giving rise to a temperature

spectrum [57]. By comparing the left and right sides, conclusions can be drawn due to the different patterns [57]. The images remain for a few minutes, slowly fading away after [56].

A feasibility study conducted in 2009 [56] showed that SpectraSole was able to detect 74% of the foot problems among the patients with the worst foot status. Furthermore, 10% of the detected cases had not been detected in the preceding ordinary examination [56].

TempStat™ [55] is a personal home care device intended to be used in the patients daily self-examination routine [58]. The device is depicted in Figure 2.5. TempStat™ contains a magnifying convex mirror in the central region, in order to help the patient to observe the sole of its feet [58]. It contains two plastic pads made primarily of liquid crystalline cholesteric ester [58]. This way, this device enables the patient to visually examine his feet as well as see a graphical representation of the plantar temperature pattern [58].

Figure 2.5: TempStat™. It can be seen that the right foot contains a hot stop in the upper part, indicative of an ulcer. Reproduced from [58]

TempStat™ works in the same way as SpectraSole Pro 1000 and a patient survey demonstrated that it is able to clearly detect hot spots (see Figure 2.5) [58].

In addition to these commercially available devices, several patents have been issued over the years but have not made it into the market such as patent U.K. 0802913.4 [59]. This invention in addition to the LCT method contains a high-resolution video camera allowing the visualisation of the sole of the feet as well as higher storage of the image data obtained [59].

Liquid crystal thermography technology offers rapid temperature imaging and recent improvements, such as insensitivity to pressure and lower cost, have made it possible to use it in a clinical environment [59]. Furthermore, LCT is able to give temperature readings of the entire foot in one measurement procedure [26].

However, LCT presents two major drawbacks, low image resolution, and limited life time [51]. Furthermore, the capture of the data needs to be closely monitored in order to avoid errors [51]. For example, on one hand, if the foot is in contact with the platform for a long period of time, the temperature in the crystals will tend to an equilibrium [51]. On the other hand, if the duration of contact is not long enough the crystals will not be sensitised sufficiently to give accurate results [51]. Moreover, some images may sometimes be difficult to interpret [26].

2.2.1.2 Infrared thermometry and thermography

Infrared radiation (IR) is an electromagnetic radiation invisible to the human eye that is emitted by any object whose temperature is higher than 0 K. Therefore, by detecting this type of radiation, the temperature of the emitting object can be determined.

IR thermometry has been shown to be an effective tool to assess skin temperature and it has been used for many years in clinical environment [60]. There are already several handheld IR thermometers available and their low cost and decreased size make them feasible to implement in foot-care [60].

One example of these IR thermometers is TempTouch® [61] depicted in Figure 2.6. To use this method, the patient starts by approximating the thermometer to a specific region of the foot [61]. The thermometer includes a proximity sensor that is able to detect its distance to the foot [61]. When TempTouch® is at the right distance, the patient is informed and the temperature is measured [61]. After the first measurement, the patient repeats the process on the contralateral foot and the temperature difference is displayed on screen [61].

Figure 2.6: TempTouch®. Reproduced from [62]

A randomised trial used IR thermometry, with TempTouch®, as an additional procedure to the standard therapy [63]. It was concluded that the group without the additional IR thermometry was significantly more likely to develop foot ulcers than patients with the additional IR thermometry [63]. Furthermore, the study indicates a 60% reduction in foot ulceration [63].

This method, although being easily used by patients and relatively cheap, needs considerable patient's adherence in order to individually measure several spots in both feet each time.

Another method that relies on IR is IR thermography. This method has been used in several clinical applications, such as breast thermography and skin disease, and produces a coloured visualisation of the IR emitted at the measurement site [53].

IR thermography has been commonly used as a way to assess foot temperature in several studies such as [64], where the purpose was to compare the foot temperatures between diabetic and familial amyloid polyneuropathy patients. Furthermore, a study conducted in 2015 by Mendes *et al.* [65] reinforced the applicability of this technique in the assessment of diabetic foot risk screening.

Despite its use in studies to assess foot temperature, its use to detect and predict foot ulcers and wounds is still at an early stage with several studies and patents issued such as [66, 67].

One interesting example is the study carried out by Fraiwan *et al.* [23]. They developed an ulcer detection system based on a mobile thermal camera, FLIR ONE [68], attached to a smartphone and a mobile application [23]. This mobile application, through image processing, is able to predict ulcer formation [23]. The system was meant for domestic use enabling the patient to self-check his feet for any possible ulcers without needing to go to the diabetic clinic [23]. The mobile application was tested in existing thermal images and it successfully detected the regions with a high temperature difference between the two feet [23].

Just like LCT, IR methods are not capable of monitoring the feet continuously, but rather are meant to be used as a quick assessment tool. In addition, IR thermometers need a considerable amount of patient compliance in order to obtain a rigorous assessment. However, IR methods are preferred to LCT since they do not require direct contact with the patient's skin [23], making it a better option for clinical environments.

2.2.1.3 Electrical contact thermometry

Electrical contact thermometry means using appropriate temperature sensors, either arrays or individual, to measure the skin temperature in contact [53].

A commercially available product based on this method is the Podimetrics Mat™ [69], depicted in Figure 2.7. This device is part of an in-home telemedicine system that is capable of measuring foot temperature and its asymmetry [70]. The user starts by standing on the mat for ap-

Figure 2.7: The Podimetrics Mat™. Reproduced from [71]

proximately 20 seconds, while the device records the plantar temperature [70]. When the reading is done, the mat notifies the patient and transmits the information wirelessly to the manufacturer's servers [70]. There, the information is saved and processed [70].

This device contains an array of around 2,000 thermistors, protected under a water-resistant cover [70]. The thermogram generated has an accuracy of ±0.6°C and a precision of 0.1°C [70].

A feasibility study conducted in 2017 [70] concluded that when the threshold of asymmetry was of 2.22°C, the system was able to identify 97% of the DFU, on average, 37 days before any clinical signs. However, this high rate of detection was also accompanied by a rate of false positive of 57% [70]. This value is rather high and it is not desirable as could lead to patients'

non-adherence. When the threshold was set to 3.2°C, the false positive rate decreased to 32% but so did the sensitivity to 70% [70].

Other devices use a different design such as a shoe insole [50, 72, 73], see Figure 2.8. The greatest advantage of this design is the ability to continuously monitor plantar temperature as it can be placed inside the shoes.

One example of such devices is the one developed by Murillo *et al.* [50]. The measuring device developed is capable of measuring the plantar temperature in four different regions: hallux, first metatarsal, arch, and heel. The insole consisted of four LM35D – precision temperature sensors [74] – placed on a plastic-EVA foam cover and it was designed to be comfortable and economical [50]. The insole was, then, connected to a monitoring system, which was set to register the temperature every minute in the four different regions [50]. The data collected was then transferred to a PC for analysis and processing [50].

The system was tested in 10 participants, 5 diabetic patients and 5 healthy participants, while sitting up straight in a chair for 15 minutes [50]. The system was able to detect temperature differences between the two groups [50].

Despite the promising results, the system was not tested in dynamic situations. Furthermore, the dimensions of the monitoring system developed (a plastic box of $15 \times 9 \times 45$ cm), to which the insole is connected, limit the portability of the device [50].

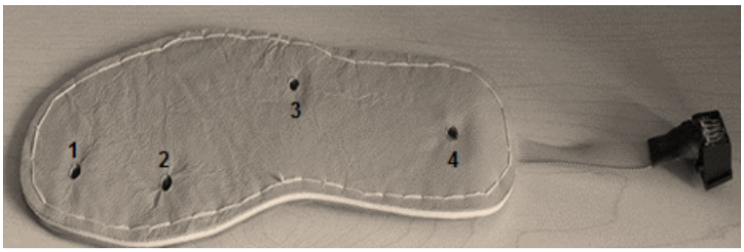

Figure 2.8: An insole device. Reproduced from [50]

Another example is the device developed by Reddy *et al.* [73]. The insole is very similar to the one previously described having four TMP35 — low voltage temperature sensors [75] — embedded in hard foam with a thickness of 5 mm [73]. The sensors were placed in four different regions of the foot using average data: the hallux, between the first and second metatarsal heads, the lateral side of the foot and the heel [73]. The data from the sensors was digitised and stored using a myRIO unit with a pack of batteries connect [73].

The device was placed inside a standard shoe and was then used to measure foot temperatures of healthy participants as they walked on a treadmill at different velocities [73].

When analysing the data recorded, Reddy *et al.* noticed two measurement problems [73]. One was the foot lifting off the insole during walking, leading to measuring the air between the foot and insole's temperature instead of the foot's [73]. This was mostly observed on the hallux and the heel sensors. The other problem arose from misplacement of sensors, leading to measuring the temperature of not desirable areas of the foot, or of places where the foot was not in contact with the insole [73].

These problems can be easily addressed. To ensure that the foot does not lift off the insole, one could place the insole in direct contact with the foot and secure its position with a sock, for example (see Figure 2.9) [73, 76]. The problem of the misplacement of sensors can be solved by tailoring individual insoles for each participant [73].

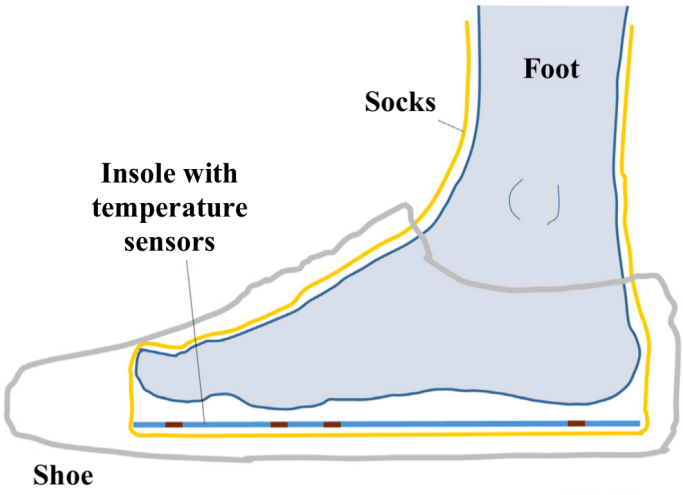

Figure 2.9: Placing the insole in direct contact with the foot to prevent erroneous data. Adapted from [76]

Electrical contact thermometry is very useful in diabetic foot temperature measurements as it allows for continuous monitoring at a relatively low cost. However, several aspects need to be taken into consideration when applying this technology to foot measurements, such as response time, calibration and effect on the test object [53]. Depending on the heat capacity of the temperature sensor and the thermal conductivity of the material between the foot and the temperature sensor, it may take a certain amount of time for the sensor to produce an associated change in resistance [53]. Furthermore, the calibration for skin is rather difficult and excessive pressure from the sensor on the foot could alter blood supply leading to different temperatures [53]. In addition, if used continuously, protective measures to the device should be taken in order to prevent early deterioration.

2.2.2 Temperature and other physical properties methods

In recent years, due to an increase in research in this subject, several techniques have been emerging that make use of temperature measurement in combination with other physical properties to assess a foot at risk and/or predict foot ulceration.

The most common one is pressure since it has been well established that higher pressures are linked with ulceration [24]. By combining temperature measurements and plantar pressure assessment, one can more accurately evaluate a foot at risk and predict foot ulceration [24].

One example is the device developed by Bernard *et al.* [47]. By designing an insole with thermistors and load sensors, they were able to develop a device which monitors high-risk areas of

the sole of the feet for indices of ulceration [47]. The device is composed of three thermistors and three load sensors placed in three high-risk areas: hallux, first metatarsal and heel [47]. Attached to the device is a data acquisition system which receives, interprets and saves the data [47]. In case of concerning readings, an alarm to the patient is emitted [47]. Unlike the previous devices, the patient's foot values are compared with a pre-programmed set of indicators [47].

Another emerging technology is the SmartSox, which is based on fibre optics embedded on a standard sock [24]. These highly flexible and thin optical fibres are based on fibre Bragg gratings (FBGs) [24]. Basically, infrared radiation is sent through multiple FBGs and each one reflects back a specific wavelength depending on the strained caused by external forces and temperature [24]. This way, angular motion, temperature and pressure changes at each FBG can be obtained and monitored by the microprocessor connected [24].

In Figure 2.10 it is represented the SmartSox. It contains 5 embedded FBGs in the plantar region to measure temperature and pressure. An additional 6th FBG is placed on top of the hallux to measure the range of motion [24].

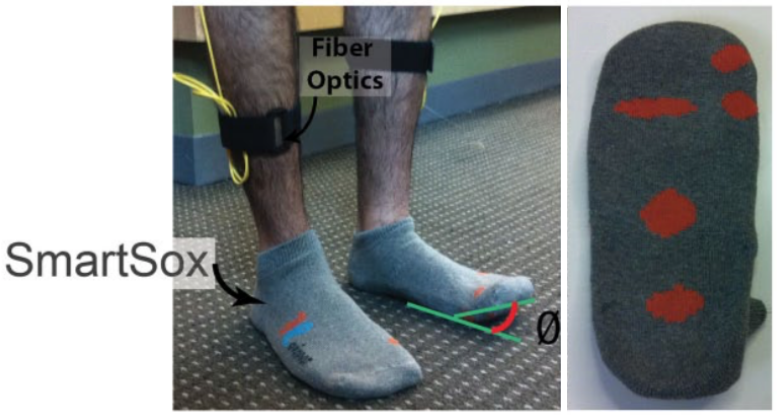

(a) (b)

Figure 2.10: (a) SmartSox prototype. (b) Positions of FBG sensors in the sole of the feet. Reproduced from [24]

The device is intended for clinical implementation with a short measurement protocol of 50-60 steps and was tested in 33 patients in this situation [24]. The measurements obtained were compared to those of a reference system [24].

During the tests, no cross-talks between the parameters of interest were found, suggesting that SmartSox could be used to monitor simultaneously all three parameters [24]. There was a moderate and significant agreement with the reference system indicating that the SmartSox is sensible enough to detect dangerous conditions and is able to identify foot at risk and predict DFU [24].

This device is innovative in two aspects: design and measurement method. First, the fact that the device is a sock makes it well accepted by the patient and makes it possible to be used with any type of footwear, unlike most devices [24]. Second, the usage of FBGs instead of the

traditional electrical sensors could reduce the risk of electrostatic accumulation and overheating to the patient and facilitates the cleaning process [24]. However, FBGs are not a low-cost technology and it was proved that they are too fragile for such an application, since several prototypes were broken during the human testing phase [24].

In addition, this device still needs some improvements. SmartSox does not have enough spatial resolution to cover the entire foot and there is no guarantee that the measured areas correspond to the exact same anatomical regions in the reference system [24]. Furthermore, the temperature measured might not reflect the exact temperature of skin [24].

A third emerging study developed wearable materials for monitoring foot ulcers based on temperature and pH [31]. The main innovation of this study was the use of a pH sensor to monitor the ulcers state [31]. In fact, an increase in pH can be indicative of infection due to the bacteria that proliferate in the wound.

Although this study is at a very initial stage and has not been tested in patients yet, Salvo *et al.* concluded that an electrode layered with graphene oxide (GO), at a concentration of 4 mg/mL, is a potential candidate to measure pH in patients, with a sensitivity of 43 mV/pH [31].

2.2.3 Additional factors that influence foot temperature

Foot temperature of healthy individuals is, on average, 30.6°C [77]. However, this temperature is highly influenced by several factors, other than ulceration.

As stated earlier, the premise of temperature based methods is that a local temperature difference larger than 2.2°C between the two feet is indicative of ulceration. Therefore, devices based on this concept need to take into consideration these external factors that may mask this temperature difference, leading to erroneous readings.

One factor to consider is the ambient temperature. Foltyński *et al.* [78] studied the influence of ambient temperature on foot temperature of diabetic patients with one ulcerated and one non-ulcerated foot. They concluded that foot temperature highly depends on ambient temperature [78]. It is known that an ulcerated foot has higher temperatures that the non-ulcerated one. However, this study showed that this relationship highly depends on ambient temperature. Foltyński *et al.* concluded that the higher the ambient temperature, the closer the temperature of both feet are [78]. For example, when the ambient temperature was between 24°C and 28°C, the temperature difference between the two feet was up to 4°C. However, when the ambient temperature was between 30°C and 34°C, the temperature difference was close to zero [78]. This suggests that the threshold value of 2.2°C widely accepted should be ambient temperature dependent and not fixed.

Physical activity also plays an important role on foot temperature. Reddy *et al.* investigated the impact that walking had on foot temperature of healthy individuals [76]. It was concluded that there is a temperature increase in the feet and that the rate of change depends on cadence [76]. Another study conducted by Najafi *et al.* studied the impact of walking on foot temperatures in diabetic patients with and without Acute Charcot [79]. They found that the plantar temperature increased sharply in patients with Acute Charcot with the number of steps whereas the change was significantly lower in patients without Acute Charcot [79]. Reddy *et al.* also examined the

effect of viscoelastic heating during cyclical normal loading, on porcine tissue, and concluded that heating does occur due to the viscoelastic properties of the tissue [80]. Furthermore, the amount of heating depends on the amplitude and frequency of the loading and can play a confounding factor for detection or prediction of diabetic foot ulceration [80].

Although no studies were found regarding how activity levels influence plantar temperature in patients with and without foot ulcers, one can expect that the level of activity might play a role in these temperatures, and ultimately may mask the temperature difference between the two feet.

Finally, external pressure exerted on the skin also plays an important role in its temperature [81]. Upon the release of the applied pressure, the local skin temperature quickly increases and then gradually decreases [81]. The larger the pressure and the longer the application time, the higher the peak temperatures observed [81]. Once again, no studies comparing this effect between ulcerated and non-ulcerated tissue was found.

2.2.4 Summary

The interest in foot monitoring in diabetic patients is increasing and, with recent advances in wearable technology, new and innovative devices will continue to appear. Most of the devices that currently exist are not available commercially and/or are not meant to be used by the patient at home. Being home monitoring and self-assessment a critical part in the prevention and early detection of DFU, an effort to develop this kind of devices should be made.

In an attempt to evaluate feet at risk in diabetic patients, one should consider and evaluate the risk factors. For this reason, several devices that measure plantar pressure have been created and are commercially available. Being the pathway for foot ulceration complex and not straightforward, techniques based on this method are not able to fully assess a foot at risk. In addition, the variability among patients makes impossible to define an accurate threshold for high plantar pressure.

Temperature methods seem to be the best ones which are, in fact, capable to predict the onset of ulceration before any other clinical signs. For this reason, several devices have been emerging, whether based on LCT, IR or electrical temperature sensors. These devices are able to accurately predict an ulcer, making an early treatment possible and, thus, preventing other serious complications such as infection and amputation.

Most of the devices are meant to be used under static conditions, needing the patient to be standing or sitting while recording the data. However, some recent devices are capable of recording temperature under dynamic conditions, such as sensing insoles. In fact, dynamic capable devices are preferred over static ones for two main reasons. On the one hand, as it has been stated previously, high-risk DFU patients experience a sharp increase in plantar temperature with a few steps. For this reason, any walking prior to a single measurement of the foot temperature might mask the temperature difference between the two feet and give inaccurate readings. On the other hand, a device that is capable of constant monitoring, not only will provide a more detailed temperature profile of the foot throughout the day and during activities, but will also burden to a lesser

degree the patients, since they do not need to incorporate into their daily routines a foot temperature examination. This surely plays an important role in patients' compliance and adherence to an ulcer predicting system.

Being so, devices based on electrical contact thermometry are preferred over technologies such as LCT and IR, since they currently do not allow for continuous monitoring.

The device's design also has a major impact on its usability and success among patients. An ergonomic design guarantees that the device meets the patient's needs and is functional at the same time. In addition, the device should not present major disruptions to the patient's daily life, in order not to discourage its regular use. Accordingly, designs such as insoles or socks are the most appealing ones.

Moreover, if the device is to be used continuously, protective measures should be taken in order to prevent deterioration. Careful attention to these measures should be paid since they need to guarantee that the temperature detected is, in fact, the foot temperature. Taking this into consideration, devices based on socks might not be suitable due to its fragility when compared to insoles.

Ulcer monitoring is also an important step to make sure that the ulcer is healing properly. The development of devices and techniques that are able to monitor the healing of foot ulcers is also increasing but it still is at a very early stage.

2.3 Types of temperature sensors

Nowadays there are several options when it comes to measuring temperature. However, not all of these options are suitable for the same situations.

When it comes to incorporating temperature sensors into a device to monitor foot temperature, there are three main types of temperature sensors that might be a right fit to the purpose: resistance temperature detectors, thermistors, and monolithic temperature sensors.

2.3.1 Resistance temperature detectors

Resistance temperature detectors (RTD) are one of the types of electrical resistance temperature sensors and are made of high-purity conductive metals such as platinum or nickel [82, 83]. There are two main constructions. The metal can be wound into a coil or deposited onto a ceramic substrate (see Figure 2.11) [84]. The premise of the RTD is that the metal's resistance changes with temperature and by passing a current and monitoring its output voltage, one can infer the temperature [82, 83]. This current can cause self-heating in the resistive wires leading to errors in the readings [82]. To avoid this, RTDs are usually connected into a Wheatstone Bridge network which has additional connecting wires for lead-compensation [83]. Other approaches are choosing a small-sized resistance device with a quick response time or a larger resistance device with better heating release; or even keeping the measuring current to low values [82].

The material used will highly influence the sensor's properties, being platinum the most common one. In general, its output is very linear giving accurate temperature measurements and is

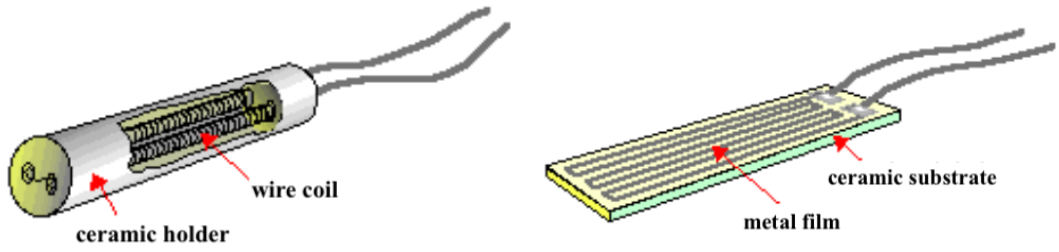

(a) (b)

Figure 2.11: (a) Wire RTD construction. (b) Thin-film RTD construction. Reproduced from [84]

stable over a wide temperature range (−200°C to 600°C) [83, 85]. However, they have low thermal sensitivity, meaning that a small change in temperature will produce a very small change in the output and they are more expensive than their alternatives [83, 85].

2.3.2 Thermistors

Thermistors are another example of temperature sensitive resistance devices. These are a special type of resistor that changes their resistance with temperature [83]. Thermistors are made of a semiconductor material, normally ceramics such as the oxide of nickel or manganese [82, 83]. An example of a thermistor can be seen in Figure 2.12(a).

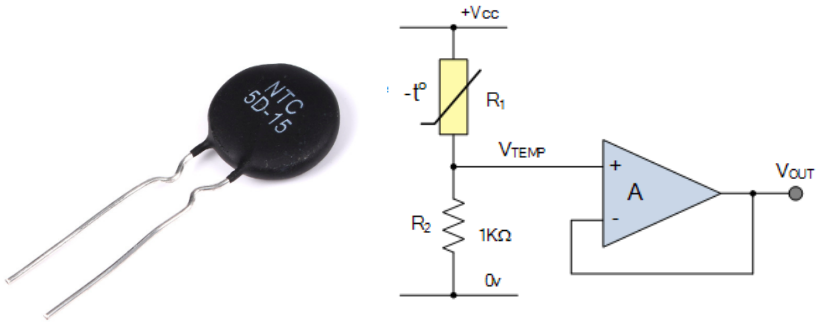

(a) (b)

Figure 2.12: (a) An example of a thermistor, a NTC-5D15 from Exsense Electronics Technology. Reproduced from [86]. (b) A common temperature sensing circuit using a thermistor. Reproduced from [87]

The main advantage of this type of temperature sensor is its high sensitivity [82, 83]. In addition, it also has a very fast response to thermal changes [83, 85]. However, its durability is low, being a fragile sensor, and it is also externally powered being highly susceptible to self-heating [85, 87]. It is non-linear and its working temperature range is narrow, normally around −40°C to 250°C [85].

Thermistors need a bias current and a few external components. In Figure 2.12(b), a common temperature sensing circuit using a thermistor is shown. A constant voltage is applied across the thermistor and resistor connected in series and the voltage output across the fixed resistor R_2 is measured [87, 88]. When the resistance of the thermistor changes, due to a change in temperature, the measured output also changes [87]. The additional amplifier could be used as a differential amplifier for high sensitivity and amplification [87].

2.3.3 Monolithic Temperature Sensors

Monolithic temperature sensors are a modern development in thermometry and have all the elements of a full circuit incorporated in only one chip or integrated circuit (IC) [82]. This means that the device is capable of producing a signal that is directly proportional to temperature without needing to add components or being calibrated [89]. An example is depicted in Figure 2.13. The premise of this type of sensors is that the voltage drop between the base and emitter of a transistor increases as temperature increases [89]. So, by amplifying this voltage change, it is easily obtained an analog signal that is directly proportional to temperature [89].

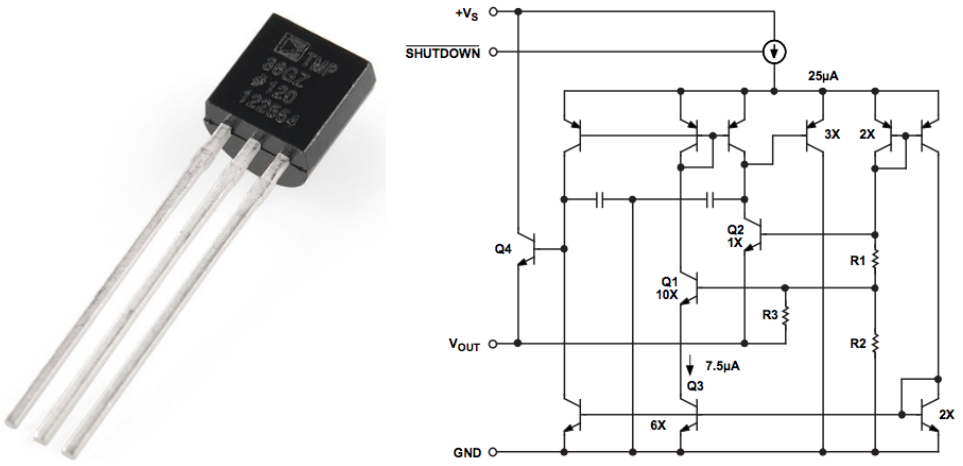

(a) (b)

Figure 2.13: (a) An example of a monolithic temperature sensor, a TMP35 from Analog Devices, and (b) its equivalent circuit. Reproduced from [75]

Just like thermistors, these sensors are fragile, require an external power supply and work within a narrow range of temperatures [82]. However, monolithic temperature sensors have a linear response throughout [82]. Furthermore, they are inexpensive, ready and easy to use [89].

2.3.4 Summary

When choosing the best temperature sensor type to the desired application, several aspects need to be considered, such as operating temperature range and design.

Starting with the temperature range needed, when it comes to a device to measure the foot temperature, the span desired is narrow. This way, thermistors and IC chips fit the application.

In terms of design, thin-film RTDs are the best fit. These are flexible and capable of measuring temperature over a larger area, unlike thermistors and IC chips. However, their cost is also much higher when comparing to the other two types, presenting a major obstacle to the development of a low-cost device. Furthermore, their sensitivity is considerably lower when comparing to thermistors and IC chips, which is not desirable in this situation.

Considering thermistors and IC chips, they do not have many operating differences. However, thermistors need additional external components in order to be used. This presents extra manufacturing steps over IC chips which are ready-to-use sensors.

IC chips overall present a great choice for measuring skin temperature. They have a reasonable sensibility, being able to detect small temperature changes, are easy to use and are low-cost.

2.4 Foot orthoses for diabetic patients

Foot orthoses can be defined as any material placed between the sole of the foot and the inside of the shoe [90] or more specifically all types of in-shoe medical devices designed to treat foot or lower-extremities pathologies [91]. These are prescribed for a variety of situations, from biomechanical corrections to comfort enhancement and impact attenuation [92].

There are several distinct types of foot orthoses, each one having its advantages and disadvantages [90, 92]. This gives a wide variety of insoles which best application depends on the situation and patient [90]. This type of devices can be classified according to their manufacturing method, function or rigidity [90, 92].

When it comes to the manufacturing method, insoles can be either casted or prefabricated [90]. Casted orthoses are tailored specifically to a patient's foot whereas the prefabricated ones are mass-produced and standardised in their shape by the manufacturers, giving general arch support or cushioning function [90, 92].

In terms of functionally, foot orthoses can be functional or accommodative [90]. A functional orthosis is, for example, made of rigid materials and is intended to reduce pronation [90]. On the other hand, an accommodative orthosis can be a flat insole made of cushioning materials to reduce plantar pressures [90].

Finally, the rigidity is mainly determined by the material used and the orthoses can be classified into three different groups: rigid, semi-rigid and soft [92].

Being diabetic patients prone to foot pathologies, foot orthoses have been widely used among diabetic patients being even advised by NICE guidelines for feet at risk [90, 93]. Its main usage is to relieve areas of high plantar pressure but can also be used to reduce shear and shock, accommodate fixed deformities and stabilise and support flexible deformities [94]. These characteristics are mainly obtained by choosing the right materials for the fabrication of the insole, as well as its profile [94].

When designing a temperature system based on an insole it is important to take into consideration certain aspects in order not to harm the patient's foot or even potentiate foot ulceration. Therefore, although the purpose of this dissertation is the development of a temperature system and not necessarily a foot orthosis, several aspects inherent to the design of orthoses can be useful in the design of the aforementioned temperature system. For this reason, a general insole design overview was made followed by a comparison of the different materials currently used in the fabrication of insoles for diabetic patients.

2.4.1 Insole design

There are several insole designs that best fit different situations and foot deformities [90].

Guldemond *et al.* [95] studied twelve different insole designs on plantar pressure and walking convenience. The different designs consisted of different combinations and heights of a metatarsal dome, varus and valgus wedges and arch supports [95] (see Figure 2.14).

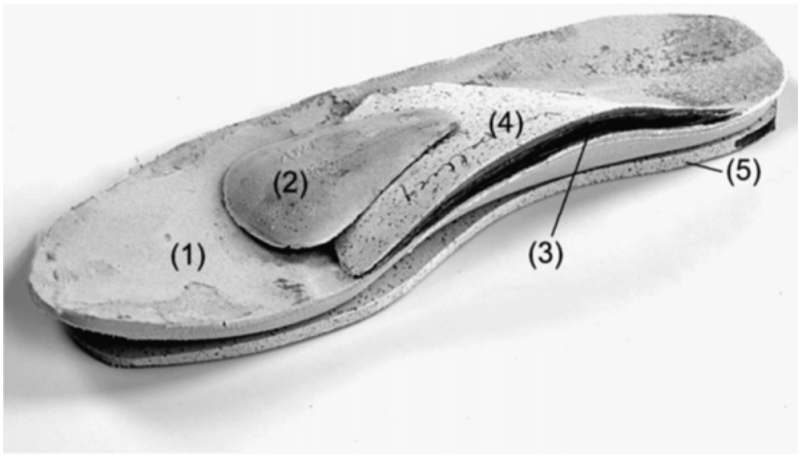

Figure 2.14: The insole with different components. (1) Basic flat insole, (2) metatarsal dome, (3) arch support, (4) extra arch support, (5) wedge (medial). Reproduced from [95]

It was concluded that an insole with a metatarsal dome and extra arch support had the biggest effect on lowering the plantar pressures [95]. However, this insole did not satisfy the patients' walking needs [95]. The insole that had the best feedback from patients in terms of walking convenience was the flat insole [95].

When it comes to the thickness of the insole, a thick insole provides more cushioning. However, if the insole is too thick, it might force the dorsal surface of the toes against the shoe upper [90]. General thickness of insoles for diabetic patients are 6 or 12 mm [94].

2.4.2 Insole materials

The insole material highly influences its success and durability [92, 94]. The important material's characteristics when fabricating insoles for diabetic patients were defined by Paton *et al.* [94] as density, resilience, compressive stiffness, static coefficient of friction and shear, durability

and compression set. These characteristics are generic and will vary depending on the ultimate goal [92]. In fact, when intended for a temperature system other characteristics must be considered such as the material's thermal conductivity, its easiness of manufacture and cost.

Therefore, the following physical characteristics are of utmost importance for the intended measuring device:

- **Thermal conductivity** is the ability of a material to conduct heat. A high value of thermal conductivity means that the material is a good heat conductor, whereas a low value means that the material is a poor heat conductor or insulator [96]. A high value of thermal conductivity is desired since it will allow for a rapid heat transfer from the foot to the temperature sensor. This is of extreme importance, since the sooner the sensors detect a dangerous temperature profile, the sooner the patient is given that information. Furthermore, in order to guarantee the reliability and consistency of the temperature measurements, the insole material properties, both thermal and mechanical, should not change with temperature within its expected working range.

- **Stiffness** is defined as the material's resistance to deformation [94] being the complementary concept flexibility. The material's stiffness needs to be well though of. On the one hand, a stiff material might be beneficial to achieve motion control, support, and stability [94]. On the other hand, a low stiffness material may be necessary to mould the insole to the foot contours to redistribute pressure away from bony prominences [94]. Therefore, the material should be soft enough so that it moulds to the patient's feet providing comfort and protection, but not too soft as to prevent the protuberance of the embedded sensors and wires.

- **Wear resistance and shear strength:** An insole is mainly subjected to compression and shear forces [94]. Wear is defined as the removal of surface material as a result of mechanical action [97], whereas shear is defined as a load composed of two equal opposing forces that tend to displace one part of an object in relation to an adjacent part along the force's plane [94]. It is desirable that the insole material is both wear and shear resistant. Being wear resistant means that the insole is capable of withstanding the cyclic loading of gait and does not expose the sensors and wires to the skin. Having a high shear strength means that the insole will not deform upon shear preventing sensor dislocation. Both of these two physical properties will ensure the durability of the device [94].

- **Coefficient of friction:** Friction is defined as the forces between the surfaces of two objects that act parallel to these surfaces and prevent them from slipping or sliding [94]. The higher coefficient of friction, the higher the frictional forces [94]. The difference between friction and shear is that shear occurs within the object [94]. When walking, if the coefficient of friction is too high, the foot tissues will be put under shear stress and this might be destructive to the tissue [94]. In fact, the shear forces could cause displacement of a tissue layer in respect to another, leading to foot ulceration in diabetic patients [94]. By minimising the coefficient

of friction below the shear force required to displace foot tissue, slippage between the foot and the insole occurs, redistributing the shear forces [94].

- **Easiness of manufacture and cost:** The material for the insole should allow an easy embedment of sensors and wires without damage to either the electrical components and the insole material. Furthermore, in order to keep the cost of the device to a minimum, it is also important to consider the overall costs of manufacture.

The materials used for foot orthosis can be grouped in several categories such as plastics, composites, and foams, being the most common silicone rubber, ethylene vinyl acetate (EVA) and polyurethane commercialised as Poron® [98]. In Table 2.2, the previously described properties for each of these materials are stated.

Table 2.2: Physical properties of common insole materials.

	Silicone rubber	EVA	Poron® 4701-40 Soft
Thermal conductivity	Average value is around 0.2 W/m.K [99, 100].	0.34 W/m.K [101].	From 0.065 to 0.127 W/m.K, depending on the density chosen [102].
Stiffness	Low stiffness [103].	Stiff [94].	Low stiffness [94].
Wear resistance and shear strength	Good wear and shear resistance [104].	Good wear and shear resistance [105].	Good wear and shear resistance [102].
Coefficient of friction	0.93 [106].	Higher than Poron® [94].	Low coefficient [94].
Easiness of manufacture and cost	Can be easily manufactured using moulds and casts or even three dimensional printing. Embedment of sensors is relatively simple as well. Overall low cost [103].	Sensor embedment can be a challenge due to being a foam material, making reproducibility difficult. More expensive than silicone rubber.	Sensor embedment can be a challenge. Similar price to EVA.

Note: No studies comparing the coefficient of friction between skin and the three different materials was found. Paton *et al.* [94] compared EVA and Poron®. Zhang *et al.* [106] compared silicone rubber with other materials such as nylon or alluminium. Due to the lack of numerical values of the comparison performed by Paton *et al.*, this property will not be considered.

Given the properties described, silicone rubber seems to be the best material for the desired application. The three materials have similar physical properties when it comes to thermal conductivity or wear and shear resistance, however, silicone rubber is far easier to work with and to embed sensors and wires in. Furthermore, it has excellent weather and chemical resistance [107, 108] and is physiological inert affecting to a lesser degree the living tissues that are in contact with it [104].

2.4.2.1 Silicone rubber

Silicone in its broader term refers to the class of synthetic compounds which consist of polymer chains of alternately connected silicon and oxygen atoms [109]. Silicone rubbers (or silicone elastomers) are elastomers based on high-molecular-weight linear polymers, normally polydimethylsiloxane (PDMS), which can be modified by introducing functional groups [109]. In Figure 2.15, the backbone structure of silicone rubber is presented.

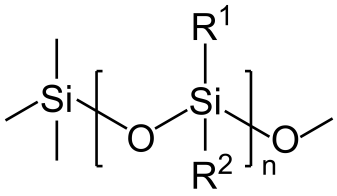

Figure 2.15: Repeat unit of silicone rubber. Adapted from [109]

It is their Si–O siloxane structure that gives them different properties when compared to other organic polymers, whose backbone structure consists of carbon atoms linked together [109]. The fact that there are no double bonds in the molecular chain contributes to its chemical inertness [109]. Furthermore, the covalent bond energy in Si–O is much higher than in carbon-to-carbon of other organic rubbers leading to the higher stability of silicone rubbers [109].

Each silicon atom of the Si–O linkage has a normal valency of four and, therefore, can connect to four different atoms [109]. Being so, it connects to two oxygen atoms (the adjacent atoms in the backbone structure) and to other two atoms, generating two pendant groups, as can be seen in Figure 2.15. The most common pendant groups in silicone rubbers are: methyl (CH_3), phenyl (C_6H_{11}), propyl (C_3H_7) or a combination of these [109].

The polymer chains are connected to one another by covalent bonds and cross-linked into a three dimensional structure [109]. This cross-linking takes place at the end of the polymer chains, where reactive groups react with the cross-linking agent to give a cured elastomer. Silicones that cure at room temperature (Room-temperature-vulcanising silicones) can be divided in one or two component systems, depending on the number of components supplied:

- **One component systems** use the moisture in the air as the cross-linking agent. The moisture hydrolises the functional groups, providing sites for the formation of a network structure [109]. Since their cure to a cross-linked structure is initiated by an external air-bore substance, the degree of cure obtained highly depends on the silicone's cross-sectional thickness [109]. This also means that curing time increases with thickness as measured from the exposed surface inward [109].

- **Two component systems** are supplied in the form of two components: the base and the curing agent. These systems enjoy a major advantage over one component systems in the way that they do not require moisture to cure [109]. Therefore, they are not limited to external factors to cure. They require, however, skilful weighing of both components and thorough

blending in order to achieve good results [109]. Additionally, special care should be taken when working with two component systems, as they are susceptible to cure inhibition caused by contaminants [109].

Despite the fact that silicone rubber has excellent chemical and mechanical properties for the overall scope of the project, its thermal conductivity is low and can pose a problem in a temperature sensing system [110]. For this reason, an attempt to improve this physical property should be made.

2.4.2.2 Enhanced Silicone Rubber

As stated previously in section 2.4.2, silicone rubber has low thermal conductivity and therefore is not suited for thermal interfaces. However, in order to overcome this, several studies have focused on improving the thermal conductivity of silicone rubber by incorporating thermally conductive fillers [107, 108, 110].

One example is silicone rubber filled with aluminium oxide (Al_2O_3). Gao *et al.* [107] studied the influence on the thermal conductivity of a silicone rubber when filled with Al_2O_3. It was concluded that larger particles induced a higher increase of thermal conductivity for the same amount of filler volume fraction [107]. The thermal conductivity increased non-linearly with increasing filler volume fraction. For example, for the larger particle (75μm in diameter) at a filler volume fraction of 0.15, the increase was around 60%, whereas at a volume fraction of 0.62 was of more than 800% [107].

Despite the tempting results for higher filler volume fractions, the impact on the mechanical properties was not investigated. Since the volume fraction of the filler is larger than the one of silicone rubber itself, one can suspect that the mechanical properties were highly modified.

Another example is silicone rubber filled with zinc oxide (ZnO). Mu *et al.* [108] studied the influence of volume amount, as well particle size, of ZnO on silicone rubber, both in terms of mechanical properties and thermal conductivity.

It was verified that a low volume of ZnO leads to better mechanical properties (elongation at break, hardness, and tensile strength). However, when the amount exceeded 0.12 of filler volume fraction, these properties worsened. [108]

In terms of thermal conductivity, the higher the filler volume, the higher the thermal conductivity of the composite for either particle size [108]. In addition, for higher filler volume fractions, a substantial increase in thermal conductivity happened when a hybrid filler content was added to the silicone rubber [108]. In fact, it was concluded that a filler composed of two different sized particles is able to get the same thermal conductivity as a single sized filler, but at a lower amount [108].

In conclusion, filling silicone rubber with ZnO can be beneficial both in terms of mechanical properties and thermal conductivity. However, a trade-off should be made between these two groups of properties, since a filler volume larger than 12% will have a negative impact on the mechanical properties. [108].

A special interest has been shown in carbon nanofillers, such as carbon nanotubes (CNTs) [111], graphene nanoplatelets [112] or even carbon nanocomposites [110].

CNTs have high thermal and electrical conductivity, being of great interest to be used as fillers [113]. Liu *et al.* [111] loaded silicone elastomer with CNTs, both single-walled (SWNT) and multi-walled (MWNT) nanotubes. They verified that the CNTs were well dispersed on the silicone elastomer and that at a filler mass fraction of 0.038 there had been an increase of 65% in the thermal conductivity [111]. This increase was, however, lower than anticipated [111].

Lin *et al.* [110] developed a nanocomposite made of silicone rubber first filled only with graphene nanosheets (GNS) and then also filled with graphene-silver nanowire. They verified that GNS increased the thermal conductivity, having experienced an increase of 128.8%, at 10 parts per hundred rubber (phr) [110]. When adding the graphene-silver nanowire to the previous composite at 6 phr, the increase was of 540% [110]. This showed, that the silver plays an essential role in generating new heat conduction networks in graphene [110].

2.4.3 Summary

Foot orthoses are widely used among diabetic patients and provide valuable insight when developing a temperature sensing insole, both in terms of design and materials.

There are several insole designs providing different options for different situations. Since the goal of this dissertation is not the development of a foot orthosis, the main concern is to develop a device that will not, in any way, harm or potentiate ulceration. Therefore, when looking at different profile design options, it can be concluded that a flat insole not only will not harm the patients' feet but it is also the profile more easily accepted by the patient.

The material used also has a huge impact on the characteristics and properties of the insole. When looking at the different materials commonly used, silicone rubber proved to be the most promising one, facilitating the sensor and wire embedment, despite its low thermal conductivity.

Several studies have proved that by adding thermally conductive fillers to silicone rubber it is possible to produce silicone composites with enhanced thermal conductivity. Although most of these studies focus only on the composite's final thermal conductivity, the addition of these fillers also has an impact on its mechanical properties, as shown by Mu *et al.* [108].

Since silicone rubber has favourable mechanical properties for its intended use and one of the goals is the overall low-cost of the device, it is desirable to keep the filler volume fraction to a minimum.

Being so, the use of CNTs seems to be the most appropriate option since they are capable of the largest increase in the thermal conductivity at lower fraction volumes.

When embedding electronics in a substrate, the electrical conductivity of that substrate should be low to prevent noise and interferences in the measurements. CNTs, in addition to having high thermal conductivity, have high electrical conductivity and therefore, may pose a problem when added to silicone rubber. Being so, coating to electrical components should be added beforehand.

2.5 Three Dimensional Printing

Three dimensional printing (3DP) or additive manufacturing (AM) is a technology that, through the deposition of sequential layers of material, is able to form complex three dimensional (3D) structures [29, 114].

In order to actually print an object through 3DP, one starts by designing a digital model of the intended object [114, 115]. Having the digital model in an appropriate standard 3DP file format, such as STL or AMF, the file is sent to the 3D printer [116]. The printer, controlled only by the computer [116], is then ready to print the object layer by layer [114, 115].

3DP can be divided into different processes, depending on the method of layer manufacturing [117]. The American Society for Testing and Materials has defined seven different categories of AM [118], which are as follows:

- **Vat Photopolymerisation** uses an energy source, such as a laser beam, to selectively cure liquid photo-curable polymers inside a vat. Typically, the vat contains a platform on the inside that descends after each layer is cured [117], see Figure 2.16.

- **Material Extrusion** involves selectively dispensing a material filament through an extrusion nozzle. The material is then deposited layer-by-layer at the build platform. The nozzle is able to move horizontally and the platform moves vertically after each layer has been deposited [117]. Thermoplastics are the most common material used, needing a heated extrusion [29], see Figure 2.17.

- **Direct Energy Deposition** is similar to Material Extrusion but here the nozzle can move in multiple directions and it is not fixed to a single axis [117]. The extruded material is melted upon the deposition by an energy source [117], see Figure 2.18.

- **Powder Bed Fusion** consists in selectively melting and fusing regions of powdery materials on the build platform using a thermal energy source [29, 117]. After a layer has been fused, the workbench descends and a new layer of powder is tiled on top, see Figure 2.19.

- **Binder Jetting** is similar to Power Bed Fusion in terms of also using powdery materials. In Binder Jetting, a binder is selectively extruded to join the powder in the build platform [29]. After the layer has been bound, the workbench descends and a new layer of powder is deposited by the powder roll, see Figure 2.20.

- **Material Jetting** uses a photosensitive resin as printing material [119]. After being selectively deposited, the material is cured and the process is repeated for all layers [29], see Figure 2.21.

- **Sheet Lamination** cuts individual sheets of materials using knives or lasers [117, 119]. After a layer has been cut, another one is added on top [119]. A roller is responsible for gluing each new layer to the existing object [119], see Figure 2.22.

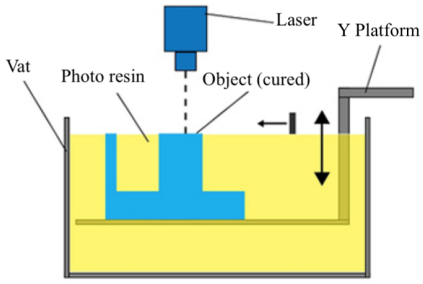

Figure 2.16: Vat Photopolymerisation. Reproduced from [117].

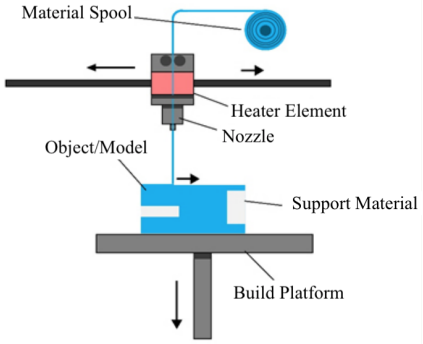

Figure 2.17: Material Extrusion. Reproduced from [117].

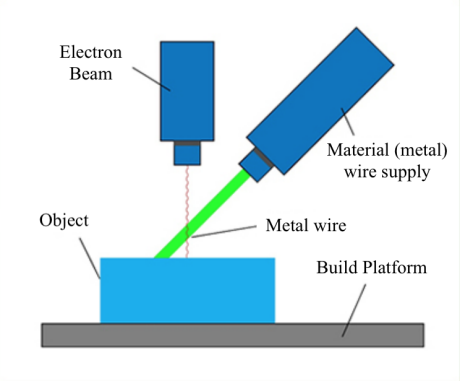

Figure 2.18: Direct Energy Deposition. Reproduced from [117].

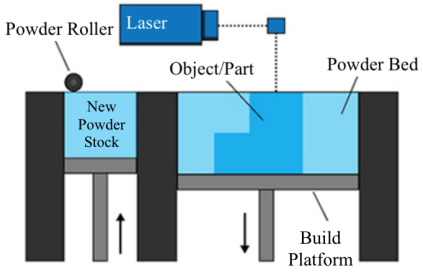

Figure 2.19: Powder Bed Fusion. Reproduced from [117].

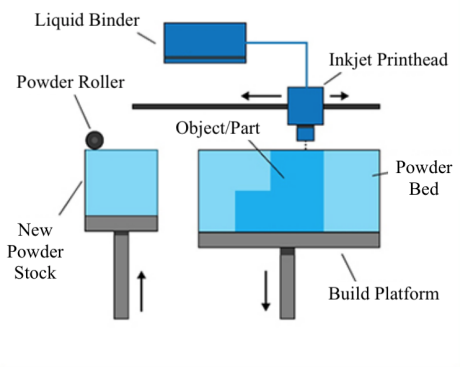

Figure 2.20: Binder Jetting. Reproduced from [117].

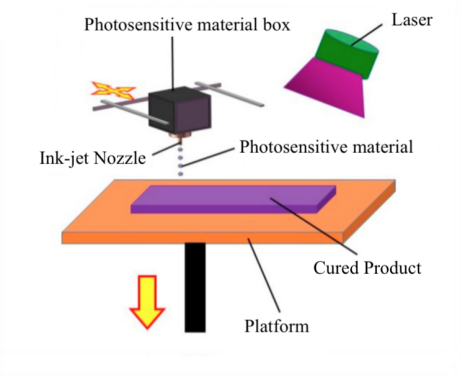

Figure 2.21: Material Jetting. Reproduced from [119].

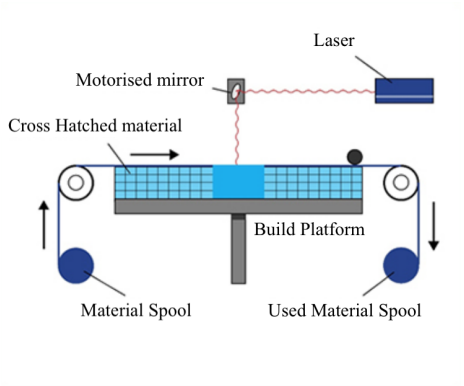

Figure 2.22: Sheet Lamination. Reproduced from [117].

Each one of these categories has its own relative advantages and limitations as well as the possible operating materials, offering different options for cost and feature detail. In Table 2.3 this information is presented.

Table 2.3: Materials that can be used with each 3DP process and their relative advantages and limitations [117, 119]

Process	Materials	Advantages	Limitations
Vat Photopolymerisation	Photopolymers	High level of accuracy Quick Process Models up to 200 kg	Single material Relatively expensive Lengthy post processing
Material Extrusion	Thermoplastics Eutectic metal Ceramics	Widespread Low cost Materials easily accessible	Low resolution Rough surface Low printing speed
Powder Bed Fusion	Any powder based materials	Large variety of materials High accuracy Powder acts as support structure	Low printing speed Lack of structural properties Finish depends on powder grain size
Binder Jetting	Metals Polymers Ceramics	Low cost Large variety of materials Fast process Colourful printing	Needs post surface treatment Not suitable to structural parts
Material Jetting	Polymers	Multiple materials simultaneously High accuracy Low waste	Limited materials Support material is required
Sheet Lamination	Sheet material (paper, plastic film, etc.)	Low cost Ease of material handling	Design limitations Limited mechanical properties Limited material usage
Direct Energy Deposition	Metals	Ability to control the grain structure Good surface quality	Limited material use May require post processing

Although having been invented several decades ago, this form of fabricating objects has been drawing much attention recently due to major improvements in its performance [29]. In fact, AM has already been used in several different fields of science such as medicine and manufacturing. [29, 119]

AM presents several advantages to traditional manufacturing techniques like stamping or casting [120]. First, AM is capable of producing objects with complex geometries that no other technique is [120]. Moreover, being the process digital, the level of operator expertise needed is low as well as the human interaction with it. This allows for, for example, overnight builds, dramatically decreasing the time of production [120]. This characteristic also enables a fast production on a global scale, since the digital model file can be easily shared [120]. There is a reduction of waste considering the material is added layer by layer and not carved out of a stock billet [120]. Lastly, should the design change, no additional tools need to be customised or added, unlike injection moulding or machining [120].

On the other hand, AM is still at a very infant development phase and presents two major disadvantages when compared to some traditional methods. First, the current technology is not suited for mass production purposes since its fabricating speed is still considerably lower [120]. Nevertheless, AM is still a very useful technique in the customised production which normally does not require mass production. [120]. Secondly, most of the AM processes use proprietary materials that are not well categorised and are weaker than its traditional forms [120]. This has been a major field of study in an attempt to create new and innovative materials that are able to be used in 3DP [121].

2.5.1 Multiprocess Three Dimensional Printing: object sensorisation

Until recently, the resulting structures of 3DP processes were normally limited to one material and were just capable of rendering a basic shape [29]. This limited its end-use functionality and 3DP was seen as a rapid prototyping method of single material objects for form and fit evaluation [29]. Being so, the concept of multiprocess (or hybrid) 3DP arose.

Multiprocess 3DP is defined as AM enhanced with complementary processes, such as robotic placement, cutting or machining [29]. In fact, 3DP processes can be stopped and restarted allowing the incorporation of complementary processes or embodiments in the structure [29, 119]. With this, one can, in a nonassembly process, fabricate objects that, besides being complex in shape, can also be complex in functionality, providing more useful end-use products [29, 119].

One of the main interests in multiprocess 3DP has been the sensorisation of the objects created [29, 119]. Depending on the type of sensor incorporated, the final object can have several features, such as thermal or chemical, combined with the inherent geometric benefits of 3DP [119]. Research has focused on two different ways of sensoring the printed objects, either by fully printing the sensor itself or by embedding an existing sensor in a printed object [29].

In order to 3D print electronic systems and sensors, conductive materials need to be incorporated in the process [28]. Conductive inks are inks infused with some type of conductive particles,

such as graphite [122]. Recent developments in the field, such as the materials used, have made this type of ink more easily accessible and widely used in 3DP [122].

Conductive inks can be used to form electrical interconnects, allowing the electrical communication within the system [29]. Furthermore, these inks can also be used to print directly electronic components such as resistors and sensors [28]. By adopting different materials of varying suspension densities, one can modulate the electrical properties of such components [28].

In stretchable substrates, electrical interconnections have been considered a challenge [123]. Nevertheless, studies have been emerging in order to overcome this obstacle, such as the one where Ota *et al.* were able to manufacture highly twistable Galistan-based channels [28].

When comparing these inks to traditionally printed circuit boards made with copper, one concludes that they still suffer from high resistance [29]. This results in a reduction of performance and power, making its reliability a concern [29]. Nevertheless, its usage in 3DP will allow the development of 3D printed electronic systems facilitating personalised electronic devices [28].

2.5.1.1 3DP Temperature sensors

One way of incorporating sensors into 3D printed objects is by printing the sensor itself. Printing temperature sensors requires resistive inks [124]. The used ink is the sensing material since its electrical properties change with temperature [119]. Several types of ink have been used with this purpose, such as based on silver nanoparticles [125], carbon nanoparticles [126, 127] or conducting PDMS [128].

One example of a 3D printed temperature sensor is the one developed by Courbat *et al.* [125]. Using silver nanoparticles ink and paper for printed electronics as the substrate, they were able to inkjet-print a resistive temperature sensor. The sensor is depicted in Figure 2.23. The underlying mechanism is that temperature influences the resistance of the printed silver wires. Due to the instabilities of Ag lines on paper, especially under humidity, passivation with parylene was made. [125]

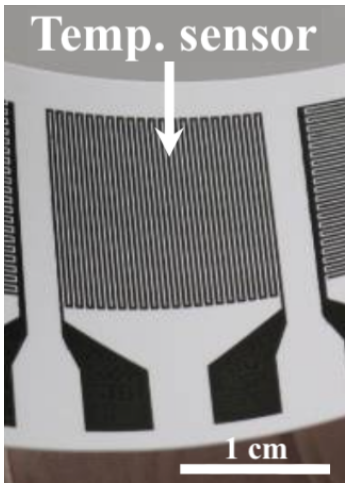

Figure 2.23: Inkjet printed temperature sensor. Adapted from [125]

The sensor showed good linearity between $-20°C$ and $60°C$, in a 30% relative humidity environment. Even with the parylene coating, at higher values of humidity, hysteresis was observed. The temperature coefficient of resistance (TCR) was of $0.0011°C^{-1}$, making it suitable for temperature measurements. [125]

Overall, the developed sensor could be used for temperature measurements between $-20°C$ and $60°C$, in low humidity environments.

Honda *et al.* [127] printed temperature sensors through a shadow mask printing technique on Kapton® substrates. They evaluated the usage of three different materials for the temperature sensor: CNT, poly(3,4-ethylenedioxythiophene) polystyrene sulfonate (PEDOT:PSS) and a mixture of the two.

They concluded that the sensor made out of CNT and PEDOT:PSS was the one with the highest value of TCR ($0.006°C^{-1}$ against $0.0029°C^{-1}$ and $0.0039°C^{-1}$ for CNT and PEDOT:PSS respectively) [127]. However, the sensor exhibited levels of hysteresis that might be too high for practical health monitoring [127]. A passivation to the sensor should have been added in order to decrease the hysteresis levels.

As proof of concept, the sensor was tested on human beings and it was capable of detect small skin temperature changes [127].

Another example of PEDOT:PSS usage as the temperature sensing material is the skin-conformable inkjet-printed temperature sensors developed by Vuorinen *et al.* [129]. They printed graphene/PEDOT:PSS with stretchable silver conductors on top of a stretchable polyurethane substrate with native adhesive. The developed sensor is shown in Figure 2.24.

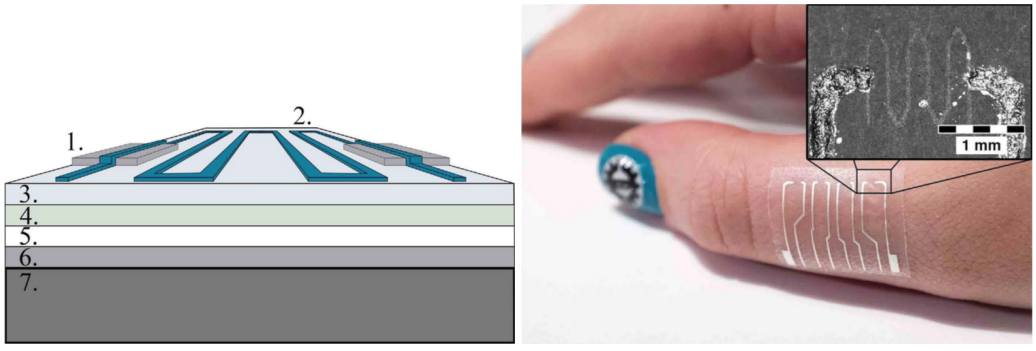

(a) (b)

Figure 2.24: (a) Schematic representation of the temperature sensor: 1. silver conductors, 2. wave patterned graphene/PEDOT:PSS temperature sensor, 3. polyurethane surface layer, 4. adhesive layer, 5. protective paper, 6. PET film, 7. cooling/heating element. (b) Photograph of sample attached to skin. Adapted from [129]

Tests were conducted in the temperature interval of $35°C$ to $45°C$ in an inert argon atmosphere and in an ambient atmosphere. Since humidity has a severe impact on graphene/PEDOT:PSS, a fluoropolymer coating was added to the sensor in order to improve stability. [129]

In the inert environment, the developed sensor was able to measure temperature with a TCR of $0.0064°C^{-1}$ and low levels of hysteresis [129]. When in the ambient environment, the value of

TCR dropped to 0.0034°C^{-1} and showed increased levels of hysteresis [129]. This proved that the coating was not totally effective.

Although not being able to compete in efficiency with already existing temperature sensors, the developed device could be used to monitor skin temperature, being a simple indicator of fever [129].

Lastly, Ali *et al.* [130] inkjet-printed a temperature sensor with an innovative design suitable for flexible substrates using silver nanoparticles ink. The sensor consists of two back-to-back printed patterns connected in series by wires. This way, if the sensor is bent on either side, one of the patterns will experience tension, increasing its resistance, whereas the other side will experience compression, decreasing its resistance [130]. As a result, the overall resistance of the sensor will remain practically the same. The developed sensor is depicted in Figure 2.25(a). The pattern dimensions were also investigated, being the dimensions shown in Figure 2.25(b) the final ones.

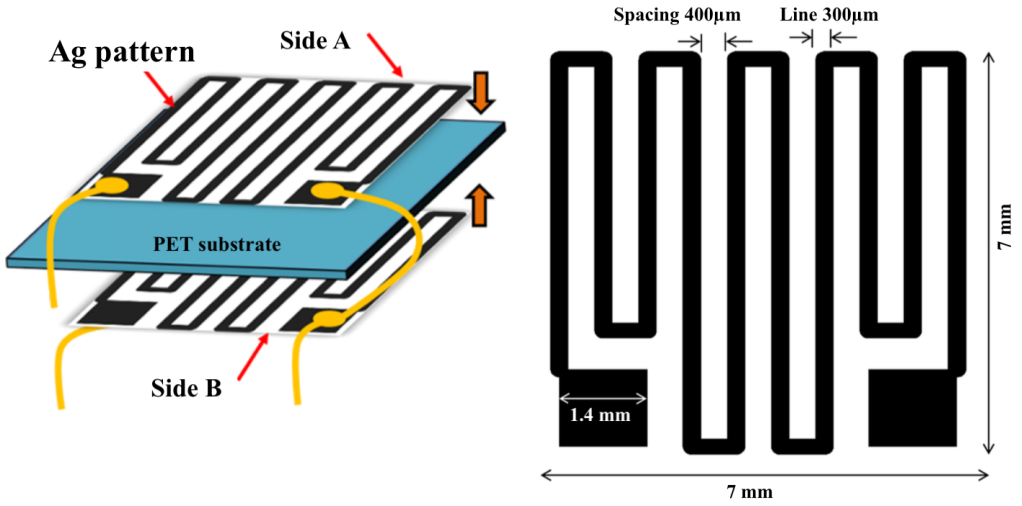

(a) (b)

Figure 2.25: (a) Schematic representation of the developed flexible sensor. (b) Schematic representation of the printed pattern. Adapted from [130]

The sensor was tested between the 0°C and 130°C and it was observed that up to 100°C the relationship between the resistance and temperature was linear with a TCR of 0.001076°C^{-1} [130].

To verify the usability under deformation, the sensor was bent up to 8 mm and only a nominal change in resistance was found (under 1 Ω) [130]. To ensure bending reliability, the sensor was bent over 5mm for more than 300 cycles and no change in resistance was found [130]. This way, the sensor proved to be a useful tool to measure temperature under flat, flexible or bent surfaces.

Several other studies were conducted on this subject, such as [131], where direct laser writing was used to print temperature sensors based on up-conversion luminescence. In general, these devices are still not able to compete with the already existing ones but are capable of doing basic temperature monitoring [129].

2.5.1.2 Embedding sensors in 3D printed objects

Another way of incorporating sensors into 3D printed objects is by embedding already existing sensors. In fact, 3DP processes can be interrupted allowing the insertion of existing electrical components, such as IC chips, into the structure.

Ota *et al.* [28] demonstrated the process for embedding electrical components into printing objects and it is represented in Figure 2.26.

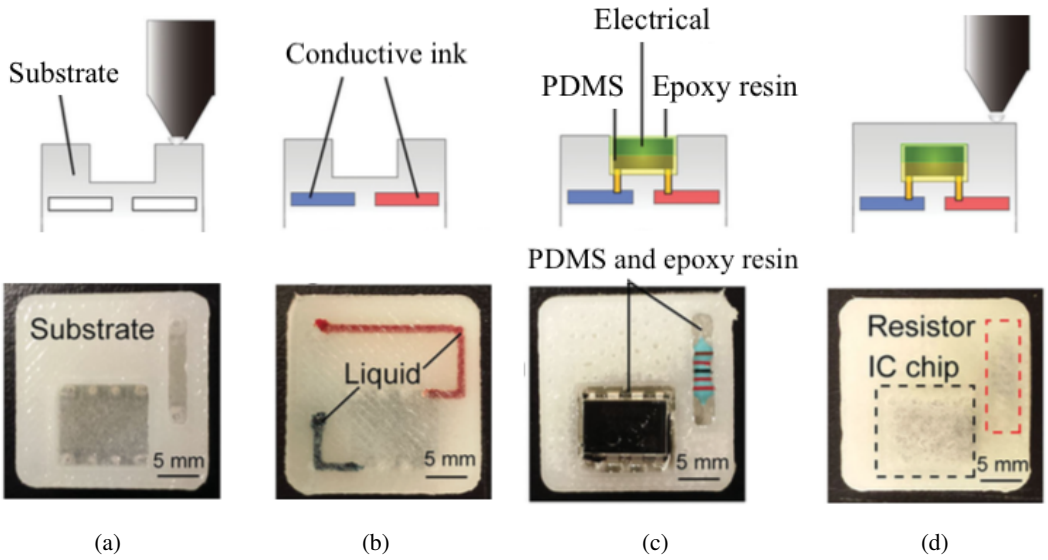

Figure 2.26: Schematic and real representation of IC chips and other electrical components in 3DP. (a) Substrate fabrication, (b) Conductive ink injection, (c) Component assembly, (d) Embedding components. Adapted from [28]

First, a substrate layer containing microchannels and slots for the component(s) is printed (Figure 2.26(a)). Next, the microchannels are filled with conductive ink in order to form the interconnections (Figure 2.26(b)). Then, the IC chip and/or other solid state electronic components are embedded within the substrate slots, making sure that the components' terminals are inserted in the microchannels. PDMS and epoxy resin can be added on top of the inserted component in order to obtain a flat surface (Figure 2.26(c)). Lastly, the 3DP process can continue (Figure 2.26(d)).

This process allows the insertion of components in several spacial orientations, enabling a wide range of device designs. Furthermore, integration of IC chips in the printed object enables advanced circuit functionalities that, currently, cannot be achieved by the 3D printed components [28].

As an example, Ota *et al.* developed a fully integrated smart glove [28]. The smart glove contained printed conductive channels in order to create interconnections, as well as actuators, sensors and circuit components. Furthermore, it also integrated IC chips through the process previously described [28]. The glove, as well as its fabrication process, is shown in Figure 2.27.

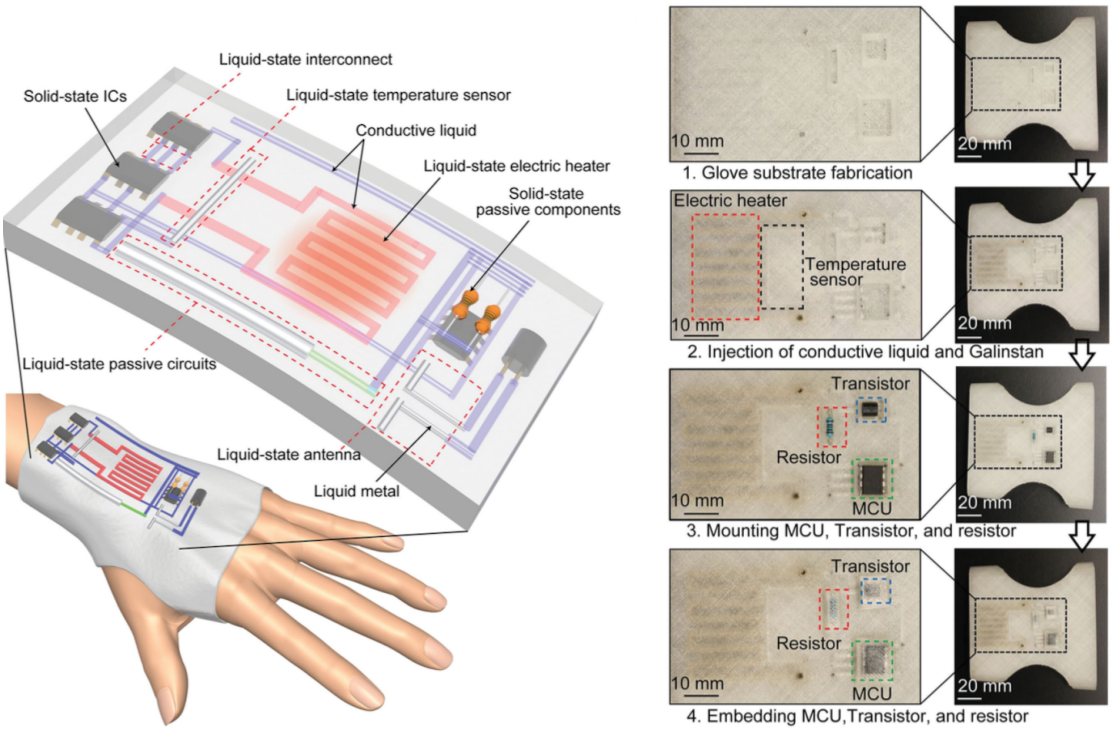

(a) (b)

Figure 2.27: (a) Schematic representation of the smart glove. (b) Fabrication process of the smart glove. Reproduced from [28]

The glove was developed for patients in need of thermotherapy, where heat supply is needed at the point of injury to enhance blood flow [28]. They further demonstrated the temperature sensing and heat delivery capability of the glove [28].

2.5.2 Summary

Since 3DP was invented, it has immensely grown over the years and it is now becoming widely used as a manufacturing tool. 3DP is superior in several aspects when comparing to the traditional manufacturing methods. However, current 3DP is only capable of producing rendering shape objects. The possibility to further enhance the capabilities of 3DP is now a major field of study in an attempt to create multifunctional devices.

The medical field is to benefit greatly from these advancements. In fact, sensors have been widely used in the medical community to monitor and diagnose patients. Multiprocess 3DP opens a new degree of freedom in manufacturing and design of which the biomedical field will benefit a lot. Indeed, the development of a 3DP device for continuously monitoring the temperature of a diabetic foot could be a turning point in the current situation described in Chapter 1.

In fact, there are several studies that report having successfully 3D printed a temperature sensor, some of them even designed for human use. This further indicates the usage of 3DP as a potential manufacturing method of medical devices.

Chapter 3

Preliminary tests

Prior to the development of an insole, the sensor depth and CNT loading in silicone rubber were optimised. Being so, this chapter describes the methods and results of these preliminary tests.

3.1 Methods

In order to optimise the sensor depth and the amount of CNT mixed in the silicone, small samples were designed, manufactured and submitted to thermal and mechanical experiments. The usage of these smaller samples instead of a full insole is to facilitate experiments, as well as to use less material.

In order to optimise the sensor depth, three sensor depths were studied: 0.5 mm, 1.0 mm and 1.5 mm. Since it has been established that CNTs increase silicone's rubber thermal conductivity, but no studies on its mechanical properties were found, two CNT concentrations were also studied: 0wt% and 2.96 wt%. Additionally, a 3D printed sample was also manufactured in order to evaluate 3DP as a suitable manufacturing method. The descriptions of all samples are presented in Table 3.1.

Table 3.1: Description of all samples.

		Sensor depth	CNT loading
Samples no.	Manufacturing method	mm	wt%
1	Compression moulding	0.5	0
2	Compression moulding	1.0	0
3	Compression moulding	1.5	0
4	Compression moulding	0.5	2.96
5	Compression moulding	1.0	2.96
6	Compression moulding	1.5	2.96
7	3D Printing	1.0	0

3.1.1 Samples' design

These samples are to be regarded as parts of an insole and, therefore, should follow a design adequate to an insole.

This way, the samples were designed to have a full thickness of 6 mm and a flat surface. The samples consisted of a cuboid shape with a 50×50 mm face and contained a gap for placing the sensor with a lateral opening for the connecting wires. The SolidWorks® models of the moulds for compression moulding are represented in Figure 3.1. Figure 3.2 depicts the SolidWorks® models of the sample to be 3D printed. Full dimensions can be consulted in Appendix A.

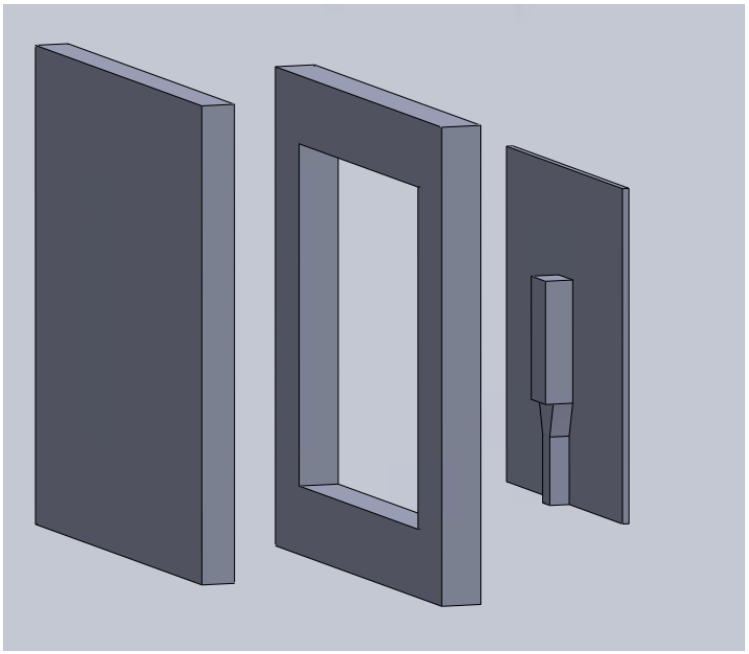

(a) (b) (c)

Figure 3.1: Samples' Solidworks® models for compression moulding. (a) Lower mould. (b) Middle mould with 6 mm thickness. (c) Upper mould with varying thickness.

Different sensor depths were tested in the case of compression moulding, requiring different mould dimensions. For this reason, three upper moulds (see Figure 3.1(c)) were designed with different thicknesses, one for each sensor depth. In addition, these upper moulds have a squared face of 49×49 mm in order to allow the excess of silicone rubber to exit while curing. In the 3DP case, since only one sensor depth was tested, the thickness of each part was defined accordingly.

The moulds for compression moulding were laser cut using a perspex sheet with the appropriate thickness, with the exception of the upper moulds which were 3D printed out of polylactide.

3.1.2 Samples' manufacturing

Prior to the manufacturing of the samples, the silicone rubber had to be prepared accordingly with the manufacturer's specifications.

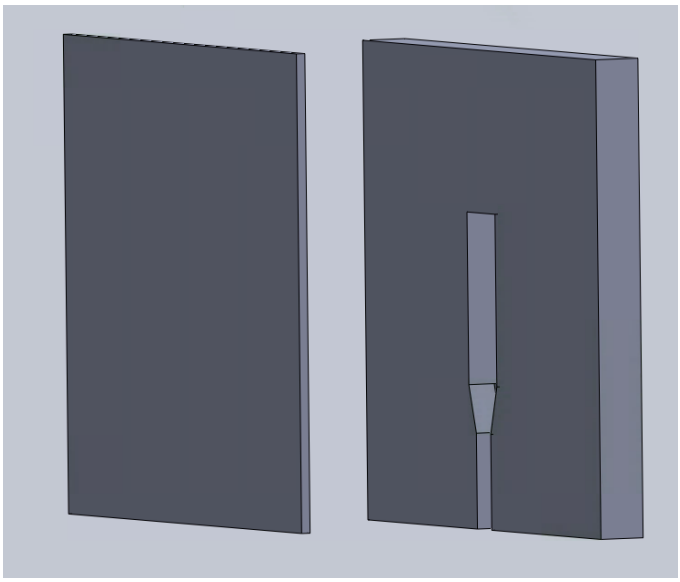

(a) (b)

Figure 3.2: Sample's Solidworks® models for 3DP. (a) Upper part. (b) Lower part.

3.1.2.1 Silicone rubber

Different silicone rubbers were used depending on the manufacturing method.

For compression moulding, one component silicone systems are not desirable due to the lack of air contact, as this would impose additional difficulty and time in the curing process. For this reason, two component silicone systems are preferred. Being so, it was used the addition cure silicone rubber AS40, commercialised by EasyComposites™. Its datasheet can be found in Appendix B. In addition to the traditional and transversal silicone rubber properties, AS40 has very high dimensional accuracy and low shrinkage. This guarantees the accuracy of the dimensions of the samples produced. Therefore, its preparation started by weighting silicone rubber and adding the catalyst on a 10:1 weight ratio. For samples that required CNT loading, SWNT were added after the catalyst. All the components were, then, mixed until obtaining a homogeneous mixture. The mixture was placed inside a degassing chamber at -0.95 bar. This step is highly needed since after mixing, the material is filled with air bubbles which will definitely compromise the mechanical properties of the cured silicone rubber. When in the degassing chamber, the silicone starts by expanding and releasing air bubbles. After a while, it collapses back to its original volume, but it is still releasing air. The process was stopped when no additional air bubbles were observed in a period of 1 minute. This step took around 10 minutes. Having the silicone rubber degassed, it is then ready to be used.

AS40 has a pot life of 30 minutes which, although not being a problem for the compression moulding process, poses a challenge when 3DP. 3DP jobs can take several hours to complete and, therefore, this silicone is not suitable for such a process, since it would require frequent refilling of the printer cartridge. For this reason, one component silicone was used. This type of silicone

systems is compatible with 3DP since the material is dispensed in thin filaments that become in contact with air once printed, thus allowing a rapid and effective curing process. Hence, Forever White commercialised by Everbuild® was used. Its datasheet can be found in Appendix C and no additional preparation was needed.

3.1.2.2 Temperature sensor

The temperature sensors used were LM35CA from Texas Instruments. Already calibrated, with an output voltage linearly-proportional to the centigrade temperature in an operating range between $-40°C$ and $110°C$, this IC temperature device is a good fit for the desired application. Furthermore, it has an accuracy of $\pm 0.24°C$ and low-self heating in still air. The sensor's datasheet can be viewed in Appendix D.

The sensors were soldered on conductive copper wires prior to their embedment. Due to the high electrical conductivity of CNT, an additional coating was required for the sensors used in silicone rubber loaded with this filler.

3.1.2.3 Compression moulding

For the manufacturing of the compression moulded samples, the middle mould (see Figure 3.1(b)) was placed on top of the lower mould (see Figure 3.1(a)). The degassed silicone rubber with 0wt% CNT was then poured into the cavity until fully filled. At last, the upper mould (see Figure 3.1(c)) was placed on top. Due to possible expansion of the silicone rubber when curing, all moulds were kept in place using G-clamps. In Figure 3.3 it is depicted the experimental setting. The silicone rubber was then left to cure for 24 hours, accordingly with the manufacturer's instructions.

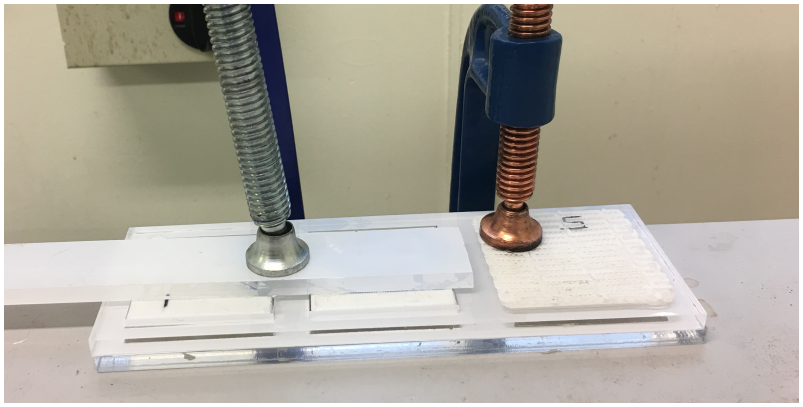

Figure 3.3: Experimental setting for the manufacturing of the compression moulded samples.

When the silicone rubber had fully cured, the upper and lower moulds were removed and an LM35CA was placed into the sample's cavity. Sequentially, silicone rubber – with or without CNT – was poured on top until the cavity of the middle mould was completely filled. The bottom mould was then placed on top, in order to provide a flat surface for the upper samples' face, and held in place with G-clamps. The samples were left to cure for 24 hours once again.

3.1.2.4 3D Printing

EnvisionTEC 3D-Bioplotter®

The 3D-Bioplotter® is a series of AM printers specifically designed to process biomaterials. Its printing process is quite simple. It has a material cartridge filled with the material to be printed. Using air pressure, the material is dispensed selectively through a needle tip from a 3-axis system. The material then solidifies on the printing bed giving rise to the printed object. The 3D printer specifications are presented in Appendix E. Its main features that are of specific interest to this project are: capability of using up to five different materials in the same printing job; the printer is not limited to proprietary materials being the only requirement that the material solidifies; and is capable of printing a strand as thin as 0.100 mm. Furthermore, the printer allows the user to define several parameters for each material, such as temperature, pressure, and speed of the nozzle, which ultimately define the properties of the printed object.

Providing an .STL file, the printer's software splits the model into layers of a designated thickness specified by the user.

For the inner structure of the printed object, three different patterns can be chosen, providing different mechanical stability. These patterns differ in the orientation angles between layers, see Figure 3.4.

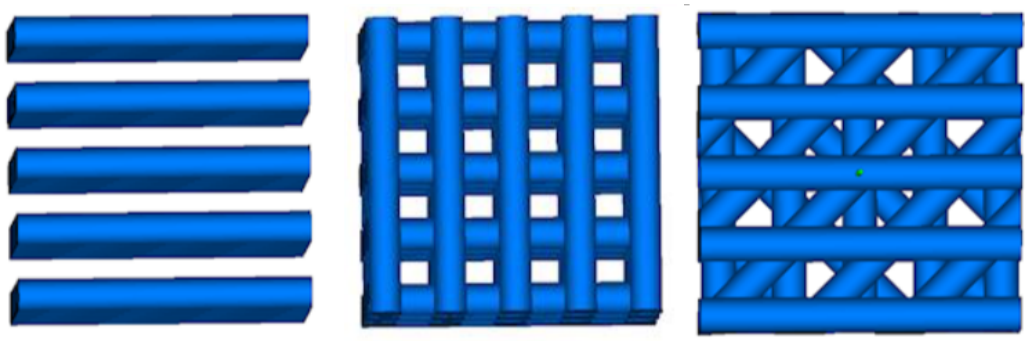

(a) (b) (c)

Figure 3.4: Different inner structures of the printed object. (a) Layers are printed with the same orientation. (b) Layers are printed with an orientation angle of 90º between them. (c) Layers are printed with an orientation angle of 45º between them. Reproduced from [132]

Layers that are printed in the same orientation (see Figure 3.4(a)) have the lowest mechanical stability among the three possibilities, whereas layers that are printed with orientation angles of 45º have the highest. Additionally, the porosity of the inner structure also differs. As it can be easily seen in Figure 3.4, inner structures where the layers are printed in the same direction have higher porosity than the others. Structures with layers at 45º have the lowest porosity.

Manufacturing process

In the sample to be 3D printed, the sensor is at a depth of 1.0 mm. Furthermore, the sensor is at 0.8 mm from the lower face of the sample, and its cavity has a height of 4.2 mm (see Appendix A). To guarantee a better accuracy of the printed object, the lower model (see Figure 3.2(b)) was sliced into 25 layers of 0.2 mm thickness each. To facilitate the printing process and uniformise the printing parameters, the upper model (see Figure 3.2(a)) was also sliced into layers of 0.2 mm, thus into 5 layers.

Prior to the printing of the sample, the 3D-Bioplotter® printing parameters were tuned for the silicone in order to achieve the best printing conditions. In Table 3.2 the final printing parameters are presented.

Table 3.2: Parameters for the 3DP of the samples using EnvisionTEC 3D-Bioplotter®.

Parameter	Value
Pressure	6.0 bar
Needle diameter	0.5 mm
Needle off-set	0.5 mm
Needle speed	5.5 mm/s
Temperature	20°C

The layers were printed with at an orientation angle of 45º between them, resulting in a higher mechanical stability and lower porosity.

The manufacturing of the sample through 3DP was done in three steps. Firstly, the lower model was printed. Secondly, the sensor was placed in its cavity, without removing the printed object from the printing bed. Lastly, the upper model was printed on top of the lower one.

By doing the process sequentially and without removing the lower part from the printing bed upon completion, no possible errors from misplacement of layers by the printer are likely to happen.

3.1.3 Thermal testing

In order to evaluate the effectiveness of using LM35CA embedded in silicone rubber at different depths for a temperature sensing insole, thermal tests were performed.

For this, the data from the sensors was collected using a data acquisition system, NI myDAQ from National Instruments and LabVIEW as the acquisition software. Due to the relatively rapid variation of temperature values, the acquisition rate used was of 10 Hz.

The data was then exported to a .txt file which was, afterwards, used for analysis and processing on MATLAB®.

3.1.3.1 Sensor's self-heating

Although the LM35CA has low self-heating in still air (see Appendix D), this is not guaranteed when the sensor is embedded in silicone rubber. For this reason, a simple experiment was conducted to see if this self-heating had an influence in the temperature measurements when the sensor is embedded in silicone rubber and is meant to be used continuously during several hours.

Being so, sample 2 – the sample in each the sensor is more deeply embedded on both sides – was placed on a table at room temperature and its temperature was recorded during 11 hours. Additionally, room temperature, using a non-embedded LM35CA sensor, was also monitored.

3.1.3.2 Sample's thermal response

To test the thermal response of the samples, both to an increase and a decrease in temperature, a heating plate controlled by a proportional-integral-derivative (PID) controller was used. Figure 3.5 depicts a schematic of the heating plate and PID controller set up as well as a photograph.

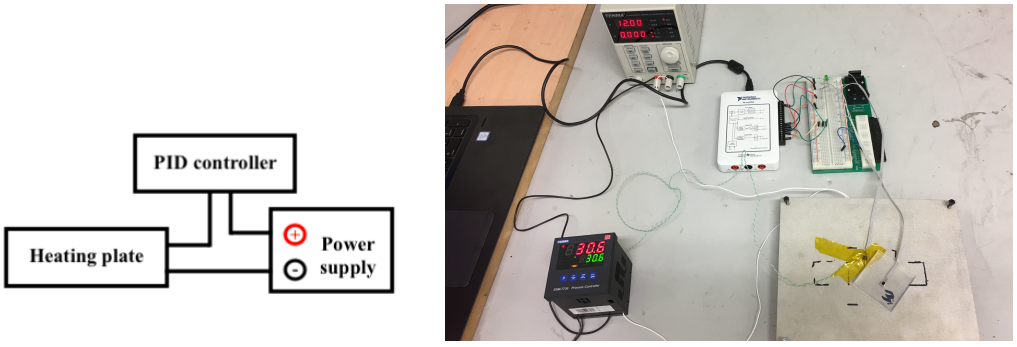

(a) (b)

Figure 3.5: (a) Schematic of the experimental set up of the heating mat and PID controller and (b) corresponding photograph.

The protocol for the heating and cooling experiments is depicted in Figure 3.6.

Both experiments were performed three times for all samples. Additionally, the same experiments were performed using a non-embedded sensor for reference purposes.

3.1.3.3 Thermal analysis

Prior to the analysis of the data obtained from the sensors, the raw values were treated.

Pre-processing

First, the voltage data was converted into temperature values. As stated earlier, LM35CA is already calibrated with voltage output linear to temperature change. From the datasheet (see Appendix D), it can be seen that the output is given by (3.1).

$$V_{out} = 0\ \text{mV} + 10.0\ \text{mV/°C} \tag{3.1}$$

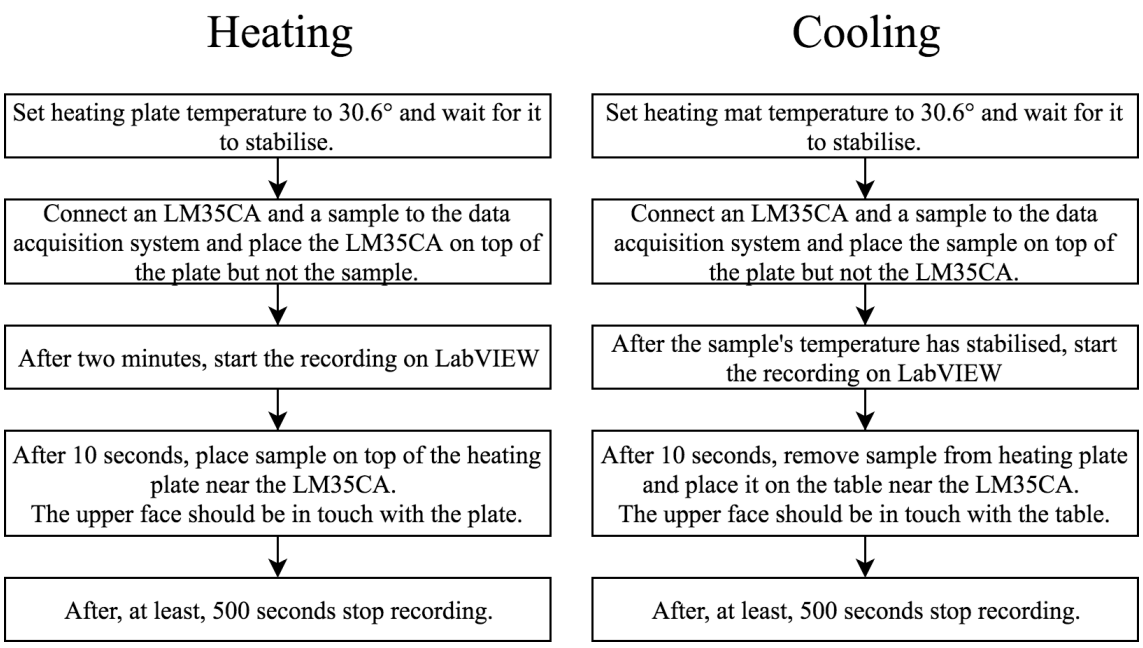

Figure 3.6: Steps for the heating and cooling experiments.

Additionally, the transfer function is given by (3.2).

$$V_{out} = 10 \text{ mV/°C} \times \text{t} \tag{3.2}$$

Secondly, after obtaining temperature values, the data was filtered using a moving average filter in order to smooth the signal and attenuate possible noise, while maintaining its original response. The filter's equation is represented by (3.3), where M is the number of points used, 50, x the raw signal and y the filtered signal.

$$y[i] = \frac{1}{M} \sum_{j=-\frac{\text{M}-1}{2}}^{\frac{\text{M}-1}{2}} x[i+j] \tag{3.3}$$

As can be induced, the first 50 samples of the filtered signal need to be disregarded, as they result from the average using non-existing values from the input signal. Therefore, after the filtering step, the initial 5 seconds of the signal were omitted.

Data analysis

The samples' response to heating and cooling can be seen as a dynamic step-response for a first order system. First-order systems are systems whose input-output relationship is a first order differential equation. This response is depicted in Figure 3.7.

In the heating scenario, the initial steady state can be identified as the initial sample's temperature – ideally equal to room temperature, the dynamic state the heating of the sample and the final

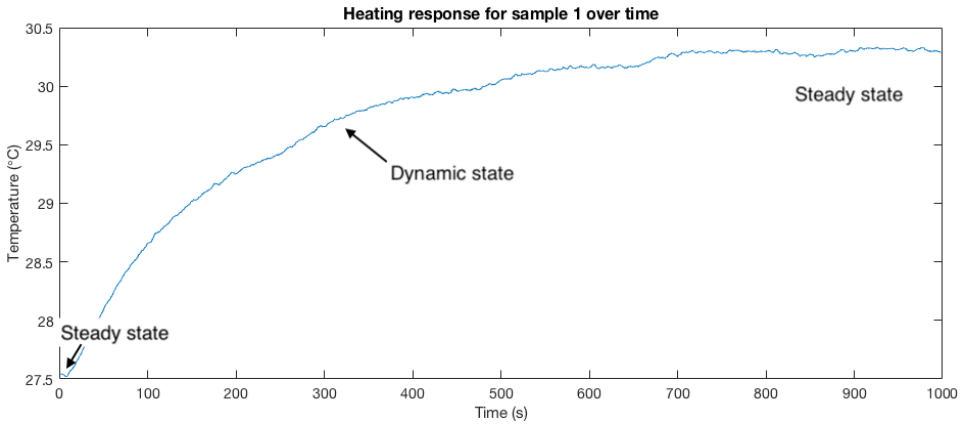

Figure 3.7: Dynamic response to step change. Data from the heating response of sample 1.

steady state the final sample's temperature – ideally equal to the plate's temperature. Being the step function, the sudden increase in temperature.

In a step response of a first order system, the time constant τ is defined as the time taken to reach 63% of total change, as can be seen in equation (3.4)).

$$\Delta y(\theta + \tau) = 0.63\Delta y(\infty) \tag{3.4}$$

θ represents any initial time delay, as for example, the ten initial seconds on the protocol; Δy represents the change at a given period of time, being, therefore, $\Delta y(\infty)$ the total change. A more detailed explanation of this subject is presented in Appendix F.

Furthermore, the system's settling time T_s is defined as the time required for the system's response to remain within a certain percentage of its final value, typically 2% or 5%. This way, if the tolerance band of the system's response is set at 5%, T_s will be the time taken for the system to reach 95% of the total change, corresponding to 3τ (see Table F.1). Since the goal is to maximise the fastness of the sample's thermal response, the system's settling time, T_s, is an excellent performance measure between the different samples. Therefore, this value was computed for each sample, assuming a tolerance band of 5%.

Ergo, for the heating experiment, the sample's temperature during the first 5 seconds was averaged and taken as the initial steady state. The heating plate's temperature was averaged, as well, during for the whole duration of the measurement and taken as the final steady state. Analogously, for the cooling experiment, the sample's temperature during the first 5 seconds was averaged and taken as the initial steady state and room temperature was averaged during the whole duration of the experiment and its value was taken as the final steady temperature. After computing the time taken to reach 63% in total change, the initial time delay, $\theta = 5$ s, was subtracted to finally obtain τ. This was done for each of the three experiments for each sample, and the average and standard deviation of τ computed for each sample. To obtain the settling time, the time constant and standard deviation were then multiplied by three.

3.1.4 Mechanical testing

In addition to the thermal response, the durability of the different samples when used during long walking periods was determined. For this, the samples were submitted to a mechanical test consisting on cyclic compression loadings that simulated gait.

The average diabetic patient walks 6,342 steps a day [133]. Furthermore, the peak plantar pressure among patients with diabetic ulceration is equal to 351.60 ± 92.5 kPa [134], accounting for a maximum pressure of 444.1 kPa.

This way, considering the highest pressure possible, 444.1 kPa, and the application area of the sample, 50 mm $\times$ 50 mm $= 0.0025$ m^2, it is possible to determine the corresponding force to be applied using (3.5),

$$P = \frac{F}{A} \tag{3.5}$$

where P represents the pressure, F the force applied to area A.

Being so, the samples were submitted to cyclic loads of 1,110 Newton at 10 Hz, using an INSTRON® 8501. The number of cycles applied is described in Table 3.3. The situations were performed sequentially on each sample. For this reason, the number of cycles that was in fact applied in each situation had in consideration the number of cycles previously applied.

Table 3.3: Number of cycles in each mechanical test.

Situation no.	Total no. of cycles	No. of cycles applied	Description
1	6,342	6,342	One day of use
2	44,394	38,052	One week of use
3	196,602	152,208	One month of use
4	589,806	393,204	Three months of use
5	1,179,612	589,806	Six months of use

After each situation, the sample was visually examined and the sensor was wired to the data acquisition system to see if it was still working properly. If after this examination, the silicone rubber had been perforated, exposing the sensor, or if the sensor no longer worked, the sample was considered to have reached failure and no more mechanical testing was done in that sample.

The test was performed on samples 1, 2, 3, 4 and 7. The choice of the samples was based on the different parameters among them: sensor depth (samples 1, 2 and 3), CNT loading (sample 1 and 4) and manufacturing method (sample 2 and 7).

3.2 Results and discussion

3.2.1 Sample's manufacturing

In Figure 3.8 the upper face and sideview of samples 1, 4 and 7 are depicted.

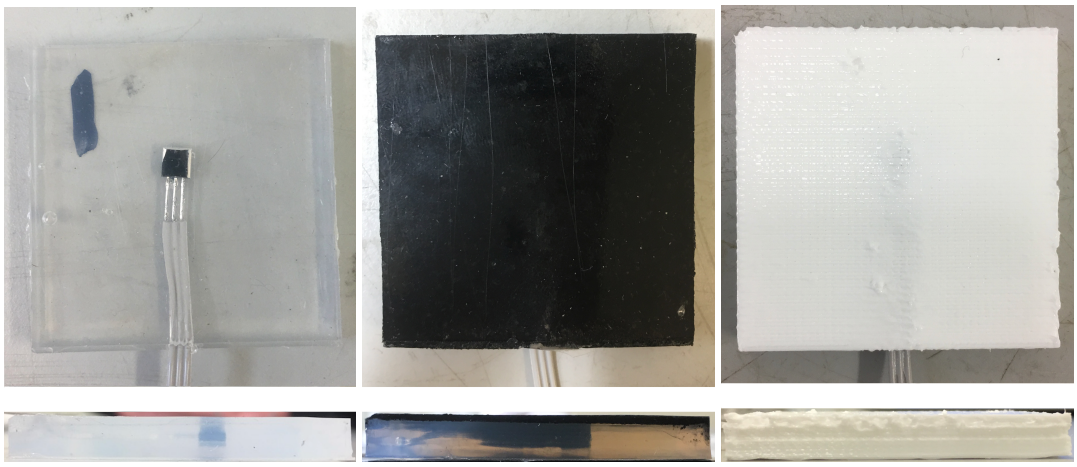

(a) (b) (c)

Figure 3.8: Top and side view of (a) sample 1, (b) sample 4, (c) sample 7.

The samples with the embedded sensors were successfully manufactured. This proves that both methods, compression moulding and 3DP, can be used in the manufacturing of silicone objects with embedded sensors. However, in both methods some problems or additional concerns needed to be taken into consideration in order to successfully manufacture the samples.

When manufacturing through compression moulding, special attention should be paid when pouring the silicone rubber into the moulds, as air bubbles can be easily incorporated into the mixture. This is not desirable and can alter significantly the thermal and mechanical results of the sample.

Additionally, when placing the G-clamps, the pressure level should be the same across all samples. This is very important and crucial since both the perspex sheet and the 3D printed upper moulds will bend under high levels of pressure exerted by the G-clamp. If the upper moulds are bent, that means that the final dimensions of the manufactured sample will not be the desirable ones. Not only that, but the dimensions across samples will be different depending on the G-clamp tightness.

As for during the 3DP process, after placing the sensor, the printing parameters, concerning the needle offset position, may need to be tuned and/or additional layers above the sensor may need to be printed. This has to do with the fact that the sensor, and its connected wires, do not provide a flat surface with constant height throughout. So, after placing the sensor, the needle will not have a single offset position throughout the sample. This led to some difficulties during the beginning of the printing process of the upper layer.

3.2.2 Thermal testing

3.2.2.1 Sensor's self-heating

In Figure 3.9 it is depicted the room temperature and the temperature of sample 2 over time. Additionally, in Figure 3.10, the difference between the sample's temperature and room temperature over time is also shown.

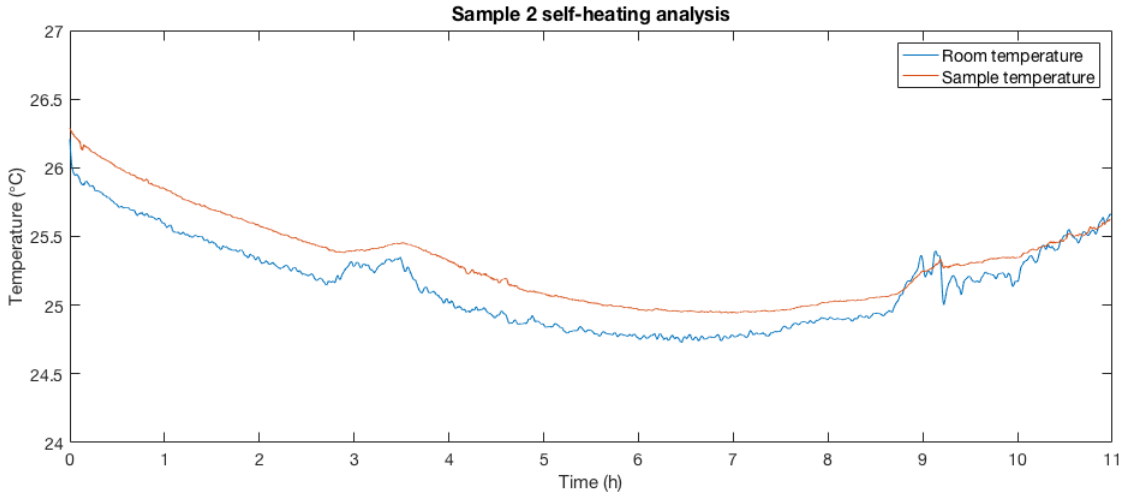

Figure 3.9: Sample 2 temperature over time when left at room temperature.

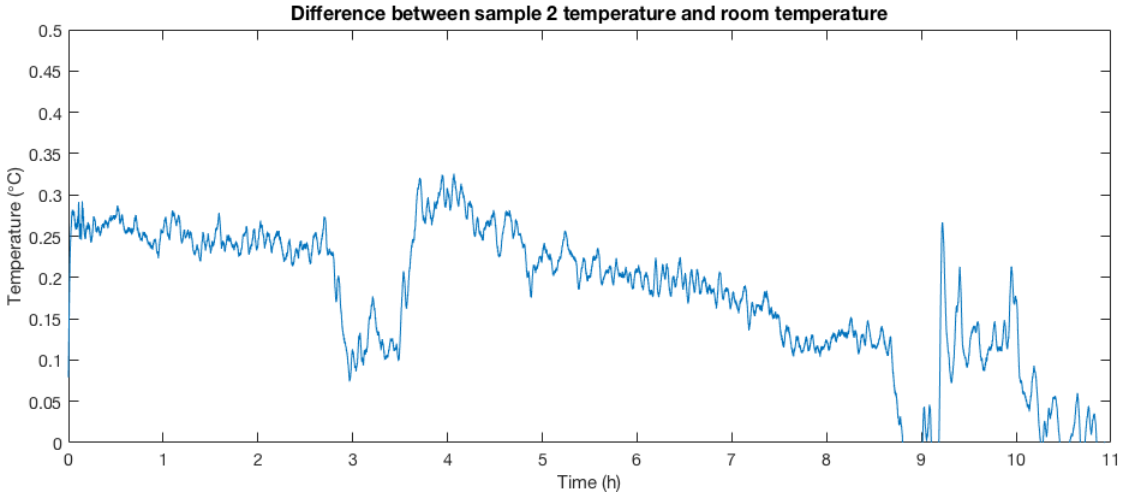

Figure 3.10: Difference between sample's temperature and room temperature over time.

As it can be seen from Figures 3.9 and 3.10, the sample's temperature was around 0.25°C higher than room temperature from the start and throughout most of the measurement time. However, this does not seem to be a result of the sensor's self-heating. The sensor was wired seconds before the measurement started, so no self-heating prior to the experiment is likely to have happened. So, this small initial temperature difference can be attributed to slight variations in temperature around the room.

Additionally, room temperature was not constant throughout the experiment as it can be observed from Figure 3.9 that the sample's temperature followed the same pattern of room temperature. Furthermore, when looking at the difference during the 11 hours of measurement, the difference does not increase with time.

Being so, it can be concluded that the sensor's self-heating does not influence the temperature measurements when the sensor is embedded in silicone rubber.

On another note, the peaks and irregularities in Figure 3.10 between hour 9 and 10 come from sharp variations in room temperature. In fact, these fluctuations have little to no impact in the sample's temperature, giving rise to those peaks in the temperature difference. This means that the insole will not be affected by sharp, and possibly insignificant, temperature variations only responding to lasting and longer, and probably meaningful, temperature changes.

3.2.2.2 Samples' thermal response

In Figure 3.11 it is depicted the average of the thermal responses of all seven samples when submitted to the heating experiment. As it can be seen, the samples' responses can be considered as a step-response for a first order system.

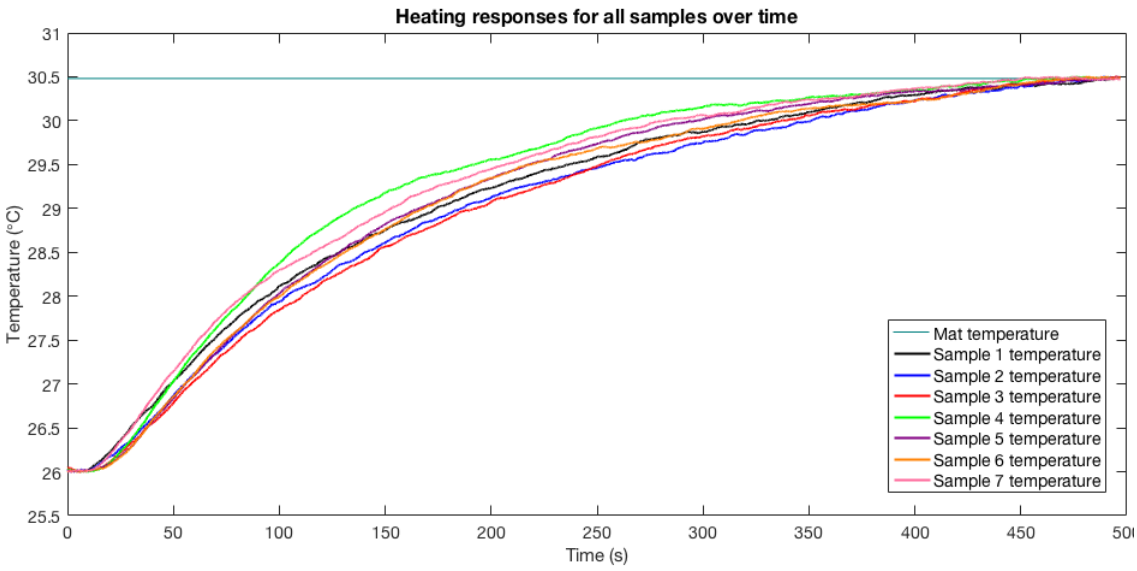

Figure 3.11: Heating response over time for all samples.

Additionally, in Table 3.4 the average time taken for the samples to reach 95% of its final temperature and standard deviation for the heating and cooling experiments is shown. The increase in percentage between heating and cooling times is also shown. The same information for the non-embedded sensor was added as sample 0.

Sensor depth optimisation

Looking at the heating values for samples 1, 2 and 3, it is easily observed that the deeper the sensor within the silicone rubber, the longer it takes for its temperature to settle, as expected. However,

Table 3.4: Average time taken to reach 95% of total change, 3τ, and standard deviation for all samples for both experiments, and the increase in percentage between heating and cooling times.

	Heating	Cooling	
Sample no.	3τ (s)	3τ (s)	Variation (%)
0	44.7 ± 1.3	74.2 ± 8.8	65.9
1	298.9 ± 8.5	358.5 ± 86.1	19.9
2	388.0 ± 58.0	493.9 ± 19.7	27.1
3	446.2 ± 75.2	438.9 ± 26.9	-1.6
4	258.1 ± 18.3	488.7 ± 14.4	89.3
5	311.3 ± 29.1	540.77 ± 47.0	73.7
6	322.6 ± 30.8	495.8 ± 34.1	53.7
7	293.1 ± 25.8	315.9 ± 10.9	7.8

it seems that the relationship between the time it takes to reach 95% of its total change and the sensor depth is not linear.

In Figure 3.12 it is plotted the sensor depth versus 3τ for the heating experiment for samples 1,2 and 3. As it can be seen, as the sensor depth increases, the increase in the time taken to reach 95% of total change is smaller. In fact, when moving from 0.5 to 1.0 mm, it took 89.1 seconds more corresponding to an increase of 30.0% in 3τ. However, when going from 1.0 to 1.5 mm, it only took 58.2 seconds more, corresponding to a smaller increase of 14.8%, which is significantly lower.

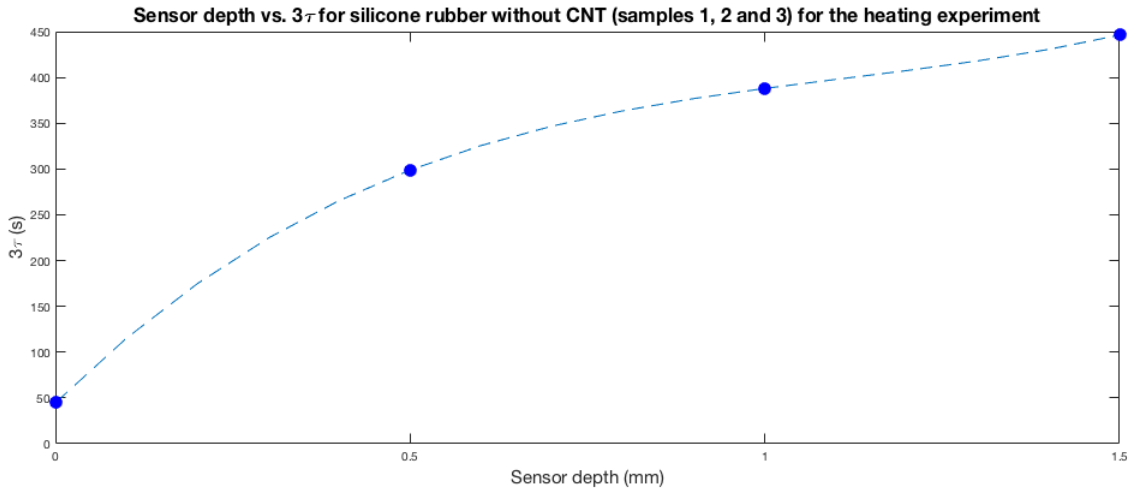

Figure 3.12: Sensor depth *vs.* 3τ for samples 1, 2 and 3 for the heating experiment.

This way, the depth of the sensor is not linearly related to the speed of the thermal response.

Looking at the values from the cooling experiment, it is clearly visible that the cooling of the samples takes longer than the heating, except for sample 3. This goes as expected since for the non-embedded sensor a similar behaviour was observed (sample 0).

However, the difference between the heating and the cooling times is significantly lower for the samples than for the non-embedded sensor. A non-embedded sensor takes 65.9% longer to cool than to heat. However, sample 1 only takes 19.9% more and sample 2 27.1%. This suggests that embedding the sensor in small amounts of silicone rubber helps to normalise its behaviour between heating and cooling conditions. Higher amounts of silicone rubber, however, seem to lead to higher differences in the sample's behaviour between the two conditions.

Sample 3 took longer to heat than to cool, unlike the rest of the samples because the sensor was at a distance of only 0.3 mm from the bottom side. Contrary to the heating experiment, where the heat is being transferred from the heating mat to the sample through one of the sample's faces; in the cooling experiment, the heat is being transferred from the sample to the environment. Therefore, heat is being transferred from all the sample's surfaces and not only from the face that is meant to be in contact with the skin. For this reason, sample 3 took longer to heat than to cool, because the sensor is at a distance of only 0.3 mm from the bottom face but at a distance of 1.5 mm from the heat source.

Comparing the cooling times between the samples, sample 2 was the one which took longer to cool. This comes from the fact that samples 1 and 3 have the sensors closer to one of the faces of the sample. Sample 1 has the sensor at 0.5 mm from its upper face and in sample 3 the sensor is only 0.3 mm away from the lower face. However, in sample 2, the sensor is 0.8 mm from the lower face and 1.0 mm from the upper one. This way, by having the sensor farther away from any of the sample's surfaces, sample 2 will take longer to notice a decrease in temperature.

Analogously, looking at samples 1 and 3, one would expect that sample 3 would cool faster than sample 1 since the sensor is closer to one of the sample's faces. However, the samples were placed on the table with the surface meant to be in contact with the skin down. So, the heat dissipation was happening mainly through the thicker side for sample 3 and the thinner for sample 1. This way, despite the fact that sample 3 has the sensor closer to one of the faces, sample 1 cooled down faster.

Carbon nanotube loading optimisation

In Table 3.5 the values of 3τ for samples 1 to 3 and 4 to 6 are presented for the heating experiment, as well as their corresponding variation when adding CNT to the silicone rubber.

It can be seen that adding CNT does indeed increase silicone rubber's thermal conductivity, since the values of 3τ for samples 4, 5 and 6 are significantly lower when comparing to samples 1, 2 and 3, respectively. Furthermore, it seems that the deeper the sensor is, the more significant the change is, since the variation in modulus increased with sensor depth.

Additionally, sample 5 and sample 6 have very similar values of 3τ, despite the difference in sensor depth. This suggests that when embedding the temperature sensor in silicone rubber with CNT loading, the depth of the sensor does not play an important role in the thermal response,

Table 3.5: Values of 3τ for the heating experiment for samples 1 to 3 and 4 to 6, and corresponding variation.

Sample no.	3τ (s)	Sample no.	3τ (s)	Variation (%)
1	298.9 ± 8.5	4	258.1 ± 18.3	-13.6
2	388.0 ± 58.0	5	311.3 ± 29.1	-20.0
3	446.2 ± 75.2	6	322.6 ± 30.8	-27.7

as sample 6 only took 11.3 seconds more than sample 5. This reiterates the observation that the deeper the sensor is, the stronger the impact of CNT loading.

In Table 3.6 the same information is presented but for the cooling experiment.

Table 3.6: Values of 3τ for the cooling experiment for samples 1 to 3 and 4 to 6, and corresponding increase.

Sample no.	3τ (s)	Sample no.	3τ (s)	Variation (%)
1	358.5 ± 86.1	4	488.7 ± 14.4	36.3
2	493.9 ± 19.7	5	540.77 ± 47.0	9.4
3	438.9 ± 26.9	6	495.8 ± 34.1	13.0

As opposed to the heating values, adding CNT to the silicone rubber diminishes its sensibility to a decrease in temperature, as 3τ increased significantly. However, the same trend was observed with sample 5 taking longer then the others and sample 4 being the fastest one.

Manufacturing method

With the purpose of comparing both manufacturing methods, compression moulding and 3DP, in Table 3.7 it is presented the values of 3τ for the heating and cooling experiments for samples 2 and 7 and the decrease in 3τ when 3D printing the sample instead of compression moulding it.

Table 3.7: 3τ values for samples 2 and 7 for the heating and cooling experiments and the corresponding decrease in percentage.

	Heating	Cooling
Sample no.	3τ (s)	3τ (s)
2	373.6 ± 75.3	478.9 ± 19.7
7	293.1 ± 25.8	315.9 ± 10.9
Variation (%)	-24.6	-36.0

As it can be seen, sample 7 has a much faster heating response than sample 2 taking 80.5 seconds less to reach the same change in temperature. This can be attributed to the different inner structure of the samples.

Sample 2 has a much more compact structure than sample 7. The inner structure of sample 7 is composed of several layers of filaments placed at an orientation of 45º between them. Being so, this structure is less compact and more porous than the structure obtained through compression moulding. Overall, this facilitates the heat transfer from the heating plate to the sensor, since it allows other heating transfer mechanisms, such as convection, leading to an earlier change in the sensor's output.

Similarly to the other samples, the cooling of the 3D printed sample also takes longer than the heating. However, the difference in the 3D printed sample is much lower when compared to sample 2. In sample 2, the cooling took an additional 105.9 seconds, which is to say 27.1% longer, whereas in sample 7 it only took 22.8 seconds more, 7.8%. Once again, the inner structure of the sample is the most likely cause of this difference.

3.2.3 Mechanical response

3.2.3.1 Sensor depth optimisation

The results from the mechanical loading for samples 1 through 3 are presented in Table 3.8.

Table 3.8: Results from mechanical loading for samples 1 through 3.

Samples no.	Time to reach failure
1	Failure after 1 month.
2	Did not fail after 6 months
3	Failure after 3 months

As it can be seen, if the sensor is only at 0.5 mm from the surface, the silicone will perforate and expose the sensor to the patient's foot after one month of use. In Figure 3.13 the exposed sensor can be seen.

Similarly, when embedding the sensor at 1.5 mm, because the full thickness is 6 mm, the sample is 0.3 mm apart from the ground. After three months of use, although it is not exposing the sensor to the patient's foot, the sensor will be exposed to the lower part of the shoe, which also compromises the efficacy of the developed system.

When placing the sensor at 1.0 mm from the patient's foot, the durability of the system is increased significantly not failing after 6 months of use. In fact, although the distance was only doubled, from 0.5 to 1.0 mm, the durability of the sample was increased by at least 6 times. This suggests that the relationship between the sensor's distance to the foot and the degradation of the sample is not linear.

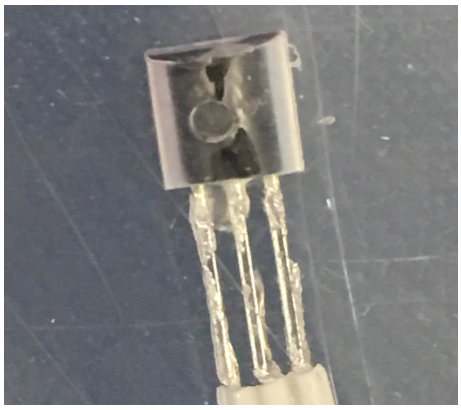

Figure 3.13: Small fissure in the silicone rubber after 1 month of use, when the sensor is at a depth of 0.5 mm.

The cause of failure in every situation was the wear of silicone rubber and not the sensor's malfunctioning. This further supports that the sensor is suitable for this use.

3.2.3.2 Carbon nanotubes loading optimisation

The results for the mechanical testing for samples 1 and 4 are presented in Table 3.9. Both samples have the sensor at 0.5 mm, but sample 4 has silicone rubber with CNT loading on top of the sensor.

Table 3.9: Results from mechanical loading for samples 1 and 4.

Samples no.	Time to reach failure
1	Failure after 1 month
4	Did not fail after 6 months

It can be easily seen that adding CNTs, with at least 2.96 wt% can be beneficial in terms of silicone rubber's resistance to wear. In fact, the durability of the sample increased at least 6 times, not having experienced any deterioration after 6 months of use, as opposed to exposing the sensor after 1 month of use.

3.2.3.3 Manufacturing method

The results for the mechanical testing for samples 2 and 7 are presented in Table 3.10. Both samples have the sensor at 1.0 mm of depth, but sample 7 was manufactured through 3DP, whereas sample 2 was obtained through compression moulding.

Figure 3.14 depicts sample 7 after 3 months of use. As it can be seen, after 3 months of use, although the sensor is not necessarily exposed (see Figure 3.14(a)), when bending the sample, a little fissure can be seen (see Figure 3.14(b)). So, although the sample is not exposing the sensor

Table 3.10: Results from mechanical loading for samples 2 and 7.

Samples no.	Time to reach failure
2	Did not fail after 6 months
7	Failure after 3 months

to the patient's foot after 3 months of use, this suggests the sensor will be exposed shortly after that, not making it to 6 months.

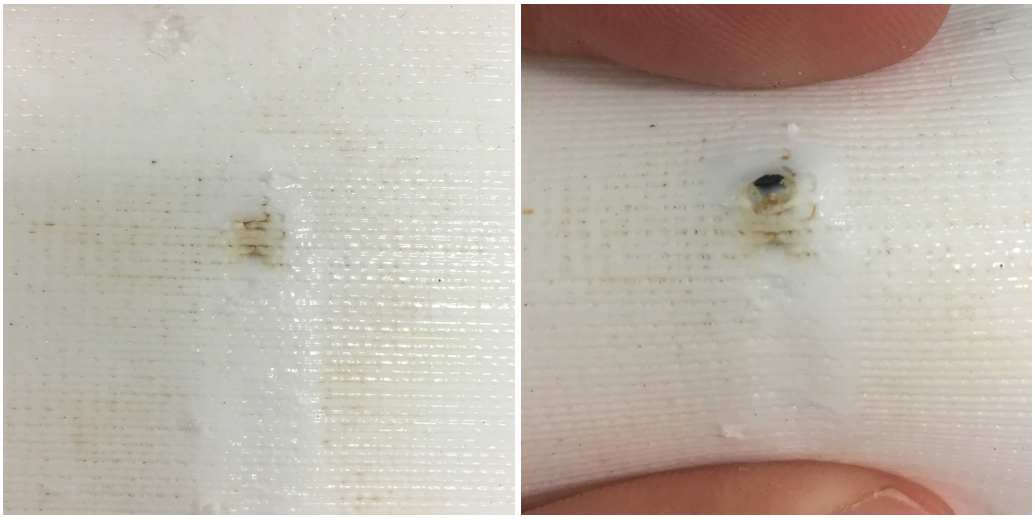

(a) (b)

Figure 3.14: Sample 7 after 3 months of use (a) when flat (b) when bent.

The earlier deterioration of the 3D printed sample in comparison to the compression moulded one is expected since they have different mechanical structures. The compression moulded sample has a mechanical structure much more compact and dense than the 3D printed one. This is inherent in the manufacturing method and reflects on the mechanical properties of the object.

3.2.4 Conclusions

When optimising the sensor depth and CNT loading, the results from both the thermal and mechanical tests need to be considered.

An obvious observation is that the shallower the sensor is within the silicone rubber, the fastest the thermal response will be, either in an increase or decrease of temperature. However, so is the deterioration of the material. In fact, for an insole of 6 mm, the only compatible sensor depth for an LM35CA is of 1.0 mm from the upper surface, since the sensor is at a good distance from both sides capable of withstanding walking loadings of up to 6 months.

Adding SWNT to silicone rubber proved to enhance both the thermal response and the mechanical resistance to wear. In fact, no negative impacts were observed when adding CNT. However, silicone rubber filled with CNT was shown to be more rigid than plain silicone rubber. For this reason, the amount of CNT should not be very high as it will possibly carry negative aspects from a mechanical standpoint. A loading of 2.96wt% should not pose a problem.

At last, 3DP proved to be a suitable manufacturing method for this purpose. Despite its good results in the thermal response, the 3D printed object showed poorer mechanical resistance, withstanding only 3 months of walking use. This unsatisfactory result can be solved by printing silicone rubber filled with CNT.

Chapter 4

Temperature sensing insole

Having the optimum sensor depth and amount of CNT, a custom made temperature sensing insole was designed and 3D printed.

4.1 Methods

4.1.1 Pressure distribution readings

Since it is well known that high pressure areas are associated with ulceration, it is these areas that are of utmost importance to monitor. Therefore, the pressure readings of an individual using the Tekscan HR Mat™.

4.1.1.1 Tekscan HR Mat™

The HR Mat™ consists on a low-profile foot pressure measurement platform that can be used in a variety of situations such as foot function analysis, pressure offloading of the neuropathic foot or even identifying areas of potential ulceration. The mat contains 8448 sensing elements on a matrix of 88 × 96, which resistance is higher when no pressure is being applied on them. The platform is capable of capturing static as well as dynamic pressure data. In Appendix G the mat's specifications are presented.

The pressure mat comes with its own software, FootMat™, for data acquisition and processing.

4.1.1.2 Acquiring pressure distribution readings

The pressure readings were taken in four different situations. These are described in Table 4.1. In the four different situations, the subject was wearing socks and the recording lasted 8 seconds. In addition to the pressure readings, the length of the individual feet was also measured.

After having the pressure readings, an intrinsic feature of the FootMat™ software was used to interpolate the average data during the 8 seconds of measurement time. The software, then, exported as output the pressure map for each foot.

Table 4.1: Situations for acquiring pressure readings using Tekscan HR Mat®.

Situation no.	Description
1	Standing still on both legs
2	Standing still on left leg, while holding a handrail for balance
3	Standing still on right leg, while holding a handrail for balance
4	Rocking back and forward on both legs, without lifting any part of the feet off the mat

Note: In the four situations, the individual was wearing socks and the pressure recorded for 8 seconds.

4.1.2 Insole design

The design of the insole was heavily based on the results from the previous optimisation of both sensor depth and CNT loading.

Having the pressure map from the FootMat™ software, the image was imported to SolidWorks® where an insole was designed. Given, the length of the footprint, the dimensions of the insole were adjusted automatically by the software.

Four temperature sensors were placed at 1.0 mm of depth under the areas of higher pressure, with silicone rubber loaded with CNT on top.

The design of the insole took into consideration the requirements of an insole to be used for diabetic patients. Therefore, the insole was designed to have a flat surface and a thickness of 6 mm.

In Figure 4.1 the insole SolidWorks® model is depicted. Full dimensions can be consulted in Appendix H.

4.1.3 Insole manufacturing

The insole was manufactured through 3DP using the EnvisionTEC 3D-Bioplotter®. The model was sliced into layers of 0.2 mm in thickness, giving rise to 25 layers for the lower part (see Figure 4.1(c)), and 5 for the upper parts (see Figure 4.1(a) and 4.1(b)).

The printing parameters used were the same of Table 3.2.

4.1.4 Insole testing

To test the efficacy of the insole developed, the four sensors were wired to an Arduino Uno and their data recorded during the situations listed in Table 4.2.

The insole was placed inside the shoe and the user was using a sock, so there was a layer of fabric between the skin and the insole. Prior to testing, the user was asked to sit still 5 minutes for the temperature of the insole to stabilise.

The same pre-processing described in section 3.1.3.3 was applied before analysing the data.

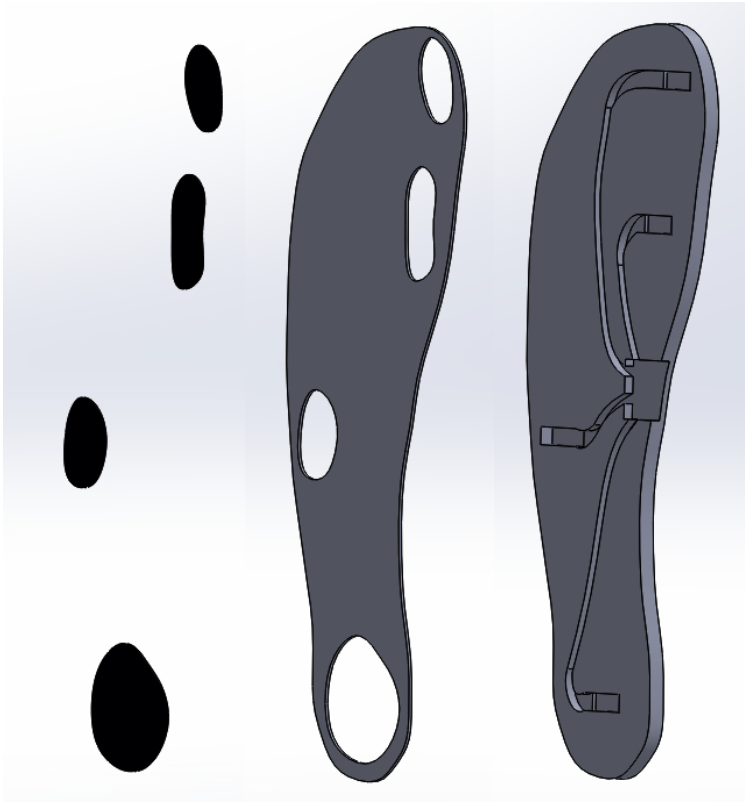

(a) (b) (c)

Figure 4.1: Insole Solidworks® model for 3DP. (a) Silicone rubber loaded with CNT layers. (b) Upper layers. (c) Lower layers.

Table 4.2: Situations for insole testing.

Situation no.	Description
1	Sit still for 5 minutes
2	Walk 100 steps
3	Run 70 meters

4.2 Results and discussion

4.2.1 Pressure distribution readings

Figures 4.2, 4.3(a), 4.3(b) and 4.4 depict the pressure maps obtained for situations 1, 2, 3 and 4 from Table 4.1. Colder colours, such as blue, mean lower pressure values, whereas, warmer colours, such as red, mean higher values of pressure.

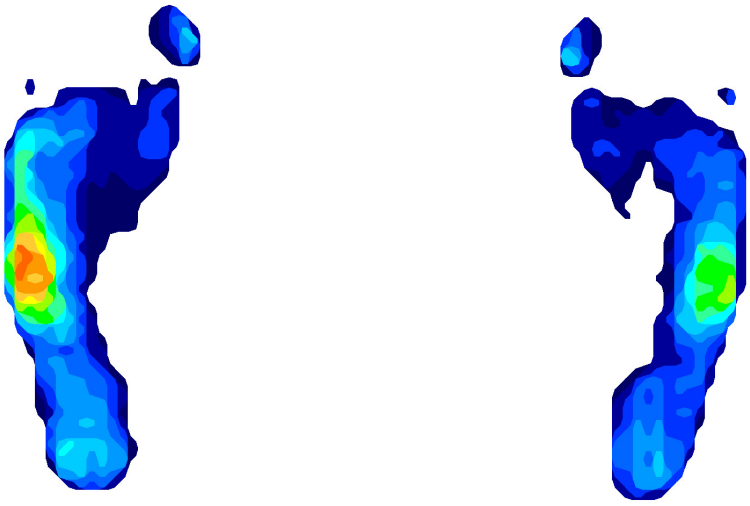

Figure 4.2: Pressure distribution obtained for situation 1 using FootMat™.

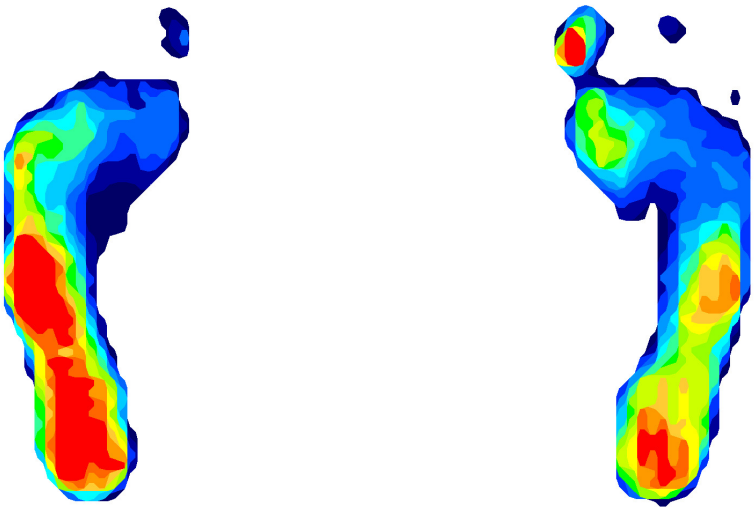

(a) (b)

Figure 4.3: (a) Pressure distribution obtained for situation 2 using FootMat™. (b) Pressure distribution obtained for situation 3 using FootMat™.

As it can be seen, the pressure readings obtained for situation 1, 2 and 3 did not cover the whole foot. Therefore, the pressure readings were not very satisfactory. In situation 1, only one

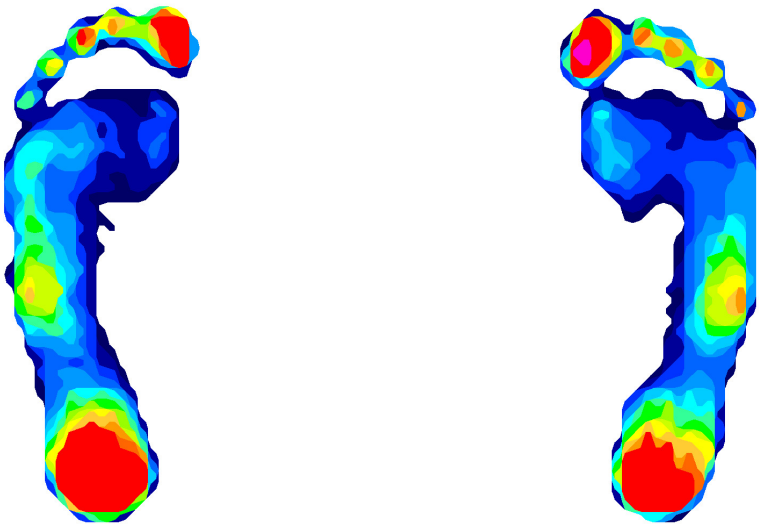

Figure 4.4: Pressure map obtained from interpolation using FootMat™.

high-pressure spot was found, in the arch of the feet (see Figure 4.2). In situation 2, a very large high-pressure spot covering half the sole of the foot was detected (see Figure 4.3(a)).

Being so, the only situation that provided satisfactory results for both feet was the fourth one. Consequently, this was the situation in which the design of the insole was based on.

4.2.2 Insole manufacturing

In Figure 4.5 a picture of the printed insole can be seen.

As it can be observed on the upper face of the insole, there is no silicone rubber filled with CNT. This is due to the fact that 3DP silicone rubber filled with CNT was not successfully achieved.

The printing of silicone rubber with CNT started by using the same printing parameters used for regular silicone rubber. However, the needle was constantly clogging needing to be replaced in order to continue to the printing job. After several testing and tuning of the printing parameters needle speed and pressure, no optimum combination was found that led to a faultless printing. This has to do with the fact that silicone rubber filled with CNT is much thicker than plain silicone rubber. Thus, it is harder to work with.

Much lower concentrations of CNT, such as 0.25wt% for example, might have solved this issue. However, this is not desirable as such lower values of CNT loading will not produce much better results when compared to plain silicone rubber, and, therefore, they are not worth the extra costs.

4.2.3 Insole testing

The data obtained for situations 1, 2 and 3 are plotted in Figures 4.6, 4.7, 4.8, respectively (see Table 4.2).

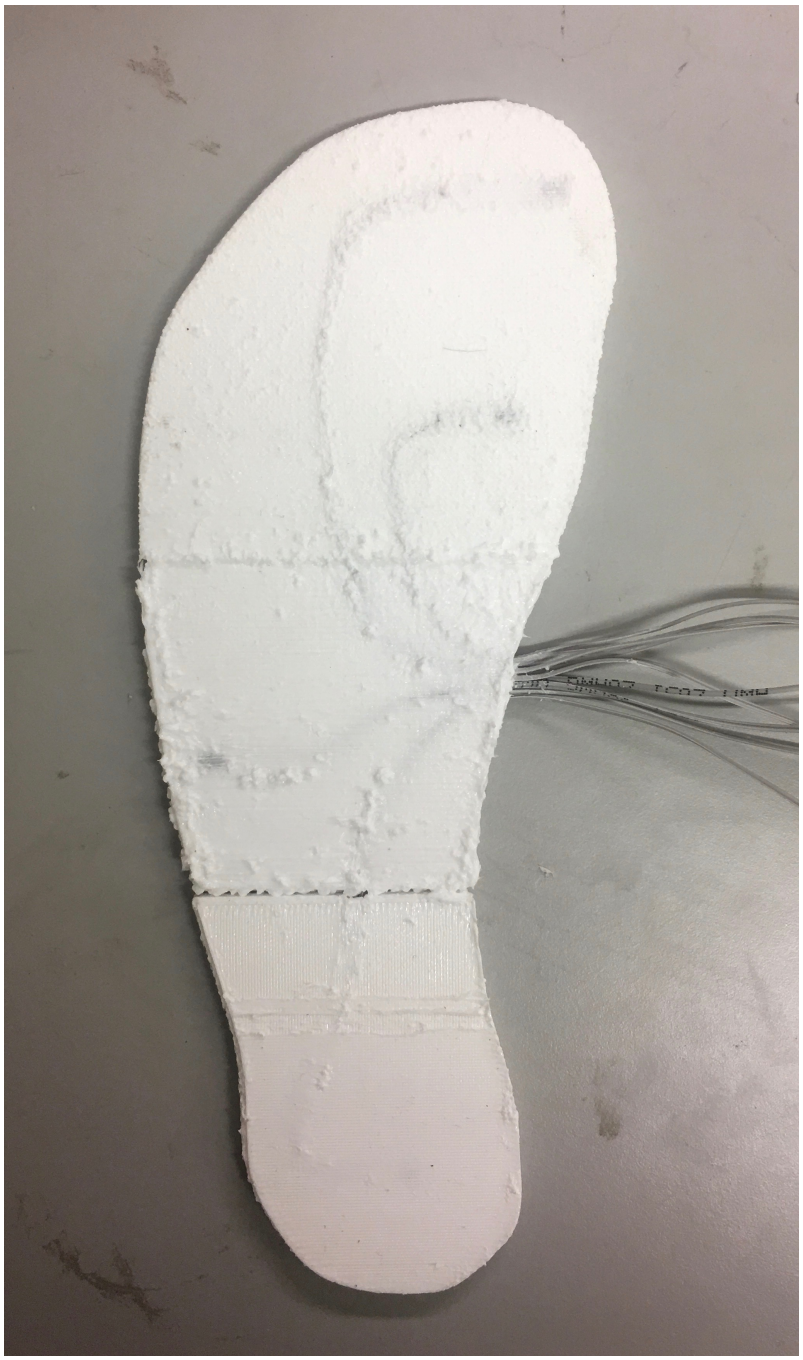

Figure 4.5: 3D printed insole.

As it can be seen, the temperature measured was not the same across the foot. In fact, the difference between the warmer region, the hallux, and the cooler region, the heel, was of 2°C. However, this is not an indicator of poor performance from the insole, as it is known that temperature is not constant across anatomical regions.

When looking at the values obtained from situations 2 (Figure 4.7) and 3 (Figure 4.8), one can say that the insole measured accurately under dynamic situations, since no sharp variations in

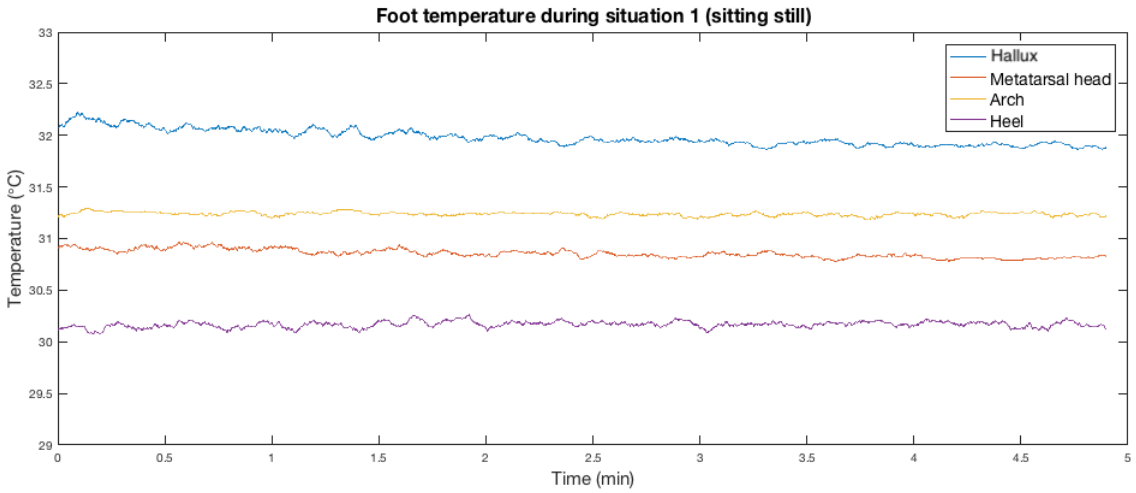

Figure 4.6: Foot temperature *vs.* time when sitting still.

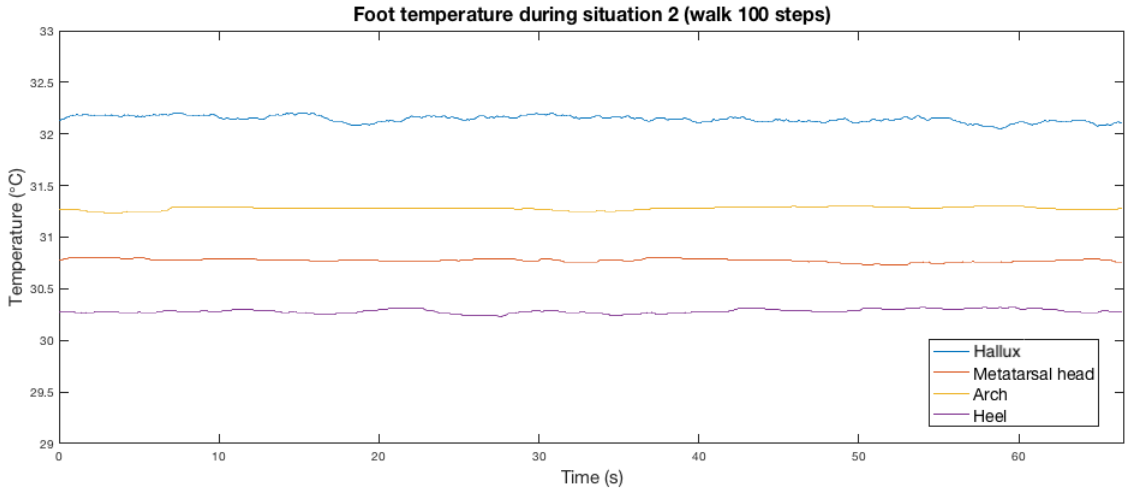

Figure 4.7: Foot temperature *vs.* time when walking.

temperature were observed.

Even though the insole was not placed directly under the foot, having a sock in between, no errors were found from possible foot liftoffs from the insole. This has to do with the fact that the shoe was tight enough so that no extra space above the foot was left. Although not being uncomfortable for the user, which was non-diabetic, for diabetic patients this might pose an extra risk of ulceration on the dorsal region of the foot. Therefore, the insole of the shoe should be replaced by the developed one, in order to leave extra upper space. Furthermore, in order to prevent erroneous measurements, the insole should be placed in direct contact with the sole of the feet as shown in Figure 2.9.

It is known that foot temperature of diabetic patients increases sharply with a few steps. Since the user does not have diabetes, this sharp increase was not observed (see Figure 4.7). However, when running, the insole was capable of detecting an increase in the arch towards the end of the experiment (see Figure 4.8).

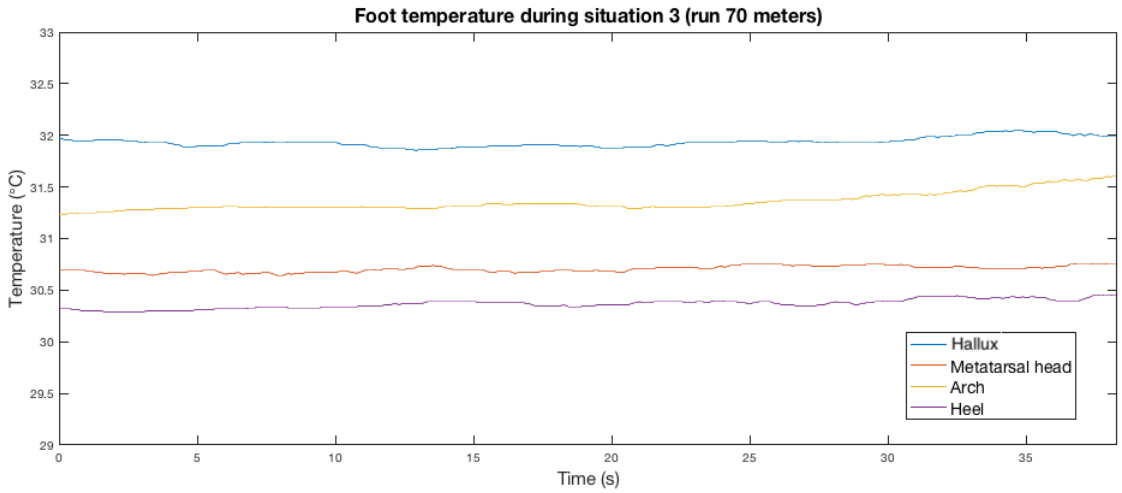

Figure 4.8: Foot temperature *vs.* time when running.

Being so, the developed insole was proven to be able to measure the foot temperature in both static and dynamic situations. Furthermore, it was able to detect fast temperature changes as a result of physical activity.

Chapter 5

Conclusions and future work

The development of a customised 3D printed insole with embedded temperature sensors was successfully achieved. Thus, the insole should be able to predict and, therefore prevent, diabetic foot ulceration, provided that it is accompanied by an adequate algorithm to analyse the acquired data. The developed insole was able to give good temperature readings in both static and dynamic situations, enabling the continuous monitoring of the foot temperature.

Silicone rubber was proven to be a suitable material for the intended object, being capable of withstanding at least 6 months of continuous use without damage. Furthermore, given a thickness of 6 mm for the insole suitable for diabetic patients, an LM35CA should be at a depth of 1.0 mm in order to optimise the durability of the insole.

Adding CNTs to silicone rubber was proven to, not only increase its thermal conductivity, but also its resistance to wear upon cyclic loadings. This largely increases the usability of the silicone rubber as it will allow for faster thermal responses and a higher longevity of the device.

3DP proved to be a suitable manufacturing method for the intended device despite the lower mechanical properties achieved. 3DP allows faster thermal responses than compression moulding and provided that it is possible to print silicone rubber filled with an adequate amount of CNTs, the lower mechanical properties should be solved.

Despite the promising results achieved, future work needs to be done in order to elevate the quality of the developed system.

Firstly, further investigation in the 3DP of silicone rubber filled with CNTs should be made. This will allow a faster thermal response as well as enhanced mechanical properties. By using larger needles, one can expect that such a problem will be overcome.

Secondly, investigating the printing of the actual sensor should also be prioritised. By actually printing the sensor, instead of embedding it, one can further automate the whole process. In addition, the overall design of the insole can also be changed as it will allow for thinner insoles, eliminating the need to replace the shoe's insole by the developed device.

Thirdly, as with 3DP one can manufacture a wide range of geometries, innovation on the insole design should also be addressed. Whether to make it as thin as possible or to create a temperature

sensing orthosis capable of diminishing plantar pressures, one should take this great advantage of 3DP as further as possible.

Bibliography

[1] K. Pointer, "What is glucose and what does it do?" 2017, available at https://www.healthline.com/health/glucose#how-glucose-works. Last checked 2018-09-09.

[2] P. V. Röder, B. Wu, Y. Liu, and W. Han, "Pancreatic regulation of glucose homeostasis," *Experimental & molecular medicine*, vol. 48, no. 3, pp. 219–237, 2016.

[3] S. L. Aronoff, K. Berkowitz, B. Shreiner, and L. Want, "Glucose metabolism and regulation: beyond insulin and glucagon," *Diabetes Spectrum*, vol. 17, no. 3, pp. 183–190, 2004.

[4] Diabetes.co.uk, "Type 1 diabetes," 2018, available at https://www.diabetes.co.uk/type1-diabetes.html. Last checked 2018-09-09.

[5] Diabetes.co.uk, "Type 2 diabetes," 2018, available at https://www.diabetes.co.uk/type2-diabetes.html. Last checked 2018-09-09.

[6] Diabetes.co.uk, "Differences between type 1 and type 2," 2018, available at https://www.diabetes.co.uk/difference-between-type1-and-type2-diabetes.html. Last checked 2018-09-09.

[7] G. Roglic, *Global report on diabetes*. Geneva, Switzerland: World Health Organization, 2016.

[8] I. D. Federation, *IDF Diabetes Atlas*, 8th ed. Brussels, Belgium: International Diabetes Federation, 2017.

[9] Diabetes UK, "Facts and stats," 2016, available at https://diabetes-resources-production.s3-eu-west-1.amazonaws.com/diabetes-storage/migration/pdf/DiabetesUK_Facts_Stats_Oct16.pdf. Last checked 2018-09-09.

[10] Diabetes.co.uk, "How many people have diabetes - diabetes prevalence numbers," 2016, available at https://www.diabetes.co.uk/diabetes-prevalence.html. Last checked 2018-09-09.

[11] H. Q. I. Partnership, "National diabetes audit complications and mortality 2015-2016," 2017.

[12] S. P. de Diabetologia, *Diabetes: Factos e Números – O Ano de 2015 – Relatório Anual do Observatório Nacional da Diabetes*. Observatório da Diabetes, 2016.

[13] S. P. de Diabetologia, *Diabetes: Factos e Números – O Ano de 2009 – Relatório Anual do Observatório Nacional da Diabetes*. Observatório da Diabetes, 2010.

[14] Diabetes.co.uk, "How to avoid diabetic complications," 2017, available at https://www.diabetes.co.uk/how-to/avoid-diabetes-complications.html. Last checked 2018-09-09.

[15] A. D. Association, "Diabetes complications," 2018, available at http://www.diabetes.org/living-with-diabetes/complications/?. Last checked 2018-09-09.

[16] N. Katsilambros, E. Dounis, K. Makrilakis, N. Tentolouris, and P. Tsapogas, *Atlas of the diabetic foot*. John Wiley & Sons, 2010.

[17] H. M. Rathur and A. J. Boulton, "The neuropathic diabetic foot," *Clinics in dermatology*, vol. 25, no. 1, pp. 109–120, 2007.

[18] M. Ndosi, A. Wright-Hughes, S. Brown, M. Backhouse, B. A. Lipsky, M. Bhogal, C. Reynolds, P. Vowden, E. Jude, J. Nixon *et al.*, "Prognosis of the infected diabetic foot ulcer: a 12-month prospective observational study," *Diabetic Medicine*, 2017.

[19] Diabetes UK, "State of the nation 2016," 2017, available at https://diabetes-resources-production.s3-eu-west-1.amazonaws.com/diabetes-storage/migration/pdf/Diabetes%2520UK%2520State%2520of%2520the%2520Nation%25202016.pdf. Last checked 2018-09-09.

[20] Diabetes UK, "Improving footcare for people with diabetes and saving money: an economic study in england," 2017.

[21] Diabetes UK, "Putting feet first: Diabetes uk position on preventing amputations and improving foot care for people with diabetes," 2015, available at https://www.diabetes.org.uk/professionals/position-statements-reports/specialist-care-for-children-and-adults-and-complications/putting-feet-first-diabetes-foot-care. Last checked 2018-09-09.

[22] M. Kerr, "Foot care in diabetes: The human and financial cost," 2017, available at http://www.londonscn.nhs.uk/wp-content/uploads/2017/04/dia-foot-care-mtg-kerr-27042017.pdf. Last checked 2018-09-09.

[23] L. Fraiwan, M. AlKhodari, J. Ninan, B. Mustafa, A. Saleh, and M. Ghazal, "Diabetic foot ulcer mobile detection system using smart phone thermal camera: a feasibility study," *Biomedical engineering online*, vol. 16, no. 1, p. 117, 2017.

[24] B. Najafi, H. Mohseni, G. S. Grewal, T. K. Talal, R. A. Menzies, and D. G. Armstrong, "An optical-fiber-based smart textile (smart socks) to manage biomechanical risk factors

associated with diabetic foot amputation," *Journal of Diabetes Science and Technology*, vol. 11, no. 4, pp. 668–677, 2017.

[25] S. Ostadabbas, A. Saeed, M. Nourani, and M. Pompeo, "Sensor architectural tradeoff for diabetic foot ulcer monitoring," in *Engineering in Medicine and Biology Society (EMBC), 2012 Annual International Conference of the IEEE*. IEEE, 2012, pp. 6687–6690.

[26] K. Roback, "An overview of temperature monitoring devices for early detection of diabetic foot disorders," *Expert review of medical devices*, vol. 7, no. 5, pp. 711–718, 2010.

[27] V. J. Houghton, V. M. Bower, and D. C. Chant, "Is an increase in skin temperature predictive of neuropathic foot ulceration in people with diabetes? a systematic review and meta-analysis," *Journal of foot and ankle research*, vol. 6, no. 1, p. 31, 2013.

[28] H. Ota, S. Emaminejad, Y. Gao, A. Zhao, E. Wu, S. Challa, K. Chen, H. M. Fahad, A. K. Jha, D. Kiriya *et al.*, "Application of 3D printing for smart objects with embedded electronic sensors and systems," *Advanced Materials Technologies*, vol. 1, no. 1, 2016.

[29] E. MacDonald and R. Wicker, "Multiprocess 3D Printing for increasing component functionality," *Science*, vol. 353, no. 6307, p. aaf2093, 2016.

[30] H. Örneholm, "The diabetic foot: Plantar forefoot ulcer, heel ulcer and minor amputation," Ph.D. dissertation, Clinical and Molecular Osteoporosis Research, 2017, defence details Date: 2017-04-06 Time: 09:00 Place: Aulan, CRC, Jan Waldenströms gata 35, Skånes universitetssjukhus i Malmö. External reviewer(s) Name: Edmonds, Michael Title: professor Affiliation: London — ISSN: 1652-8220 Lund University, Faculty of Medicine Doctoral Dissertation Series 2017:40.

[31] P. Salvo, N. Calisi, B. Melai, V. Dini, C. Paoletti, T. Lomonaco, A. Pucci, F. Di Francesco, A. Piaggesi, and M. Romanelli, "Temperature-and ph-sensitive wearable materials for monitoring foot ulcers," *International journal of nanomedicine*, vol. 12, p. 949, 2017.

[32] Medscape, "Diabetic neuropathy," 2017, available at https://emedicine.medscape.com/article/1170337-overview. Last checked 2018-09-09.

[33] Medscape, "Peripheral vascular disease," 2017, available at https://emedicine.medscape.com/article/761556-overview. Last checked 2018-09-09.

[34] I. W. G. on the Diabetic Foot, "Pathophysiology of foot ulceration," 2007, available at https://docs.google.com/file/d/0B6MIP8_uoAMfRVFoaTR2SDg0S2c/view. Last checked 2018-09-09.

[35] S. Pendsey, *Diabetic Foot: A Clinical Atlas*. Taylor & Francis, 2004. [Online]. Available: https://books.google.pt/books?id=CfB36kyjCvAC

[36] Medscape, "Diabetic foot infections," 2017, available at https://emedicine.medscape.com/article/237378-overview. Last checked 2018-09-09.

[37] D. G. Armstrong, A. J. Boulton, and S. A. Bus, "Diabetic foot ulcers and their recurrence," *New England Journal of Medicine*, vol. 376, no. 24, pp. 2367–2375, 2017.

[38] M. S. Cowley, E. J. Boyko, J. B. Shofer, J. H. Ahroni, and W. R. Ledoux, "Foot ulcer risk and location in relation to prospective clinical assessment of foot shape and mobility among persons with diabetes," *Diabetes research and clinical practice*, vol. 82, no. 2, pp. 226–232, 2008.

[39] K. L. Perell, V. Merrill, and A. Nouvong, "Location of plantar ulcerations in diabetic patients referred to a department of veterans affairs podiatry clinic," *Journal of rehabilitation research and development*, vol. 43, no. 4, p. 421, 2006.

[40] L. A. Lavery, E. J. Peters, and D. G. Armstrong, "What are the most effective interventions in preventing diabetic foot ulcers?" *International wound journal*, vol. 5, no. 3, pp. 425–433, 2008.

[41] A. J. M. Boulton, P. R. Cavanagh, and G. Rayman, *The Foot in Diabetes*, 4th ed. West Sussex, England: John Wley & Sons, Ltd, 2006.

[42] P. Sheehan, P. Jones, A. Caselli, J. M. Giurini, and A. Veves, "Percent change in wound area of diabetic foot ulcers over a 4-week period is a robust predictor of complete healing in a 12-week prospective trial," *Diabetes care*, vol. 26, no. 6, pp. 1879–1882, 2003.

[43] D. J. Margolis, L. Allen-Taylor, O. Hoffstad, and J. A. Berlin, "Diabetic neuropathic foot ulcers: the association of wound size, wound duration, and wound grade on healing," *Diabetes care*, vol. 25, no. 10, pp. 1835–1839, 2002.

[44] L. A. Lavery, R. P. Wunderlich, and J. L. Tredwell, "Disease management for the diabetic foot: effectiveness of a diabetic foot prevention program to reduce amputations and hospitalizations," *Diabetes research and clinical practice*, vol. 70, no. 1, pp. 31–37, 2005.

[45] O. A. Fawzy, A. I. Arafa, M. A. El Wakeel, and S. H. A. Kareem, "Plantar pressure as a risk assessment tool for diabetic foot ulceration in egyptian patients with diabetes," *Clinical medicine insights. Endocrinology and diabetes*, vol. 7, p. 31, 2014.

[46] S. Bus, "Innovations in plantar pressure and foot temperature measurements in diabetes," *Diabetes/metabolism research and reviews*, vol. 32, no. S1, pp. 221–226, 2016.

[47] T. Bernard, C. D'Elia, R. Kabadi, and N. Wong, "An early detection system for foot ulceration in diabetic patients," in *Bioengineering Conference, 2009 IEEE 35th Annual Northeast*. IEEE, 2009, pp. 1–2.

[48] D. G. Armstrong, K. Holtz-Neiderer, C. Wendel, M. J. Mohler, H. R. Kimbriel, and L. A. Lavery, "Skin temperature monitoring reduces the risk for diabetic foot ulceration in high-risk patients," *The American journal of medicine*, vol. 120, no. 12, pp. 1042–1046, 2007.

[49] V. J. Houghton, V. M. Bower, and D. C. Chant, "Is an increase in skin temperature predictive of neuropathic foot ulceration in people with diabetes? A systematic review and meta-analysis," *Journal of foot and ankle research*, vol. 6, no. 1, p. 31, 2013.

[50] F. L. Murillo, L. Leija, and A. Vera, "A foot temperature measuring system for diabetic patients," in *Electrical Engineering, Computing Science and Automatic Control (CCE), 2014 11th International Conference on*. IEEE, 2014, pp. 1–4.

[51] P. Sousa, V. Felizardo, D. Oliveira, R. Couto, and N. M. Garcia, "A review of thermal methods and technologies for diabetic foot assessment," *Expert review of medical devices*, vol. 12, no. 4, pp. 439–448, 2015.

[52] K. Azar, "Introduction to liquid crystal thermography," available at http://www.ewh.ieee.org/soc/cpmt/presentations/cpmt0201b.pdf. Last checked 2018-09-09.

[53] M. Bharara, J. Cobb, and D. Claremont, "Thermography and thermometry in the assessment of diabetic neuropathic foot: a case for furthering the role of thermal techniques," *The International Journal of Lower Extremity Wounds*, vol. 5, no. 4, pp. 250–260, 2006.

[54] SpectraSole, "Spectrasole," 2018, available at http://www.spectrasole.com/. Last checked 2018-09-09.

[55] A. Healthcare, "Tempstat | arche healthcare," 2018, available at https://archehealthcare.com/arche-healthcare/devices/tempstat/. Last checked 2018-09-09.

[56] K. Roback, M. Johansson, and A. Starkhammar, "Feasibility of a thermographic method for early detection of foot disorders in diabetes," *Diabetes technology & therapeutics*, vol. 11, no. 10, pp. 663–667, 2009.

[57] SpectraSole, "How to use - spectrasole," 2018, available at http://www.spectrasole.com/howtouse.htm. Last checked 2018-09-09.

[58] R. Frykberg, A. Tallis, and E. Tierney, "Diabetic foot self examination with the tempstat as an integral component of a comprehensive prevention program," *The Journal of Diabetic Foot Complications*, vol. 1, no. 1, pp. 13–8, 2009.

[59] J. Cobb, "Apparatus and method for real-time full field thermal imaging of the sole of the foot," Feb. 18 2008, U.K. 082913.4, available at http://eprints.bournemouth.ac.uk/7579/. Last checked 2018-09-09.

[60] J. G. Foto, D. Brasseaux, and J. A. Birke, "Essential features of a handheld infrared thermometer used to guide the treatment of neuropathic feet," *Journal of the American Podiatric Medical Association*, vol. 97, no. 5, pp. 360–365, 2007.

[61] G. Constantinides, "Thermometric apparatus and method," Jul. 18 2000, US Patent 6,090,050, available at https://www.google.com/patents/US6090050. Last checked 2018-09-09.

[62] L. A. Lavery, "Digital thermometry: Can it have an impact?" vol. 20, no. 10, 2007, available at https://www.podiatrytoday.com/digital-thermometry-can-it-have-an-impact. Last checked 2018-09-09.

[63] L. A. Lavery, K. R. Higgins, D. R. Lanctot, G. P. Constantinides, R. G. Zamorano, K. A. Athanasiou, D. G. Armstrong, and C. M. Agrawal, "Preventing diabetic foot ulcer recurrence in high-risk patients: use of temperature monitoring as a self-assessment tool," *Diabetes care*, vol. 30, no. 1, pp. 14–20, 2007.

[64] A. Seixas, M. do Carmo Vilas Boas, R. Carvalho, T. Coelho, K. Ammer, J. Vilas Boas, R. Vardasca, J. P. Cunha, and J. Mendes, "Skin temperature of the foot: A comparative study between familial amyloid polyneuropathy and diabetic foot patients," pp. 1048–1052, 2017.

[65] R. Mendes, N. Sousa, A. Almeida, J. Vilaça-Alves, V. M. Reis, and E. B. Neves, "Thermography: a technique for assessing the risk of developing diabetic foot disorders," *Postgraduate medical journal*, vol. 91, no. 1079, pp. 538–538, 2015.

[66] "Sleep diagnostics eden medical inc. diabetic foot scanner," 2012, available at http://www.eden-medical.com/projects/diabeticfootscanner.html. Last checked 2018-09-09.

[67] O. Postel, "Method for detecting and/or monitoring a wound using infrared thermal imaging," Feb. 18 2010, US Patent App. 12/211,535, available at https://www.google.com/patents/US20100041998. Last checked 2018-09-09.

[68] FLIR, "FLIR ONE and FLIR ONE PRO | FLIR Systems," 2018, available at http://www.flir.com/flirone/. Last checked 2018-09-09.

[69] Podimetrics, "Podimetrics," 2018, available at https://www.podimetrics.com/. Last checked 2018-09-09.

[70] R. G. Frykberg, I. L. Gordon, A. M. Reyzelman, S. M. Cazzell, R. H. Fitzgerald, G. M. Rothenberg, J. D. Bloom, B. J. Petersen, D. R. Linders, A. Nouvong *et al.*, "Feasibility and efficacy of a smart mat technology to predict development of diabetic plantar ulcers," *Diabetes care*, vol. 40, no. 7, pp. 973–980, 2017.

[71] D. Amanda Killeen, D. Rosabel Loya, and D. Jodi Walters, "Remote thermometry for early detection of chronic recurrent wounds."

[72] R. Shoureshi and S. Albert, "Smart insole for diabetic patients," May 8 2008, US Patent App. 11/556,914, available at https://www.google.ch/patents/US20080109183. Last checked 2018-09-09.

[73] P. N. Reddy, G. Cooper, A. Weightman, E. Hodson-Tole, and N. Reeves, "An in-shoe temperature measurement system for studying diabetic foot ulceration etiology: preliminary results with healthy participants," *Procedia CIRP*, vol. 49, pp. 153–156, 2016.

[74] *LM35 Precision Centigrade Temperature Sensors*, Texas Instrument, 1999.

[75] *Low Voltage Temperature Sensors TMP35/TMP36/TMP37*, Analog Devices, rev. H.

[76] P. N. Reddy, G. Cooper, A. Weightman, E. Hodson-Tole, and N. D. Reeves, "Walking cadence affects rate of plantar foot temperature change but not final temperature in younger and older adults," *Gait & posture*, vol. 52, pp. 272–279, 2017.

[77] R. A. Nardin, P. M. Fogerson, R. Nie, and S. B. Rutkove, "Foot temperature in healthy individuals: effects of ambient temperature and age," *Journal of the American Podiatric Medical Association*, vol. 100, no. 4, pp. 258–264, 2010.

[78] P. Foltyński, B. Mrozikiewicz-Rakowska, P. Ładyżyński, J. M. Wójcicki, and W. Karnafel, "The influence of ambient temperature on foot temperature in patients with diabetic foot ulceration," *Biocybernetics and Biomedical Engineering*, vol. 34, no. 3, pp. 178–183, 2014.

[79] B. Najafi, J. S. Wrobel, G. Grewal, R. A. Menzies, T. K. Talal, M. Zirie, and D. G. Armstrong, "Plantar temperature response to walking in diabetes with and without acute charcot: the charcot activity response test," *Journal of aging research*, vol. 2012, 2012.

[80] P. N. Reddy, G. Dougill, A. Weightman, E. Hodson-Tole, N. Reeves, and G. Cooper, "Experimental modelling of heat generation in porcine tissue to investigate the etiology of diabetic foot ulceration," *Procedia CIRP*, vol. 49, pp. 170–173, 2016.

[81] S. D. Mahanty and R. B. Roemer, "Thermal response of skin to application of localized pressure." *Archives of physical medicine and rehabilitation*, vol. 60, no. 12, pp. 584–590, 1979.

[82] F. Peeters, M. Peetermans, and L. Indesteege, "Temperature sensors," in *Modern Sensors Handbook*, January 2010, pp. 347–393.

[83] "Temperature sensor types for temperature measurement," Feb 2018, available at https://www.electronics-tutorials.ws/io/io_3.html. Last checked 2018-09-09.

[84] "RTDs," available at http://www.capgo.com/Resources/Temperature/RTDs/RTD.html. Last checked 2018-09-09.

[85] "Overview of temperature sensors," Aug 2016, available at http://www.ni.com/white-paper/4218/en/. Last checked 2018-09-09.

[86] *PT Series – Power Type NTC Thermistor*, Exsense Electronics Technology.

[87] "Thermistors and NTC thermistors," Apr 2018, available at https://www.electronics-tutorials.ws/io/thermistors.html. Last checked 2018-09-09.

[88] P. J. Vis, "Potential divider with NTC thermistor," available at https://www.petervis.com/GCSE_Design_and_Technology_Electronic_Products/Potential_Divider/Potential_Divider_with_Thermistor.html. Last checked 2018-09-09.

[89] "TMP36 temperature sensor," available at https://learn.adafruit.com/tmp36-temperature-sensor/overview. Last checked 2018-09-09.

[90] A. E. Williams, C. Nester *et al.*, *The pocket podiatry guide-footwear and foot orthoses*. Elsevier, 2010.

[91] P. R. L. e. Matthew B. Werd, E. Leslie Knight, *Athletic Footwear and Orthoses in Sports Medicine*, 2nd ed. Springer International Publishing, 2017.

[92] P. Crabtree, V. Dhokia, M. Ansell, and S. Newman, "Design and manufacture of customised orthotics for sporting applications (p62)," in *The Engineering of Sport 7*. Springer, 2009, pp. 309–317.

[93] "Diabetic foot problems: prevention and management," Aug 2015, available at https://www.nice.org.uk/guidance/ng19/chapter/1-Recommendations#diabetic-foot-ulcer. Last checked 2018-09-09.

[94] J. Paton, R. B. Jones, E. Stenhouse, and G. Bruce, "The physical characteristics of materials used in the manufacture of orthoses for patients with diabetes," *Foot & ankle international*, vol. 28, no. 10, pp. 1057–1063, 2007.

[95] N. Guldemond, P. Leffers, N. Schaper, A. Sanders, F. Nieman, P. Willems, and G. Walenkamp, "The effects of insole configurations on forefoot plantar pressure and walking convenience in diabetic patients with neuropathic feet," *Clinical Biomechanics*, vol. 22, no. 1, pp. 81–87, 2007.

[96] A. C. Yunus *et al.*, "Heat transfer: a practical approach," *MacGraw Hill, New York*, 2003.

[97] J. F. Shackelford, *Introduction to materials science for engineers*. Pearson Upper Saddle River, NJ, 2015.

[98] C. Nicolopoulos, J. Black, and E. Anderson, "Foot orthoses materials," *The foot*, vol. 10, no. 1, pp. 1–3, 2000.

[99] "Thermally conductive silicones - technical bulletin," Apr 2007, available at https://www.intertronics.co.uk/articles/tb012.htm. Last checked 2018-09-09.

[100] "Properties: Silicone rubber," available at https://www.azom.com/properties.aspx?ArticleID=920. Last checked 2018-09-09.

[101] "Ethylene vinyl acetate (EVA)," Jan 2018, available at https://www.makeitfrom.com/material-properties/Ethylene-Vinyl-Acetate-EVA#Thermal. Last checked 2018-09-09.

[102] *PORON®4701-40 Soft – Data Sheet*, Rogers Corporation, publication 17-007.

[103] AZoM, "Silicone rubber," Sep 2001, available at https://www.azom.com/article.aspx?ArticleID=920. Last checked 2018-09-09.

[104] S.-E. Silicone, "Characteristic properties of silicone rubber compounds," *Silicone, Shin-Etsu*, 2012.

[105] K. Mukhopadhyay, D. Tripathy, and S. De, "Wear, tear and tensile failure of silica-filled ethylene vinyl acetate rubber," *Wear*, vol. 152, no. 1, pp. 111–125, 1992.

[106] M. Zhang and A. Mak, "In vivo friction properties of human skin," *Prosthetics and orthotics International*, vol. 23, no. 2, pp. 135–141, 1999.

[107] B. Gao, J. Xu, J. Peng, F. Kang, H. Du, J. Li, S. Chiang, C. Xu, N. Hu, and X. Ning, "Experimental and theoretical studies of effective thermal conductivity of composites made of silicone rubber and Al2O3 particles," *Thermochimica Acta*, vol. 614, pp. 1–8, 2015.

[108] Q. Mu, S. Feng, and G. Diao, "Thermal conductivity of silicone rubber filled with ZnO," *Polymer composites*, vol. 28, no. 2, pp. 125–130, 2007.

[109] G. Lorenz and A. Kandelbauer. Elsevier, pp. 555–575.

[110] S.-C. Lin, C.-C. M. Ma, W.-H. Liao, J.-A. Wang, S.-J. Zeng, S.-Y. Hsu, Y.-H. Chen, S.-T. Hsiao, T.-Y. Cheng, C.-W. Lin *et al.*, "Preparation of a graphene–silver nanowire hybrid/silicone rubber composite for thermal interface materials," *Journal of the Taiwan Institute of Chemical Engineers*, vol. 68, pp. 396–406, 2016.

[111] C. Liu, H. Huang, Y. Wu, and S. Fan, "Thermal conductivity improvement of silicone elastomer with carbon nanotube loading," *Applied Physics Letters*, vol. 84, no. 21, pp. 4248–4250, 2004.

[112] Y. Song, J. Yu, L. Yu, F. E. Alam, W. Dai, C. Li, and N. Jiang, "Enhancing the thermal, electrical, and mechanical properties of silicone rubber by addition of graphene nanoplatelets," *Materials & Design*, vol. 88, pp. 950–957, 2015.

[113] Y. Mamunya, "Carbon nanotubes as conductive filler in segregated polymer composites - electrical properties," in *Carbon Nanotubes - Polymer Nanocomposites*, S. Yellampalli, Ed. Rijeka: InTech, 2011, ch. 09. [Online]. Available: http://dx.doi.org/10.5772/18878

[114] C. Groth, N. D. Kravitz, P. E. Jones, J. W. Graham, and W. R. Redmond, "Three-dimensional printing technology," *J Clin Orthod*, vol. 48, no. 8, pp. 475–85, 2014.

[115] J. U. Pucci, B. R. Christophe, J. A. Sisti, and E. S. Connolly Jr, "Three-dimensional printing: technologies, applications, and limitations in neurosurgery," *Biotechnology advances*, vol. 35, no. 5, pp. 521–529, 2017.

[116] "What is AM?" available at http://www.lboro.ac.uk/research/amrg/about/whatisam/. Last checked 2018-09-09.

[117] "The 7 categories of additive manufacturing," available at http://www.lboro.ac.uk/research/amrg/about/the7categoriesofadditivemanufacturing/. Last checked 2018-09-09.

[118] A. International, "ASTM F42/ISO TC 261 Develops Additive Manufacturing Standards," 2010, available at https://www.astm.org/COMMIT/F42_AMStandardsStructureAndPrimer.pdf. Last checked 2018-09-09.

[119] Y. Xu, X. Wu, X. Guo, B. Kong, M. Zhang, X. Qian, S. Mi, and W. Sun, "The Boom in 3D-Printed Sensor Technology," *Sensors*, vol. 17, no. 5, p. 1166, 2017.

[120] T. Campbell, C. Williams, O. Ivanova, and B. Garrett, "Could 3D Printing change the world?" *Technologies, Potential, and Implications of Additive Manufacturing, Atlantic Council, Washington, DC*, 2011.

[121] J. W. Boley, E. L. White, G. T.-C. Chiu, and R. K. Kramer, "Direct writing of gallium-indium alloy for stretchable electronics," *Advanced Functional Materials*, vol. 24, no. 23, pp. 3501–3507, 2014.

[122] S. Osborn, *Makers at Work: Folks Reinventing the World One Object or Idea at a Time*, 1st ed. Berkely, CA, USA: Apress, 2013.

[123] S. Y. Hong, Y. H. Lee, H. Park, S. W. Jin, Y. R. Jeong, J. Yun, I. You, G. Zi, and J. S. Ha, "Stretchable active matrix temperature sensor array of polyaniline nanofibers for electronic skin," *Advanced Materials*, vol. 28, no. 5, pp. 930–935, 2016.

[124] "Conductive inks | printed electronics solutions," available at www.methode.com/sensors-and-switches/conductive-and-resistive-inks.html#.WnFNAitUmEc. Last checked 2018-09-09.

[125] J. Courbat, Y. Kim, D. Briand, and N. De Rooij, "Inkjet printing on paper for the realization of humidity and temperature sensors," in *Solid-State Sensors, Actuators and Microsystems Conference (TRANSDUCERS), 2011 16th International*. IEEE, 2011, pp. 1356–1359.

[126] C. Bali, A. Brandlmaier, A. Ganster, O. Raab, J. Zapf, and A. Hübler, "Fully inkjet-printed flexible temperature sensors based on carbon and PEDOT: PSS1," *Materials Today: Proceedings*, vol. 3, no. 3, pp. 739–745, 2016.

[127] W. Honda, S. Harada, T. Arie, S. Akita, and K. Takei, "Printed wearable temperature sensor for health monitoring," in *SENSORS, 2014 IEEE*. IEEE, 2014, pp. 2227–2229.

[128] H.-S. Chuang and S. Wereley, "Design, fabrication and characterization of a conducting pdms for microheaters and temperature sensors," *Journal of Micromechanics and Microengineering*, vol. 19, no. 4, p. 045010, 2009.

[129] T. Vuorinen, J. Niittynen, T. Kankkunen, T. M. Kraft, and M. Mäntysalo, "Inkjet-printed graphene/PEDOT: PSS temperature sensors on a skin-conformable polyurethane substrate," *Scientific reports*, vol. 6, p. 35289, 2016.

[130] S. Ali, A. Hassan, J. Bae, C. H. Lee, and J. Kim, "All-printed differential temperature sensor for the compensation of bending effects," *Langmuir*, vol. 32, no. 44, pp. 11 432–11 439, 2016.

[131] A. Wickberg, J. B. Mueller, Y. J. Mange, J. Fischer, T. Nann, and M. Wegener, "Three-dimensional micro-printing of temperature sensors based on up-conversion luminescence," *Applied Physics Letters*, vol. 106, no. 13, p. 133103, 2015.

[132] *Instruction Manual for the 3D-Bioplotter*, envisionTEC, 2014.

[133] C. Tudor-Locke, T. L. Washington, and T. L. Hart, "Expected values for steps/day in special populations," *Preventive medicine*, vol. 49, no. 1, pp. 3–11, 2009.

[134] T. A. Bacarin, I. C. Sacco, and E. M. Hennig, "Plantar pressure distribution patterns during gait in diabetic neuropathy patients with a history of foot ulcers," *Clinics*, vol. 64, no. 2, pp. 113–120, 2009.

[135] S. Skogestad, *Chemical and energy process engineering*. CRC press, 2008.

[136] I. Hong and R. Tessman, "What time do you have?" 1998.

Appendix A

Solidworks® models for samples

A.1 Models for compression moulding samples

The samples manufactured through compression moulding required three different moulds. An upper mould, with different thicknesses, an inner mould and a bottom mould.

A.1.1 Upper mould

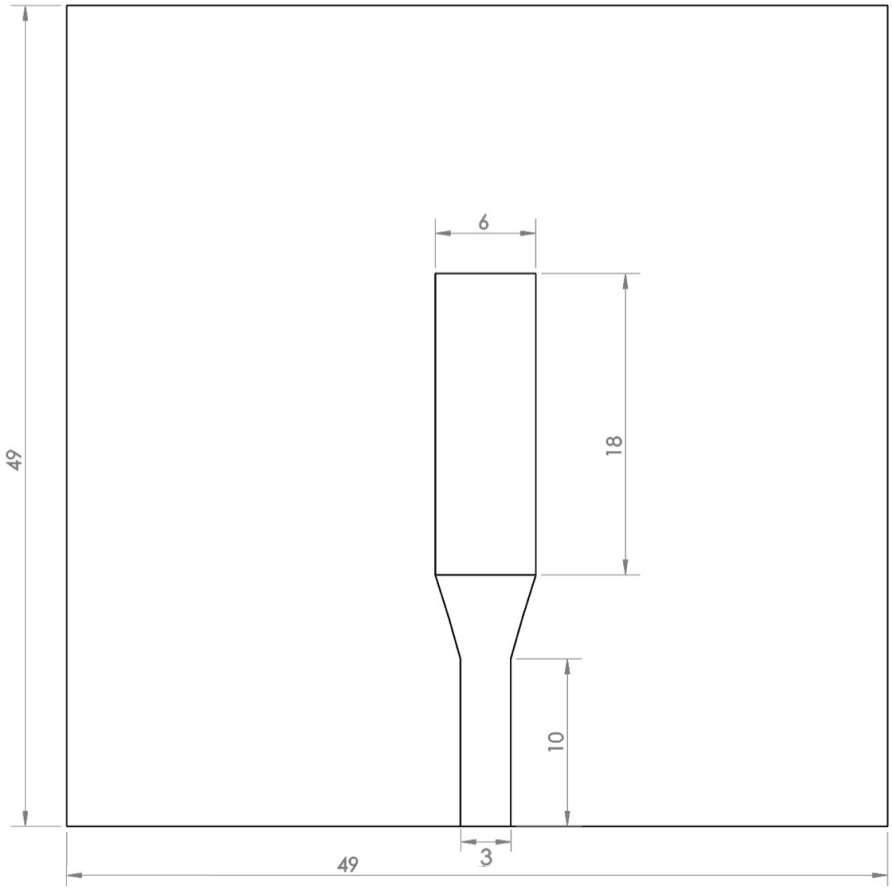

Figure A.1: Front view of upper mould (dimensions in millimetres).

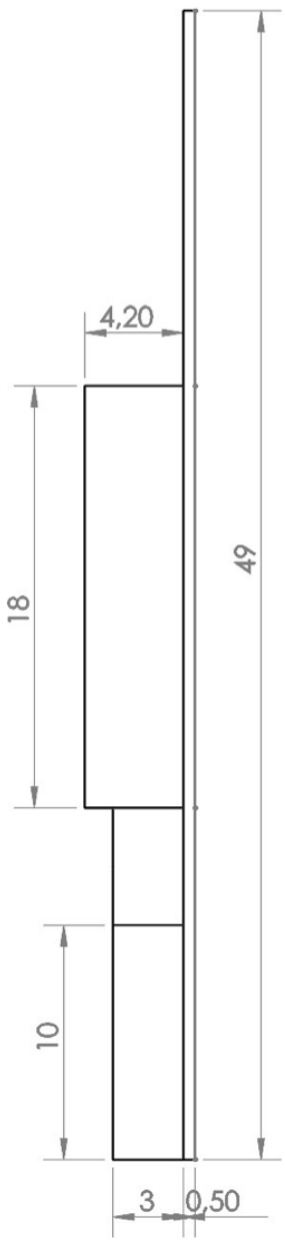

Figure A.2: Side view of upper mould with 0.5 mm thickness (dimensions in millimetres).

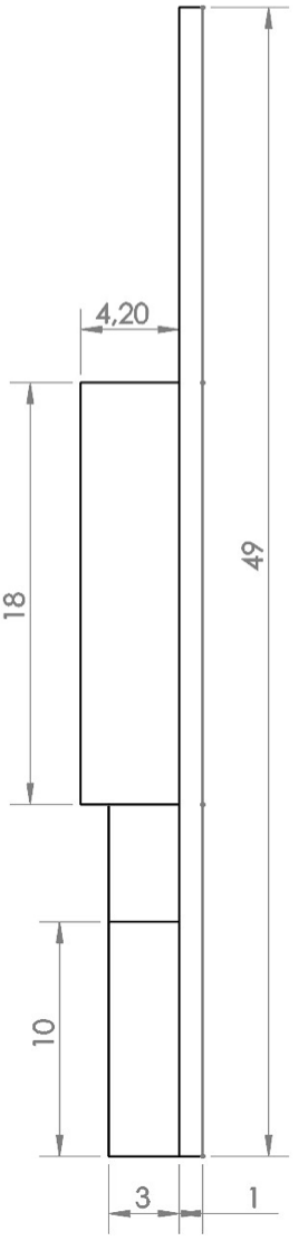

Figure A.3: Side view of upper mould with 1.0 mm thickness (dimensions in millimetres).

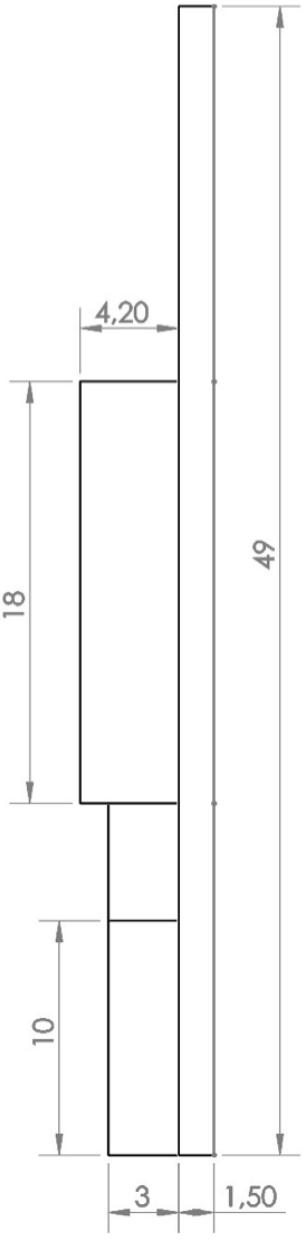

Figure A.4: Side view of upper mould with 1.5 mm thickness (dimensions in millimetres).

A.1.2 Inner mould

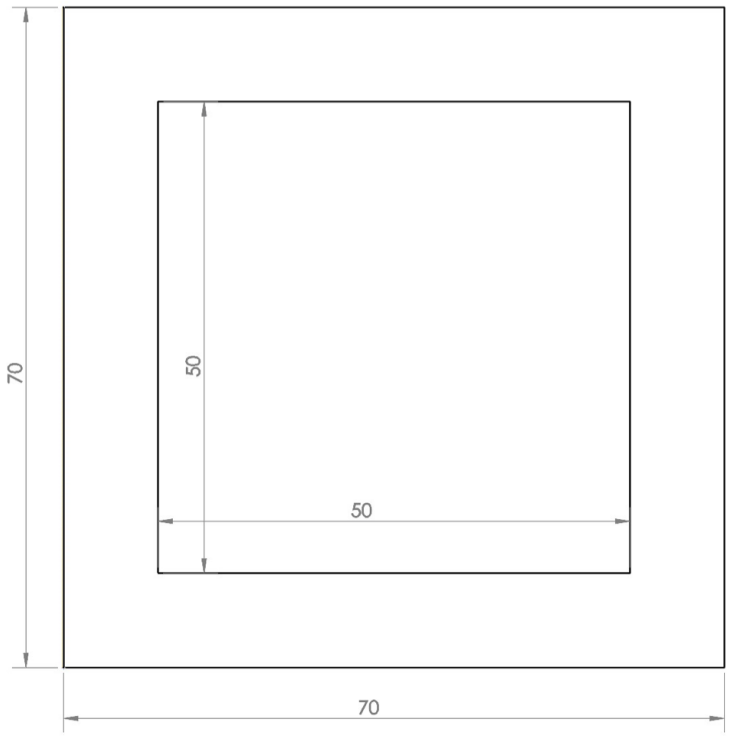

Figure A.5: Front/Back view of inner mould (dimensions in millimetres).

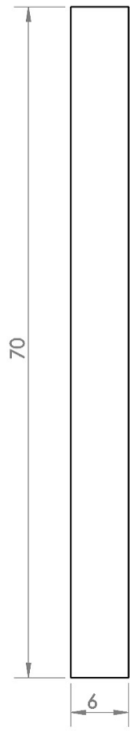

Figure A.6: Side view of inner mould (dimensions in millimetres).

A.1.3 Lower mould

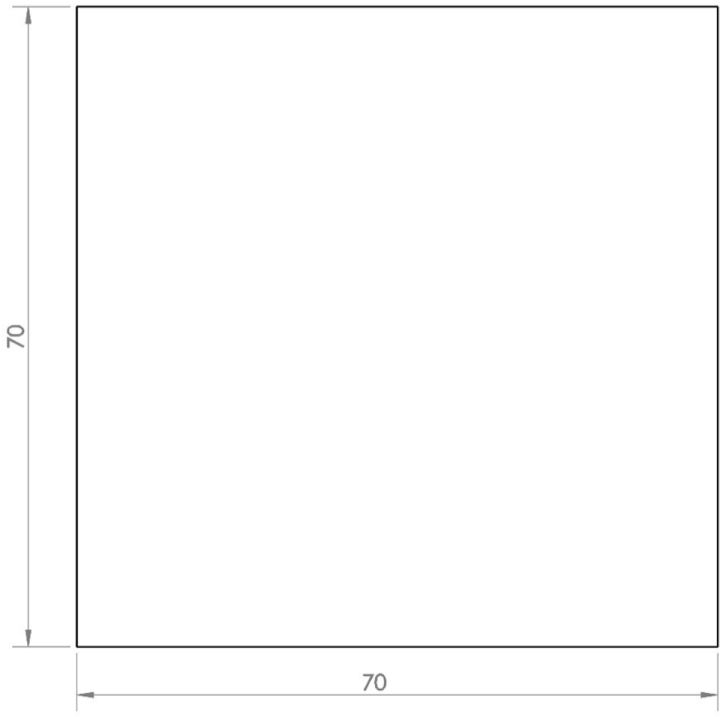

Figure A.7: Front/Back view of lower mould (dimensions in millimetres).

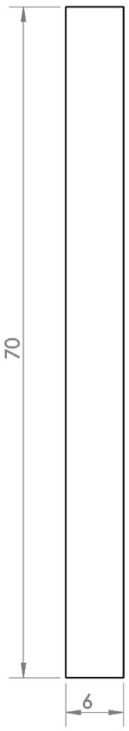

Figure A.8: Side view of lower mould (dimensions in millimetres).

A.2 Models for 3D Printed samples

The 3D samples are composed of two parts, a lower part printed first, where the sensor is embedded, and an upper part printed on top of the previous one.

A.2.1 Lower part

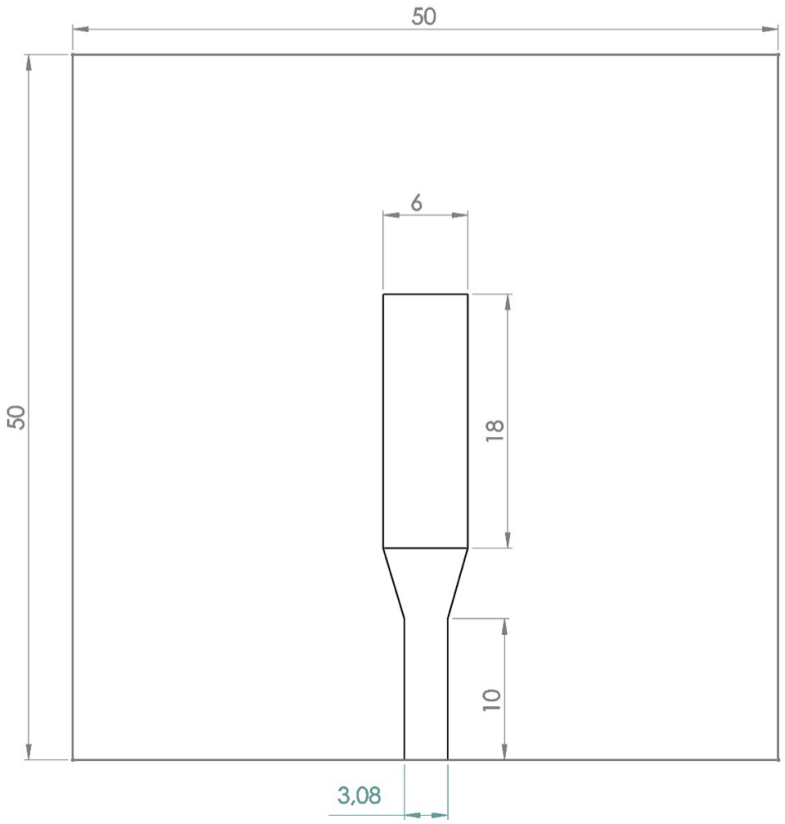

Figure A.9: Front view of lower part (dimensions in millimetres).

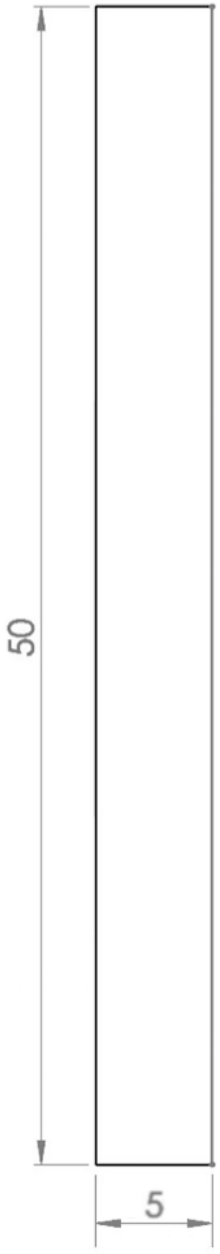

Figure A.10: Side view of lower part (dimensions in millimetres).

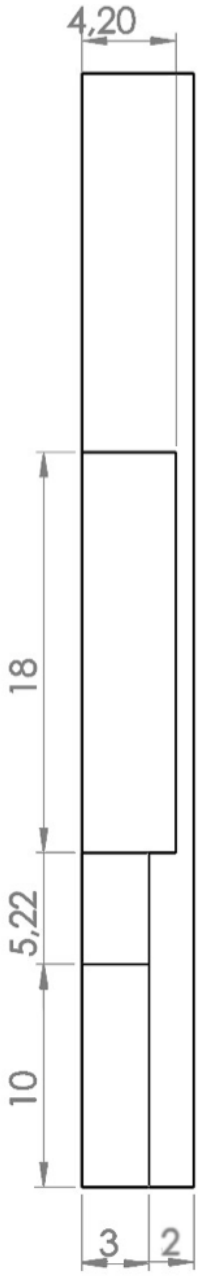

Figure A.11: Cross sectional view of lower part (dimensions in millimetres).

A.2.2 Upper part

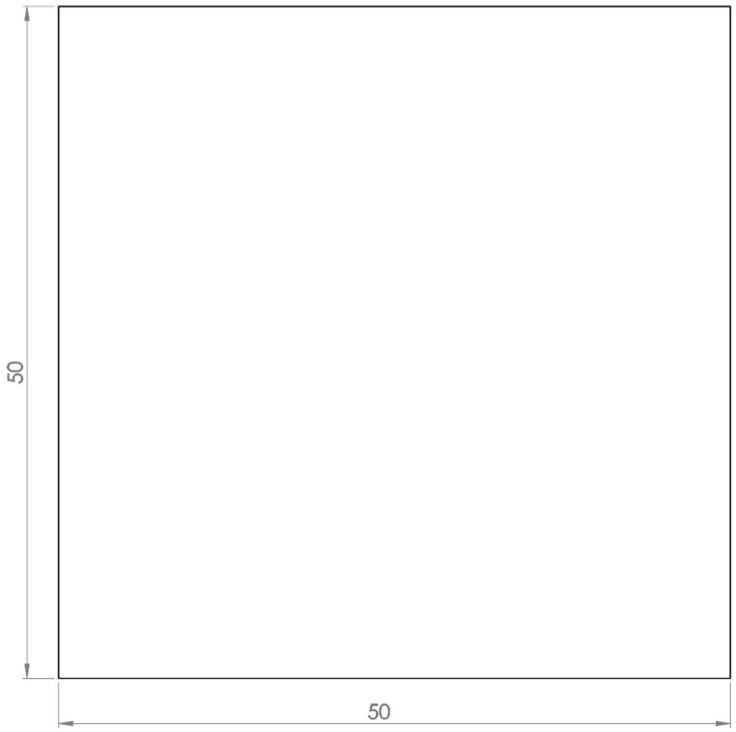

Figure A.12: Front view of upper part (dimensions in millimetres).

Figure A.13: Side view of upper part (dimensions in millimetres).

Appendix B

Silicone rubber AS40 datasheet

easycomposites™ share the knowledge

ADDITION CURE SILICONE RUBBER

AS40

Key Features

- Very accurate dimensional accuracy
- Very low shrinkage
- Translucent
- High tear strength
- Styrene and PU resistant

Product Description

AS40 is a high quality 'addition cure' (platinum cure) silicone rubber for more demanding mould making applications. Addition cure silicone rubber is a more advanced type of RTV (Room Temperature Vulcanising) silicone than the more cost effective 'Condensation Cure' silicone.

Our addition cure silicone has been chosen for its excellent dimension reproduction; it is incredibly low shrink and therefore can be used to make a mould for prototype parts that interconnect (like a nut and bolt) to engineering tolerances. It has excellent styrene and polyurethane resistance and a high tear strength.

Recommended Uses

Use our Addition Cure Silicone Rubber to produce accurate moulds of complicated parts, precisely reproducing the dimensions of the original part. Completed silicone moulds can be used for repetitive casting applications, ceramics, vacuum casting and general mould making.

Properties

The table below shows the typical uncured properties:

Property	Units	Resin	Hardener	Combined
Material	-	Silicone Rubber	Clear Liquid	Silicone Rubber
Appearance	-	Translucent Viscous Liquid	Amber Liquid	Translucent Viscous Liquid
Viscosity @20 °C	mPa.s.	40000 - 78000	200 - 300	30000 - 70000
Density @20 °C	g/cm^3	1.08	1.07	1.08

How to Use

AS40 is a chemical product for professional use. It is essential to read and understand the safety and technical information before use.

Follow the guidelines for safe use outlined in the SDS which include the use of appropriate hand and eye protection during mixing and use.

Mix Ratio

Mix Ratio 100:10 by Weight

AS40 Addition Cure Silicone should be mixed with Addition Cure Catalyst at a ratio of 100 parts of silicone to 10 parts of Catalyst, by weight. Failure to do so will result in a poor or only partial cure of the silicone, greatly reduced mechanical properties and possibly other adverse effects. Under no circumstances add 'extra catalyst' in an attempt to speed up the cure time; Addition Cure Silicones do not work in this way.

Mixing Instructions

Only weigh out and mix as much silicone as you can use within the pot life. Weigh or measure the exact correct ratio of silicone and catalyst into a straight sided container. Using a suitable mixing stick begin to mix the silicone and catalyst together to combine them completely.

Mix thoroughly together both parts of the system ensuring the container used is at least five times the volume of the material being mixed e.g. For a 2 Kg mix use a 10 litre container.

Due to the difference in viscosity of the two components extra care should be taken when mixing to ensure a homogeneous mix. When you think the mixture is homogeneous, mix again to ensure thorough mixing.

Before use the mixed silicone should be correctly de-gassed in a vacuum chamber to remove air trapped within the mix that will seriously impair the surface finish quality of the resulting mould.

Inhibiting Materials

Addition cure silicone rubbers are susceptible to cure inhibition by a number of products and materials. Take special care to ensure that the uncured silicone does not come into contact with any of the following materials or substances otherwise you may well find that the silicone does not cure at all in the contaminated areas.

Products with a high moisture content or a high sulphur content are potentially the most damaging. The known inhibiting substances include:

- Wood-mastic epoxy resin
- Natural rubber
- Silicone sealants
- Neoprene adhesive
- Vinyl adhesive
- Transparent wood glue
- Flexible compact PUR
- Plasticised PVC film*
- Foam latex and latex gloves*
- Cyanoacrylate adhesive* (super glue)
- Polyester resin
- Adhesive tape
- Coachwork polyester mastic
- Shellac
- Transparent PVC tubing*
- Condensation cure RTV
- CAF Sealant (all types)

* PARTICULARLY ACTIVE

De-Gassing

When the material is thoroughly mixed it should be placed in a vacuum chamber to de-gas. When vacuum degassing the material will expand to approximately five times its original volume and then collapse, it is at this point that the material has been successfully vacuumed.

If no vacuum chamber is available it might be possible to de-gas the mixed silicone using the 'stretch-pour' method whereby the silicone is poured into the mould by means of a very small hole in the bottom of a vessel containing the mixed silicone. The vessel should be positioned at a height of more than 1m above the set-up box and allowed to pour into a corner of the set-up box in a very thin trickle.

Pot-Life / Working Time / Cure Time

Transfer the Silicone from the mixing pot onto the part as soon as possible to extend the working time and avoid the risk of rapid cure in the mixing pot.

The pot-life/working time will vary significantly depending on the ambient temperature and the starting temperature of the silicine and Catalyst.

AS40 can be used in ambient temperatures between 15°C (59°F) and 30°C (86°F). For best results, an ambient temperature of at least 20°C (68°F) is recommended.

Pour carefully in one place in to the set-up box to avoid air inclusion. Once pouring is complete place the set-up box back in to the vacuum chamber (if possible) and degas again. If curing at elevated temperatures the mould should be allowed to stand for 10 minutes before being placed in the oven at the appropriate temperature. Shrinkage of the silicone will increase when cured at elevated temperatures.

The table below gives an indication of pot-life and cure times:

Pot-Life @ 20 °C	Demould Time @ 20 °C	Demould Time @ 60°C	Demould Time @ 70°C	Demould Time @ 80°C
30 Minutes	24 Hours	2 Hours	1 Hours	30 mins

Expansion of Cured Mould

If the silicone mould will be used at elevated temperatures it should be understood that the mould will expand to a degree. The amount of expansion for a given temperature can be calculated as follows:

L_o = Original length

L = Length at temperature

T = Temperature of silicone mould

Coefficient of expansion = 2.6×10^{-4} (mm/mm)/°C

T_{room} = 20°C

$(L - L_o) = Coef \times (T - T_{room}) \times L_o$

e.g. Increase in length of a 500 mm mould at 60°C

$(L - L_o) = 2.6X10^{-4} X (60-20) X 500 = 5.2mm$

Mechanical Properties

Cured Silicone Properties

	Units	Result
Colour		Translucent
Density 25°C	g/ml	1.05 – 1.09
Linear Shrinkage	%	0.1
Hardness 25°C	Shore A	36 - 45
Tensile Strength	MPa	> 3.5
Tear Strength	kN/m	> 13.0
Elongation at break	%	> 250
Service Temperature	°C	-60 to 250

Transport and Storage

Silicone and catalyst should be kept in tightly seal containers during transport and storage. Both the resin and hardener should be stored in ambient conditions of between 10°C (50°F) and 25°C (77°F).

When stored correctly, the silicone and catalyst will have a shelf-life of 12 months. Although it may be possible to use the silicone after a longer period, a deterioration in the performance of the silicone will occur. Pay particular attention to ensuring that containers are kept tightly sealed.

Disclaimer

Easy Composites Ltd
Unit 39, Park Hall Business Village, Longton, Stoke on Trent, Staffordshire, ST3 5XA, United Kingdom.
Tel. +44 (0)1782 454499, Fax. +44 (0)1782 596868, Email sales@easycomposites.co.uk, Web www.easycomposites.co.uk

Appendix C

Forever White datasheet

PRODUCT DATA SHEET

EVERBUILD FOREVER WHITE®

A SUPERIOR HYGIENIC SILICONE SEALANT FOR AREAS OF HIGH HUMIDITY.

PRODUCT DESCRIPTION

EVERBUILD FOREVER WHITE® contains Mould Shield which actively protects the sealant against the growth of bacteria, mildew and black mould that are commonly found in areas of high humidity. EVERBUILD FOREVER WHITE® is permanently waterproof and flexible and is produced from a superior silicone formula. EVERBUILD FOREVER WHITE® is tested and certified by an independent microbiological laboratory to show no mould growth after more than 10 yrs simulated ageing. Copies of test data are available.

USES

- For sealing showers, baths, wetrooms, sanitary ware, ceramic tiles, kitchens and all applications in areas of high humidity where maximum hygiene protection is required.
- Also ideal for sealing around window and door frames internally in areas subject to high condensation.

CHARACTERISTICS / ADVANTAGES

- Permanently waterproof.
- Highly flexible.
- 10 year proven* protection against mould and discolouration.
- High quality silicone.

Form	Paste, 1 component RTV silicone
Viscosity	100,000 - 200,000 cP
Modulus at 100% Elongation	0.35 N/mm² to ISO8339

* simulated aging

APPROVALS / STANDARDS

Certified under the harmonized European standard EN15651 for façade, cold climate and sanitary applications in compliance with the Construction Product Regulation.

PRODUCT INFORMATION

Packaging	295ml Cartridge 80ml Squeezy Tube
Colour	White, Clear, Ivory and Grey
Shelf Life	Cartridge and Squeezy tube: 24 months from date of manufacture.
Storage Conditions	Store in cool dry conditions and protect from frost.
Density	0.98 - 1.05 g/cm³
Shore A Hardness	20
Tensile Strength	Approx. 0.6 N/mm² to ISO 8339
Elongation at Break	250% to ISO8339
Movement Capability	25% EN15651-1

Service Temperature	-40°C to +180°C

APPLICATION INFORMATION

Curing Time	Approx. 2-3 mm in 24 hours at 23°C/50% RH
Skin Time	Approx. 15-20 mins at 23°C/50% RH

APPLICATION INSTRUCTIONS

- All surfaces to be sealed must be clean and dry.
- Fill deep gaps and voids with Everbuild Expanding Foam, then trim back level with bath/shower tray before applying Sealant.
- When applying to plastic & acrylic baths, fill bath half full with water whilst sealing and during cure. This provides the mid point of any movement that will be encountered.
- Always tool sealant down to ensure a proper bond is achieved.
- Tool within 15 minutes of applying.

LIMITATIONS

- Do not use in aquaria; use Aqua mate Sealant
- Do not use against surfaces that bleed oil or plasticizers, or against bitumen/pitch based products.
- It is always the user's responsibility to determine suitability of use. If in doubt request technical data or contact Technical Services department before use.

VALUE BASE

All technical data stated in this Data Sheet are based on laboratory tests. Actual measured data may vary due to circumstances beyond our control.

LOCAL RESTRICTIONS

Note that as a result of specific local regulations the declared data and recommended uses for this product may vary from country to country. Consult the local Product Data Sheet for the exact product data and uses.

ECOLOGY, HEALTH AND SAFETY

LEGAL NOTES

The information, and, in particular, the recommendations relating to the application and end-use of Sika products, are given in good faith based on Sika's current knowledge and experience of the products when properly stored, handled and applied under normal conditions in accordance with Sika's recommendations. In practice, the differences in materials, substrates and actual site conditions are such that no warranty in respect of merchantability or of fitness for a particular purpose, nor any liability arising out of any legal relationship whatsoever, can be inferred either from this information, or from any written recommendations, or from any other advice offered. The user of the product must test the product's suitability for the intended application and purpose. Sika reserves the right to change the properties of its products. The proprietary rights of third parties must be observed. All orders are accepted subject to our current terms of sale and delivery. Users must always refer to the most recent issue of the local Product Data Sheet for the product concerned, copies of which will be supplied on request.

Appendix D

Temperature sensor LM35CA datasheet

6.6 Electrical Characteristics: LM35A, LM35CA

Unless otherwise noted, these specifications apply: −55°C ≤ T_J ≤ 150°C for the LM35 and LM35A; −40°C ≤ T_J ≤ 110°C for the LM35C and LM35CA; and 0°C ≤ T_J ≤ 100°C for the LM35D. V_S = 5 Vdc and I_{LOAD} = 50 μA, in the circuit of Full-Range Centigrade Temperature Sensor. These specifications also apply from 2°C to T_{MAX} in the circuit of Figure 14.

PARAMETER	TEST CONDITIONS		LM35A			LM35CA			UNIT
			MIN	TYP	MAX	TYP	TYP	MAX	
Accuracy(1)	T_A = 25°C			±0.2			±0.2		°C
		Tested Limit(2)			±0.5			±0.5	
		Design Limit(3)							
	T_A = –10°C			±0.3			±0.3		
		Tested Limit(2)							
		Design Limit(3)						±1	
	T_A = T_{MAX}			±0.4			±0.4		
		Tested Limit(2)			±1			±1	
		Design Limit(3)							
	T_A = T_{MIN}			±0.4			±0.4		
		Tested Limit(2)			±1				
		Design Limit(3)						±1.5	
Nonlinearity(4)	T_{MIN} ≤ T_A ≤ T_{MAX}, –40°C ≤ T_J ≤ 125°C			±0.18			±0.15		°C
		Tested Limit(2)							
		Design Limit(3)			±0.35			±0.3	
Sensor gain (average slope)	T_{MIN} ≤ T_A ≤ T_{MAX}			10			10		mV/°C
		Tested Limit(2)			9.9				
		Design Limit(3)						9.9	
	–40°C ≤ T_J ≤ 125°C			10			10		
		Tested Limit(2)			10.1				
		Design Limit(3)						10.1	
Load regulation(5) 0 ≤ I_L ≤ 1 mA	T_A = 25°C			±0.4			±0.4		mV/mA
		Tested Limit(2)			±1			±1	
		Design Limit(3)							
	T_{MIN} ≤ T_A ≤ T_{MAX}, –40°C ≤ T_J ≤ 125°C			±0.5			±0.5		
		Tested Limit(2)							
		Design Limit(3)			±3			±3	
Line regulation(5)	T_A = 25°C			±0.01			±0.01		mV/V
		Tested Limit(2)			±0.05			±0.05	
		Design Limit(3)							
	4 V ≤ V_S ≤ 30 V, –40°C ≤ T_J ≤ 125°C			±0.02			±0.02		
		Tested Limit(2)							
		Design Limit(3)			±0.1			±0.1	

(1) Accuracy is defined as the error between the output voltage and 10 mv/°C times the case temperature of the device, at specified conditions of voltage, current, and temperature (expressed in °C).
(2) Tested Limits are ensured and 100% tested in production.
(3) Design Limits are ensured (but not 100% production tested) over the indicated temperature and supply voltage ranges. These limits are not used to calculate outgoing quality levels.
(4) Non-linearity is defined as the deviation of the output-voltage-versus-temperature curve from the best-fit straight line, over the rated temperature range of the device.
(5) Regulation is measured at constant junction temperature, using pulse testing with a low duty cycle. Changes in output due to heating effects can be computed by multiplying the internal dissipation by the thermal resistance.

7 Detailed Description

7.1 Overview

The LM35-series devices are precision integrated-circuit temperature sensors, with an output voltage linearly proportional to the Centigrade temperature. The LM35 device has an advantage over linear temperature sensors calibrated in Kelvin, as the user is not required to subtract a large constant voltage from the output to obtain convenient Centigrade scaling. The LM35 device does not require any external calibration or trimming to provide typical accuracies of ± ¼ °C at room temperature and ± ¾ °C over a full −55°C to 150°C temperature range. Lower cost is assured by trimming and calibration at the wafer level. The low output impedance, linear output, and precise inherent calibration of the LM35 device makes interfacing to readout or control circuitry especially easy. The device is used with single power supplies, or with plus and minus supplies. As the LM35 device draws only 60 μA from the supply, it has very low self-heating of less than 0.1°C in still air. The LM35 device is rated to operate over a −55°C to 150°C temperature range, while the LM35C device is rated for a −40°C to 110°C range (−10° with improved accuracy). The temperature-sensing element is comprised of a delta-V BE architecture.

The temperature-sensing element is then buffered by an amplifier and provided to the VOUT pin. The amplifier has a simple class A output stage with typical 0.5-Ω output impedance as shown in the *Functional Block Diagram*. Therefore the LM35 can only source current and it's sinking capability is limited to 1 μA.

7.2 Functional Block Diagram

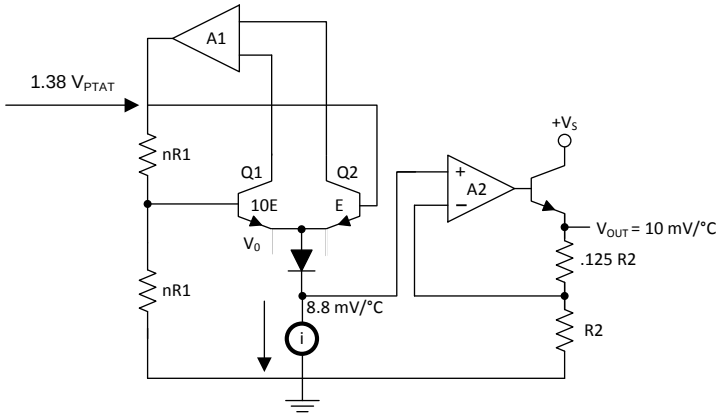

7.3 Feature Description

7.3.1 LM35 Transfer Function

The accuracy specifications of the LM35 are given with respect to a simple linear transfer function:

V_{OUT} = 10 mv/°C × T (1)

where

- V_{OUT} is the LM35 output voltage
- T is the temperature in °C

7.4 Device Functional Modes

The only functional mode of the LM35 is that it has an analog output directly proportional to temperature.

PACKAGE OUTLINE

LP0003A **TO-92 - 5.34 mm max height**

TO-92

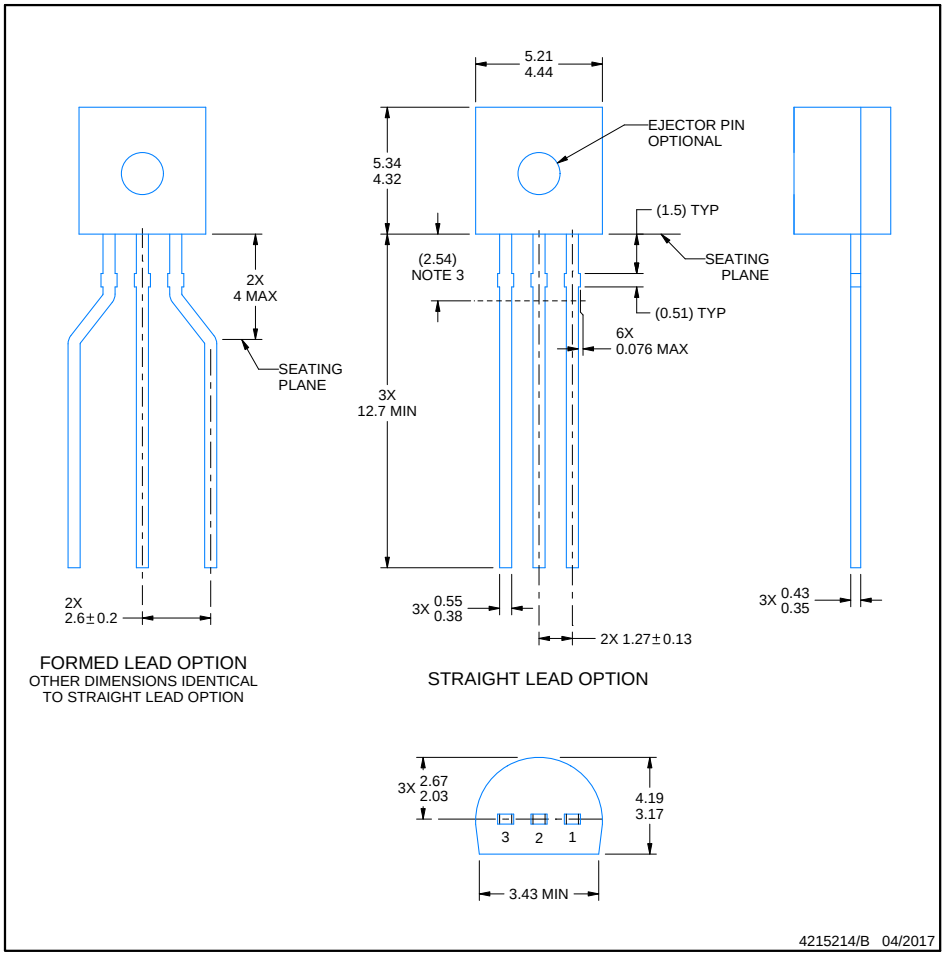

NOTES:

1. All linear dimensions are in millimeters. Any dimensions in parenthesis are for reference only. Dimensioning and tolerancing per ASME Y14.5M.
2. This drawing is subject to change without notice.
3. Lead dimensions are not controlled within this area.
4. Reference JEDEC TO-226, variation AA.
5. Shipping method:
   a. Straight lead option available in bulk pack only.
   b. Formed lead option available in tape and reel or ammo pack.
   c. Specific products can be offered in limited combinations of shipping medium and lead options.
   d. Consult product folder for more information on available options.

Appendix E

EnvionTEC 3D-Bioplotter® specifications

Machine Specification
Manufacturer Series

Axis Resolution (XYZ)	0.001 mm (0.00004″)
Speed	0.1 - 150 mm/s (0.004″ - 5.91″/s)
Pressure	0.1 - 9.0 bar (1.45 - 130 psi)
Build Volume (XYZ)	150 x 150 x 140 mm (5.91″ x 5.91″ x 5.51″)
Needle Position Control	Z-Sensor + High Resolution Camera
Camera Resolution (XY)	0.009 mm (0.00035″) per Pixel
Needle Sensor Resolution	0.001 mm (0.00004″)
Minimum Strand Diameter	0.100 mm (0.004″) - Material Dependent
Number of Materials per Scaffold	Maximum 5 Materials Using 5 Print Heads
Print Heads Included	1x Low and 1x High Temperature Head
Filters Included	Particle and Sterile Filters
Platform Temperature Control	Heating and Cooling Capable (-10°C to 80°C)
Platform Height Control	Automatic Z-height Controlling System
Material Calibration	Semi-Automatic Material Calibration
Additional Features	Automated Nozzle Cleaning Process
	4 External Temperature Sensor Ports
	Layer by Layer Photographic Log

Appendix F

Step response for a first order system

In Figure F.1 a step function and a first order system's response are represented.

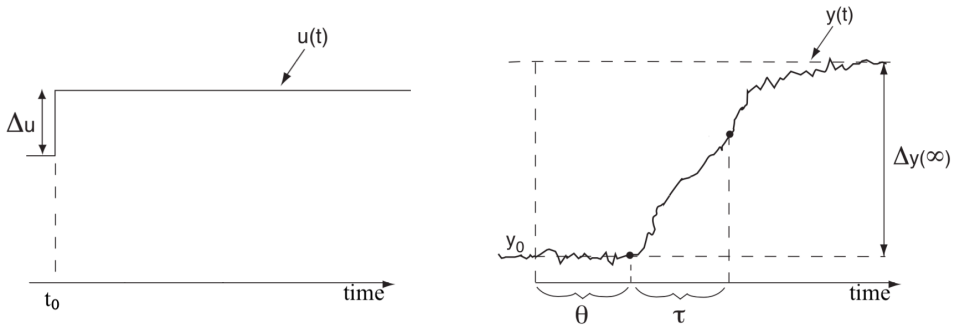

Figure F.1: (a) Step function. (b) Step response for first-order system. Reproduced from [135]

This response can be characterised by three parameters (see Figure F.1):

- Gain $k = \frac{\Delta y(\infty)}{\Delta u}$
- Delay θ: the time it takes for the dynamic phase to begin and, therefore, $\Delta y(\theta) \approx 0$. This delay can be a delay in measurement or the result of several dynamic terms that give a response that resembles a delay.
- Time constant τ: it characterises the system's inertia against change and can be defined as the additional time it takes to reach a certain percentage of the total change in y. This percentage's value depends on the order of the system. The reason for the time constant not being the time it takes to reach 100% in change is that it would take an infinitely long time to reach that state; and therefore, it would not be a meaningful value.

A first order system is a system whose input-output relationship is a first order differential equation and can be written by the standard form represented by (F.1)

$$\tau \frac{\mathrm{d}y}{\mathrm{d}t} = -y + ku, \qquad y(t_0) = y_0 \tag{F.1}$$

where τ represents the time constant, u the independent variable, y the dependent variable and k the gain.

Now, assuming that:

- the system is at rest at t_0 with $\frac{dy}{dt} = 0$, meaning that for $t < t_0$, $u = u_0$ and $y_0 = k\,u_0$.
- the independent value u changes from u_0 to a constant value at t_0.

equation (F.1) can be rewritten as equation (F.2)

$$\underbrace{\Delta y(t)}_{y(t)-y_0} = \underbrace{\Delta y(\infty)}_{y(\infty)-y_0}(1-e^{-t/\tau}) \tag{F.2}$$

So, when $t \to \infty$, then $e^{-t/\tau} \to 0$ and the system is approaching a new steady state, where $\Delta y(\infty) = k\Delta u$.

The term $1-e^{-t/\tau}$ determines how fast the system reaches this new steady state and as function of the t/τ the time taken to reach a percentage in change is shown in Table F.1.

Table F.1: Time taken to reach a certain change in output for a first order system.

t/τ	$1-e^{-t/\tau}$	Value of change
0	$1-e^{0}$	0
0.5	$1-e^{-0.5}$	0.393
1	$1-e^{-1}$	0.632
2	$1-e^{-2}$	0.865
3	$1-e^{-3}$	0.950
$\vdots$	$\vdots$	$\vdots$
∞	$1-e^{-\infty}$	1

In Figure F.2 this theoretical step response is plotted.

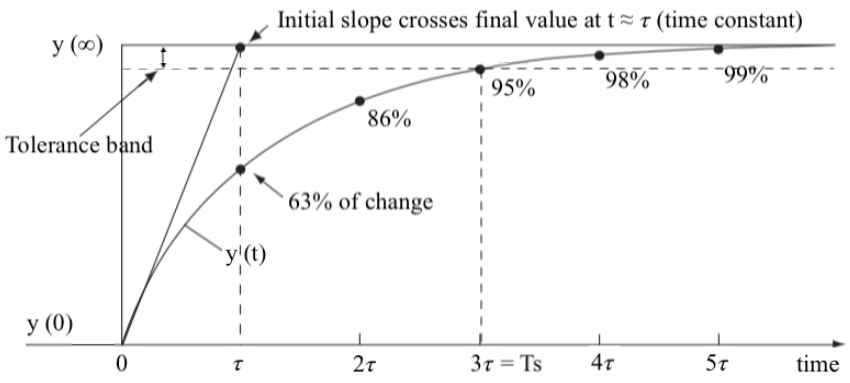

Figure F.2: Step response for first-order system. Adapted from [135] and [136].

So, for a first-order system, it means that when $t = \tau$ there has been a change of 63%. In order words, the time constant for a first order system is the time the system takes to reach 63% of its final change. This can be written mathematically by (F.3).

$$\Delta y(\theta + \tau) = 0.63\Delta y(\infty) \tag{F.3}$$

Additionally, when time equals 2τ, there has been a change of 86.5% of its total value, and so on. At last, when $t \to \infty$, the change will be complete and the system has reached its new final steady state.

Since, it will take an infinitive amount of time to reach 100% of total change, the settling time, T_s, is used instead in practical terms. This is defined as the time taken for the system's response to reach and stay within a defined tolerance band (see Figure F.2).

So, if the settling tolerance is defined as 5% error of steady state value, for example, is to say that the change is virtually complete after a period of 3 times τ.

Appendix G

Tekscan HR Mat™ specifications

Software Offerings

The ClassicMat platform supports the full suite of software applications for foot function, gait, peak plantar pressure, weight distribution, stance timing, and balance and sway analyses, and concussion assessments. The price of the mat includes one of the following software: FootMat for Clinicians, FootMat for Researchers (additional charges apply) or Sports AT. Optional add-on protocols and software may be purchased for an additional cost. A software development kit is also available that enables you to build your own applications.

All Tekscan software works with current Windows based operating systems. To view the complete computer requirements, visit: www.tekscan.com/computer-requirements.

Selection Guide and Specifications

Regardless of which mat you select, they all contain the same proven resistive sensing technology. Wireless and datalogging options are also available.

	MatScan	MatScan VersaTek	HR Mat
Sensor Model	3150	3150E	7101E
Electronics	Evolution® Handle	VersaTek® Cuff VersaTek 2-Port Hub (requires a power connection)	VersaTek® Cuff VersaTek 2-Port Hub (requires a power connection)
# of Sensels™	2,288	2,288	8,448
Active Sensing Area	43.6 x 36.9 cm (17.2 x 14.5 in)	43.6 x 36.9 cm (17.2 x 14.5 in)	48.8 x 44.7 cm (19.2 x 17.6 in)
Platform Thickness at Sensing Area	0.6 cm (0.2 in)	0.6 cm (0.2 in)	0.6 cm (0.2 in)
Sensor Resolution	1.4 sensels™ / cm^2 9.2 sensels / in^2	1.4 sensels / cm^2 9.2 sensels / in^2	4 sensels / cm^2 25 sensels / in^2
Scan Rates	100 Hz	440 Hz (100 Hz in wireless mode)	185 Hz (55 Hz in wireless mode)
Weight (includes all electronics, cables, power supplies)	1.7 kg/ 4.7 lb	3.3 kg/ 7.4 lb	3.5 kg/ 7.7 lb
Connection	USB 2.0*	USB 2.0*	USB 2.0*
Maximum Pressure Range	50-125 psi/ 345-862 kPa (adjustable)	50-125 psi/ 345-862 kPa (adjustable)	50-160 psi/ 345-1103 kPa (adjustable)

**Wireless connection is 802.11 and Datalogger connection is Micro SD card or USB 2.0.*

When you choose a system that uses VersaTek electronics, you can share electronics with other Tekscan systems (such as in-shoe, prosthetic, grip, and seating & positioning systems) to reduce your costs.

Appendix H

Solidworks® models for insole

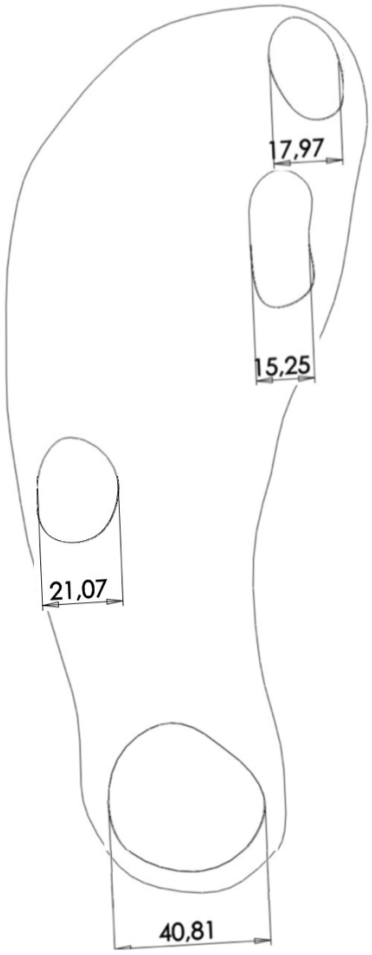

Figure H.1: Dimensions of carbon nanotubes areas in millimetres.